International Energy Agency, EBC Annex 58

Reliable building energy performance characterisation based on full scale dynamic measurements

Report of Subtask 3, part 1: Thermal performance characterization based on full scale testing - description of the common exercises and physical guidelines

María José Jiménez

International Energy Agency, EBC Annex 58

Reliable building energy performance characterisation based on full scale dynamic measurements

Report of Subtask 3, part 1: Thermal performance characterization based on full scale testing - description of the common exercises and physical guidelines

Authors Chapter 2
> María José Jiménez, Sergio Castaño, Juan de Dios Guzmán (Energy Efficiency in Buildings R&D Unit, CIEMAT, Madrid, Spain)

Authors Chapter 3
> Staf Roels, Geert Bauwens, An-Heleen Deconinck (KU Leuven, Leuven, Belgium)

Authors Chapter 4
> Gilles Flamant, Guillaume Lethé (ex-BBRI), Luk Vandaele (BBRI, Limelette, Belgium)

Authors Chapter 5
> María José Jiménez, Sergio Castaño, Laura de la Torre, Ricardo Enríquez (Energy Efficiency in Buildings R&D Unit, CIEMAT, Madrid, Spain)

Authors Chapter 6
> Imanol Ruiz de Vergara, César Escudero, Carlos García (LCCE, Vitoria-Gasteiz, Basque Country, Spain)
> Aitor Erkoreka (ENEDI Research Group, UPV/EHU, Bilbao, Basque Country, Spain)

Authors Chapter 7
> Pavel Kopecký, Kamil Staněk (CTU Prague, Czech Republic)

Authors Chapter 8
> María José Jiménez (Energy Efficiency in Buildings R&D Unit, CIEMAT, Madrid, Spain)
> Paul Strachan (University of Strathclyde, Glasgow, Scotland, UK)

Authors Chapter 9
> Gilles Flamant, Guillaume Lethé (ex-BBRI), Luk Vandaele (BBRI, Limelette, Belgium)

Authors Chapter 11
> María José Jiménez (Energy Efficiency in Buildings R&D Unit, CIEMAT, Madrid, Spain)
> Hans Bloem (Institute for Energy and Transport - Renewable Energy Unit, JRC, Ispra, Italy)

Editor:
> María José Jiménez (Energy Efficiency in Buildings R&D Unit, CIEMAT, Madrid, Spain)

Reviewed by:
> Paul Strachan, Søren Østergaard Jensen, Gilles Flamant

cover picture: Tailored heating experiment performed for one of the industrial partners of the Annex 58-project to determine the overall heat loss coefficient of a newly built dwelling based on on-site measured data. (source: Geert Bauwens, KU Leuven)

Preface

The International Energy Agency

The International Energy Agency (IEA) was established in 1974 within the framework of the Organisation for Economic Co-operation and Development (OECD) to implement an international energy programme. A basic aim of the IEA is to foster international co-operation among the 29 IEA participating countries and to increase energy security through energy research, development and demonstration in the fields of technologies for energy efficiency and renewable energy sources.

The IEA Energy in Buildings and Communities Programme

The IEA co-ordinates international energy research and development (R&D) activities through a comprehensive portfolio of Technology Collaboration Programmes. The mission of the Energy in Buildings and Communities (EBC) Programme is to develop and facilitate the integration of technologies and processes for energy efficiency and conservation into healthy, low emission, and sustainable buildings and communities, through innovation and research. (Until March 2013, the IEA-EBC Programme was known as the Energy in Buildings and Community Systems Programme, ECBCS.)

The research and development strategies of the IEA-EBC Programme are derived from research drivers, national programmes within IEA countries, and the IEA Future Buildings Forum Think Tank Workshops. The research and development (R&D) strategies of IEA-EBC aim to exploit technological opportunities to save energy in the buildings sector, and to remove technical obstacles to market penetration of new energy efficient technologies. The R&D strategies apply to residential, commercial, office buildings and community systems, and will impact the building industry in five focus areas for R&D activities:
– Integrated planning and building design
– Building energy systems
– Building envelope
– Community scale methods
– Real building energy use

The Executive Committee

Overall control of the IEA-EBC Programme is maintained by an Executive Committee, which not only monitors existing projects, but also identifies new strategic areas in which collaborative efforts may be beneficial. As the Programme is based on a contract with the IEA, the projects are legally established as Annexes to the IEA-EBC Implementing Agreement. At the present time, the following projects have been initiated by the IEA-EBC Executive Committee, with completed projects identified by (*):

Annex 1: Load Energy Determination of Buildings (*)
Annex 2: Ekistics and Advanced Community Energy Systems (*)
Annex 3: Energy Conservation in Residential Buildings (*)
Annex 4: Glasgow Commercial Building Monitoring (*)
Annex 5: Air Infiltration and Ventilation Centre
Annex 6: Energy Systems and Design of Communities (*)
Annex 7: Local Government Energy Planning (*)
Annex 8: Inhabitants Behaviour with Regard to Ventilation (*)
Annex 9: Minimum Ventilation Rates (*)
Annex 10: Building HVAC System Simulation (*)
Annex 11: Energy Auditing (*)
Annex 12: Windows and Fenestration (*)
Annex 13: Energy Management in Hospitals (*)
Annex 14: Condensation and Energy (*)
Annex 15: Energy Efficiency in Schools (*)

IEA EBC Annex 58: Reliable Building energy performance characterisation based on full scale dynamic measurements

Annex 58 in general

To reduce the energy use of buildings and communities, many industrialised countries have imposed more and more stringent requirements in the last decades. In most cases, evaluation and labelling of the energy performance of buildings are carried out during the design phase. Several studies have shown, however, that the actual performance after construction may deviate significantly from this theoretically designed performance. As a result, there is growing interest in full scale testing of components and whole buildings to characterise their actual thermal performance and energy efficiency. This full scale testing approach is not only of interest to study building (component) performance under actual conditions, but is also a valuable and necessary tool to deduce simplified models for advanced components and systems to integrate them into building energy simulation models. The same is true to identify suitable models to describe the thermal dynamics of whole buildings including their energy systems, for example when optimising energy grids for building and communities.

It is clear that quantifying the actual performance of buildings, verifying calculation models and integrating new advanced energy solutions for nearly zero or positive energy buildings can only be effectively realised by in situ testing and dynamic data analysis. But, practice shows that the outcome of many on site activities can be questioned in terms of accuracy and reliability. Full scale testing requires a high quality approach during all stages of research, starting with the test environment, such as test cells or real buildings, accuracy of sensors and correct installation, data acquisition software, and so on. It is crucial that the experimental setup (for example the test layout or boundary conditions imposed during testing) is correctly designed, and produces reliable data. These outputs can then be used in dynamic data analysis based on advanced statistical methods to provide accurate characteristics for reliable final application. If the required quality is not achieved at any of the stages, the results become inconclusive or possibly even useless. The IEA EBC Annex 58-project arose from the need to develop the necessary knowledge, tools and networks to achieve reliable in situ dynamic testing and data analysis methods that can be used to characterise the actual energy performance of building components and whole buildings. As such, the outcome of the project is not only of interest for the building community, but is also valuable for policy and decision makers, as it provides opportunities to make the step from (stringent) requirements on paper towards actual energy performance assessment and quality checking. Furthermore, with the developed methodology it is possible to characterise the dynamic behaviour of buildings, which is a prerequisite for optimising smart energy and thermal grids. Finally, the project developed a dataset to validate numerical Building Energy Simulation programs.

Structure of the project

Successful full scale dynamic testing requires quality over the whole process chain of full scale testing and dynamic data analysis: a good test infrastructure, a good experimental set-up, a reliable dynamic data analysis and appropriate use of the results. Therefore, the annex-project was organised around this process chain, and the following subtasks were defined:

Subtask 1 made an inventory of full scale test facilities available all over the world and described the common methods with their advantages and drawbacks for analysing the obtained dynamic data. This subtask produced an overview of the current state of the art on full scale testing and dynamic data analysis and highlighted the necessary skills.

Subtask 2 developed a roadmap on how to realise a good test environment and test set-up to measure the actual thermal performance of building components and whole buildings in situ. Since there are many different objectives when measuring the thermal performance of buildings or building components, the best way to treat this variety has

been identified as constructing a decision tree. With a clear idea of the test objective, the decision tree will give the information of a test procedure or a standard where this type of test is explained in detail.

Subtask 3 focused on quality procedures for full scale dynamic data analysis and on how to characterise building components and whole buildings starting from full scale dynamic data sets. The report of subtask 3 provides a methodology for dynamic data analysis, taking into account the purpose of the in situ testing, the existence of prior physical knowledge, the available data and statistical tools,… The methodologies have been tested and validated within different common exercises, in a way that quality procedures and guidelines could be developed.

Subtask 4 produced examples of the application of the developed concepts and showed the applicability and importance of full scale dynamic testing for different issues with respect to energy conservation in buildings and community systems, such as the verification of common BES-models, the characterisation of buildings based on in situ testing and smart meter readings and the application of dynamic building characterisation for optimising smart grids.

Subtask 5 established a network of excellence on 'in situ testing and dynamic data analysis' for dissemination, knowledge exchange and guidelines on testing.

Overview of the working meetings

The preparation and working phase of the project encompassed 8 working meetings:

Meeting	Place, date	Attended by
Kick off meeting	Leuven (BE), September 2011	45 participants
Second preparation meeting	Bilbao (SP), April 2012	46 participants
First working meeting	Leeds (UK), September 2012	44 participants
Second working meeting	Munich (GE), April 2013	53 participants
Third working meeting	Hong-Kong (CH), September 2013	26 participants
Fourth working meeting	Gent (BE), April 2014	49 participants
Fifth working meeting	Berkeley (USA), September 2014	37 participants
Sixth working meeting	Prague (CZ), April 2015	39 participants

During these meetings, working papers on different subjects related to full scale testing and data analysis were presented and discussed. Over the course of the Annex, a Round Robin experiment on characterising a test box was undertaken, and several common exercises on data analysis methods were introduced and solved.

Outcome of the project

The IEA EBC Annex 58-project worked closely together with the Dynastee-network (www.dynastee.info). Enhancing this network and promoting actual building performance characterization based on full scale measurements and the appropriate data analysis techniques via this network is one of the deliverables of the Annex-project. This network of excellence on full scale testing and dynamic data analysis organizes on a regular basis events such as international workshops, annual training,... and will be of help for organisations interested in full scale testing campaigns.

In addition to the network of excellence, the outcome of the Annex 58-project has been described in a set of reports, including:
Report of Subtask 1A: Inventory of full scale test facilities for evaluation of building energy performances.
Report of Subtask 1B: Overview of methods to analyse dynamic data
Report of Subtask 2: Logic and use of the decision tree for optimizing full scale dynamic testing.
Report of Subtask 3 part 1: Thermal performance characterization based on full scale testing: physical guidelines and description of the common exercises
Report of Subtask 3 part 2: Thermal performance characterization using time series data – statistical guidelines.
Report of Subtask 4A: Empirical validation of common building energy simulation models based on in situ dynamic data.
Report of Subtask 4B: Towards a characterization of buildings based on in situ testing and smart meter readings and potential for applications in smart grids
IEA EBC Annex 58 project summary report

Participants

In total 49 institutes from 17 countries participated in Annex 58. The different participants are listed below:

Austria	Gabriel Rojas-Kopeinig, Universität Innsbruck
	Susanne Metzger, Vienna University of Technology
Belgium	Gilles Flamant, Belgian Building Research Institute
	Guillaume Lethé, Belgian Building Research Institute
	Luk Vandaele, Belgian Building Research Institute (subtask 5 co-leader)
	Paul Steskens, Belgian Building Research Institute
	Gabrielle Masy, Haute Ecole de la Province de Liège
	An-Heleen Deconinck, Katholieke Universiteit Leuven
	Dirk Saelens, KU Leuven (subtask 4 co-leader)
	Geert Bauwens, KU Leuven (secretary)
	Glenn Reynders, KU Leuven
	Ruben Baetens, KU Leuven
	Roel De Coninck, KU Leuven
	Staf Roels, KU Leuven (operating agent)
	Frédéric Delcuve, Knauf Insulation
	Philippe André, Université de Liège
	Arnold Janssens, Universiteit Gent (subtask 1 leader)
	Eline Himpe, Universiteit Gent
China	Gongshen Huang, City University of Hong Kong
	Tin-Tai Chow, City University of Hong Kong
	Linda Xiao Fu, The Hong Kong Polytechnic University
	Shengwei Wang, The Hong Kong Polytechnic University (subtask 4 co-leader)
	Xue Xue, The Hong Kong Polytechnic University
Czech Republic	Kamil Stanek, Czech Technical University Prague
	Pavel Kopecký, Czech Technical University Prague
Denmark	Christian Holm Christiansen, Danish Technological Institute
	Søren Østergaard Jensen, Danish Technological Institute
	Henrik Madsen, Technical University of Denmark (subtask 3 co-leader)
	Kyung Hun (Peter) Woo, Technical University of Denmark
	Peder Bacher, Technical University of Denmark
France	Bouchie Remi, Centre Scientifique et Technique du Bâtiment
	Pierre Boisson, Centre Scientifique et Technique du Bâtiment
	Mohamed El Mankibi, Ecole Nationale des Travaux Publics de l'Etat
	Christian Ghiaus, INSA de Lyon
	Ibán Naveros, INSA de Lyon
	Guillaume Pandraud, Isover Saint-Gobain
	Simon Rouchier, Université de Savoie
Germany	Franz Feldmeier, Fachhochschule Rosenheim
	Lucia Bauer, Fachhochschule Rosenheim
	Herbert Sinnesbichler, Fraunhofer-Institut für Bauphysik
	Ingo Heusler, Fraunhofer-Institut für Bauphysik
	Matthias Kersken, Fraunhofer-Institut für Bauphysik
	Soeren Peper, Passive House Institute
Italy	Fabio Moretti, ENEA
	Hans Bloem, European Commission - DG JRC (subtask 5 co-leader)
	Lorenzo Pagliano, Politecnico di Milano
	Giuseppina Alcamo, Università degli Studi di Firenze
The Netherlands	A.W.M. van Schijndel, Technische Universiteit Eindhoven
	Rick Kramer, Technische Universiteit Eindhoven
Norway	Nathalie Labonnote, Norges teknisk-naturvitenskapelige universitet
Spain	Gerard Mor-Lleida, Centro Internacional de Métodos Numéricos en Ingeniería
	Xavi Cipriano, Centro Internacional de Métodos Numéricos en Ingeniería
	Aitor Erkoreka, Escuela Técnica Superior de Ingenieria Bilbao (subtask 2 co-leader)
	Koldo Martin Escudero, Escuela Técnica Superior de Ingenieria Bilbao

	Roberto Garay Martinez, Tecnalia Research & Innovation
	Luis Castillo López, CIEMAT
	Maria José Jiménez Taboada, CIEMAT (subtask 3 co-leader)
	Ricardo Enríquez Miranda, CIEMAT
United Kingdom	Richard Fritton, Salford University
	Chris Gorse, Leeds Beckett University (subtask 2 co-leader)
	Martin Fletcher, Leeds Beckett University
	Samuel Stamp, University College London
	Filippo Monari, University of Strathclyde
	Paul A. Strachan, University of Strathclyde (subtask 4 co-leader)
United States	Stephen Selkowitz, Lawrence Berkeley National Laboratory

IEA, EBC Annex 58, Report of Subtask 3, part 1

Thermal performance characterization based on full scale testing - description of the common exercises and physical guidelines

María José Jiménez

June 2016

TABLE OF CONTENTS

Symbols and units

A	m²	Area
A_{sol}	m²	Solar aperture
C	J/K	Effective heat capacity of a space or building
g	-	Total solar energy transmittance of a building element
H	W/K	Heat transfer coefficient of a building
H_{tr}	W/K	Transmission heat transfer coefficient
H_{ve}	W/K	Ventilation heat transfer coefficient (including infiltration)
I_{sol}	W/m²	Solar irradiance
Q	J	Quantity of heat
q	W/m²	Heat flow density
R	m²K/W	Thermal resistance
T	K	Thermodynamic temperature
t	s	Time, period of time
U	W/m²K	Thermal transmittance
θ	°C	Centigrade temperature
Φ	W	Heat flow rate
Φ_P	W	Thermal power

1. Introduction

Subtask 3 focuses on quality procedures for full scale dynamic data analysis and on how to characterise building components and whole buildings starting from full scale dynamic data tests. Subtask 3 hence contains two major topics:

1. Development of procedures for high quality dynamic data analysis. Analysing the measured data of in-situ testing requires dynamic analysis methods and models. A wide range of methodologies exist, and it is often not easy to choose the most appropriate approach for each particular case. The activities are here centred on which methodology to use for dynamic data analysis, taking into account the purpose of the in-situ testing, the existence of prior physical knowledge, the available data and the statistical tools, etc.

2. Determination of reliable performance indicators for actual thermal performance of building components and whole buildings. Dealing with questions such as the validity of the usual approximations applied to obtain the static performance indicators when characterizing highly insulated nearly zero energy buildings and the need of dynamic performance indicators.

Common exercises and free papers have been used as instruments to move forward. The methodologies have been tested and validated on the data collected for the different case studies considered along the common exercises. Free papers have given information on the current state of the art of the research activities in this area and facilitated discussions among participants in the different meetings.

This report describes a series of case studies that have been considered for common exercises, starting from quite simple systems, progressively approaching to reality, to end with full size buildings. First, two exploratory exercises considering an opaque wall were carried out. This wall is described in **chapter 2**. Then another common exercise is based on the characterization of a round robin test box described in **chapter 3**, which is seen as a scale model of a building, built by one of the participants, with fabric properties unknown to all other participants. Measurements have been performed on the test box in Belgium and Spain under real climatic conditions (**chapters 4, 5 and 6**). Afterwards the same box was tested in a climatic chamber (**chapter 7**). Next common exercise was based on one of the Twin Houses at IBP Fraunhofer in Germany, also considered for validation exercises in Subtask 4A. The experimental set up was optimised to fit the objectives of the dynamical analysis (**chapter 8**). Analogous objectives to previous exercises have been set. However new challenges are incorporated when a full size building is considered. Afterwards a full size building tested in Belgium by BBRI was also considered (**chapter 9**).The dynamic data corresponding to each of these case studies were distributed to all participants who tried to characterise the thermal performance of the building fabric based on these measurement data. Apart from the characterization of the fabric, a cross validation and blind run were also included in the exercises.

Participants were asked to describe clearly, step by step the analysis and validation carried out. These exercises demonstrated the application of different models and methods. These reports were important to facilitate identifying differences among the analysis approaches

that helped to explain differences in results. This issue was very useful to move forward in the research context of Annex 58. The exercises remarked the influence of experiment set up and test sequences and strategies on the accuracy of final results. These exercises also give evidence of the relevance of skills in different areas of expertise and capabilities to combine all of them to obtain accurate results. Necessary skills are both regarding mathematical and statistical modelling and validation techniques, and regarding pre-processing criteria, physical knowledge and application of suitable approximations assumptions. Multidisciplinary training in these combined and specific skills is being supplied by the DYNASTEE summer school on data analysis methods yearly organised since 2012. More information in: www.dynastee.info.

The multidisciplinary training has proven to provide a strong group of researchers which are able to carry out good experiments followed by appropriate use of methods from time series analysis to come up with reliable results. Besides this the methods for dynamic analysis have been further developed during the progress of the Annex work, and the latest version of the some of the developed tools can be downloaded from the DYNASTEE web page.

Calls for free papers focussing on topics which are relevant regarding the overall objective of this subtask were made for each expert meeting. Most presented contributions are related to thermal performance analysis of building "fabric". Many of these contributions report the study of different issues of modelling considering simplified situations either by simple cases studies, or by carrying out analysis based on simulated data. Relevant findings have been reported even from these simplified approaches.

Requisites on measurements and experimental set up, derived from requisites of data analysis is also considered in several reported works. In general it is concluded that the developed methodologies for dynamical analysis provide much more information about the characteristics of the building or the component than steady state methods, and moreover the results are provided using much shorter periods of experiments.

Some participants have already proven rather promising results regarding the analysis of full size buildings with a number of sensors and a number of rooms, even in the case of occupied buildings.

A list of all the free papers presented along the Annex 58 expert meetings is included in section 10.2 of **chapter 10**. Some of these works were further elaborated and published in scientific journals. A list of all these published papers is also included in section 10.3 of chapter 10. Relevant results were presented in different events organised by DYNASTEE network and their corresponding proceedings and other dissemination documents can be downloaded from its webpage (www.dynastee.info).

Guidelines for dynamic data analysis for energy performance assessment of buildings and building components have been elaborated. These guidelines are based on experiences along previous EU projects developed by DYNASTEE participants and also on lessons learned from common exercises and other activities carried out recently in the framework of Annex 58. These guidelines consist in two parts respectively related to physical and statistical aspects of data analysis. Both parts must be considered as complementary in a multidisciplinary context. The first part, dealing with physical aspects corresponds to **chapter 11** in this document. The second part, dealing with statistical aspects is the Report of Subtask 3 – Part 2 (ref. 19).

2. Opaque wall. Test at CIEMAT

2.1 Introduction

The objective of this common exercise is to identify strengths and weaknesses (reliability, inherent physical information, ...) of different available models.

The proposed case study consists on a very simple lightweight opaque and homogeneous wall. This test component was chosen simple and the tests were intentionally oversized regarding measured quantities, test period length, and test conditions, in order to investigate capabilities and limitations of different models and methods.

The simplicity in the component and the oversize in the data provide enough freedom to allow the application of a wide variety of different analysis and validation approaches, with different degree of complexity and accuracy.

Some of the analysis approaches applied to this case study have been published in references 7 and 8.

2.2 Test component description

These data correspond to a test of a simple lightweight, opaque and homogeneous wall.

It is made of ceramic bricks which size is 32cm x 16cm x 11.5cm, joined using sand and concrete mortar. Exterior is plastered with the same mortar, 2cm thick. Interior is gypsum plastered 1.5 cm thick. So the wall total thickness is 15cm made of 2cm mortar, 11.5 brick and 1.5cm gypsum.

The size of the interior surface of the wall is 298cm width and 276cm high. Figure 1 shows some constructive details and the finally constructed wall.

(a)   (b)   (c)
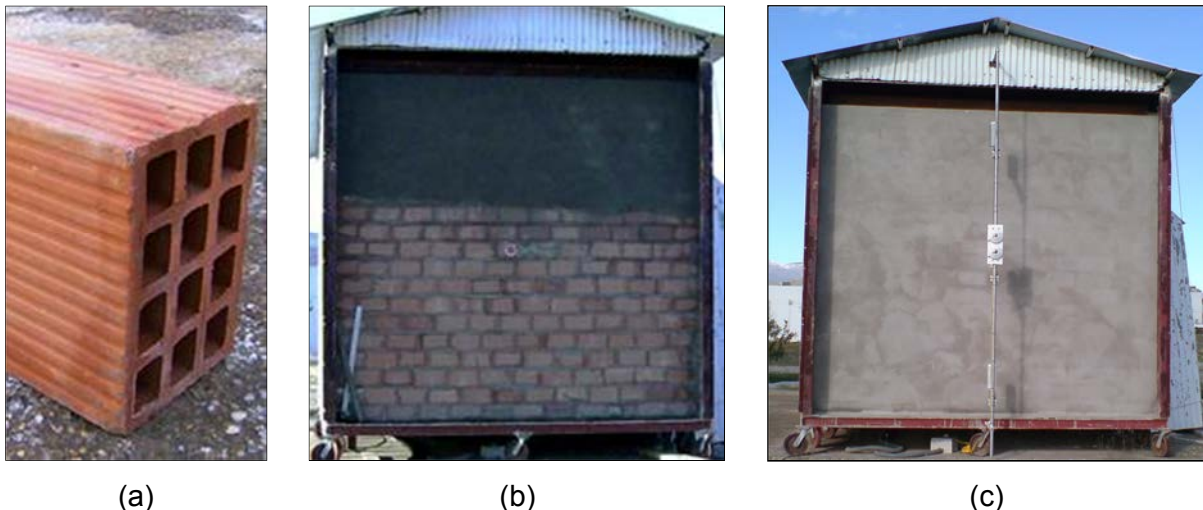
Figure 1 : Detail of the construction of the wall. (a) Hollow brick. (b) Cement mortar layering. (c) Wall finally constructed.

2.2.1 Design U and g values

U and g values have been calculated according to different expression taken from the literature frequently used in practice, and using the geometric and thermal properties summarised in Table 1.

The differences observed in the results given by these expressions give an approximated idea of the range of variability that can be obtained from the identification analysis among the different data series due to boundary conditions and other sources of uncertainty. The results obtained in this calculation can be used to carry out external validation to reject models giving results showing any of these behaviours:

- Being too far from these estimated reference values.
- Showing variability in the U and g values in a range that is remarkably higher that the range of variability theoretically calculated.

Table 1: Material properties of the different layers of the wall. Assuming usual densities for the construction, thermal conductivities included in CTE (reference 1) have been used for the given materials and densities

	Thickness (cm)	Thermal conductivity $(Wm^{-1}K^{-1})$	Density (Kg/m^3)
Plaster	1.5	0.57	1000-1300
Hollow brick	11.5	0.32	770
Concrete mortar	2.0	1.8	> 2000

The U value has been calculated according to the following expression:

$$U = \frac{1}{R_{si} + \sum \frac{l_i}{\lambda_i} + R_{se}}$$

(1)

Where R_{si} and R_{se} are respectively the internal and external surface thermal resistances of the wall, λ_i is the thermal conductivity of layer i, and l_i is its thickness.

It is well known that R_{si} and R_{se} depend on the boundary conditions in the tests such as wind speed and surface temperatures. The following three different approximations have been identified as the most frequently used in practical applications, and have been used to estimate reference parameter values and their expected range of variability:

- Taking constant standard surface thermal resistances (R_{si}=0.13; R_{se}=0.04 m²K/W) into account (ISO 6946:2007). The U value calculated for the wall is 1.76 $Wm^{-2}K^{-1}$.
- Using non-constant surface heat transfer coefficients, depending on wind speed (V) according the following expressions that include radiative effects (McAdams, 1954):

$$h_{rc} = 5.7 + 3.8V \text{ if V< 5m/s}$$

(2)

$$h_{rc} = 7.2V^{0.78} \text{ if V> 5m/s}$$

(3)

- Using non-constant surface heat transfer coefficients, depending on wind speed and surface temperatures. The following expressions have been considered for the convection surface heat transfer coefficient (Watmuff y col., 1977):

$$h_c = 2.8 + 3.0V$$

(4)

And the following expression has been considered to estimate approximately the radiative surface heat transfer coefficient:

$$h_r = 4\varepsilon\sigma T^3 \tag{5}$$

Where ε is the emissivity of the external surface and, T is its temperature. This expression is valid for parallel surfaces when their temperatures are similar (Duffie and Beckman, 1991). It is also assumed that the average temperature of surrounding surfaces is similar to the outdoor air temperature. It must be taken into account that applying this expression to estimate corresponding coefficient of the wall is a very crude approximation. However it is considered because it includes a dependence on the surface temperature that will help to detect sensitivity of U value to differences of this variable

The g value has been calculated according to the following expression (ASHRAE , 1999):

$$g = \alpha\frac{U}{h_e} \tag{6}$$

Where α is the solar absorptance of the external surface and he is the external surface heat transfer coefficient. The value $\alpha = 0.8$ has been assumed for the exterior surface of grey concrete mortar. Different approximations have been studied, according to the same three different approximations considered for the surface heat transfer coefficients used to calculate the U value.

The theoretical U and g values have been obtained for all the data series according the different approximations considered previously in this section.

Data available from April till October 2010 (both included) have been split in data series. Each of these data series include ten days. U and g values have been calculated using all the instantaneous measurements of the boundary conditions (wind speed and surface temperatures).

Figure 2 shows the parameter estimates averaged for each data series according to equations (4) and (5). Figure 3 and Figure 4 focus on the results obtained considering heat transfer surface coefficients depending on wind speed and surface temperatures. This figures show the average value and standard deviation of the parameter estimates obtained applying the considered approximations in each data series.

These figures reveal low differences among the **U values** obtained for the different boundary conditions.

- Assuming the equations (4) and (5) as approximation to estimate the surface heat transfer coefficient depending on wind speed and surface temperatures, the standard deviation among all the average values for all the data series is 2.34% and the standard deviation for the instantaneous values in each data series is in the range 3.26-4.48%. See Figure 3.

- Assuming the equations (2) and (3) as approximation to estimate the surface heat transfer coefficient depending on wind speed, the standard deviation among all the average values for all the data series is 2.37% and the standard deviation for the instantaneous values in each data series is in the range 3.99-6.18%. See Figure 4.

The variation detected by these theoretical calculations due to wind speed and surface temperatures are considered very low and undetectable in the U values estimated by identification, taking into account typical measurement uncertainties (around to 10%). Results given by the analyses reported in references 7 and 8 are a bit above these theoretical values. However agreement between theoretical and identified values is considered acceptable taking into account typical uncertainty bands.

However the differences observed in these figures among the **g values** obtained for the different boundary conditions are relatively higher.

- Considering surface heat transfer coefficient depending on wind speed and surface temperatures according to equations (4) and (5), the standard deviation among all the average values for all the data series is 8.66% and the standard deviation for the instantaneous values in each data series is in the range 16.6-27.3%. See Figure 3.

- Considering surface heat transfer coefficient depending just on wind speed according to equations (2) and (3), the standard deviation among all the average values for all the data series is 12.9% and the standard deviation for the instantaneous values in each data series is in the range 21.2-37.4%.

The variation detected by these theoretical calculations due to wind speed and surface temperatures may be not negligible in the g values estimated by identification. See Figure 4.
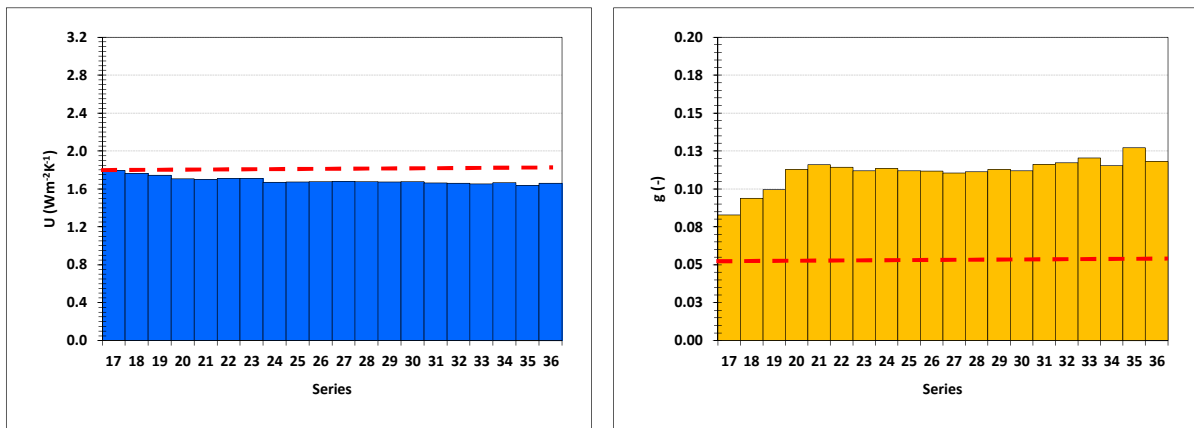
Figure 2: Parameter estimates assuming non-constant surface heat transfer resistances. Series 17 to 36 corresponds to April to October, both included. Each data series includes 10 days. Considering heat transfer surface coefficients depending on wind speed and surface temperatures (equations (4) and (5)). Dotted red lines indicate the same parameters assuming standard constant surface resistances.
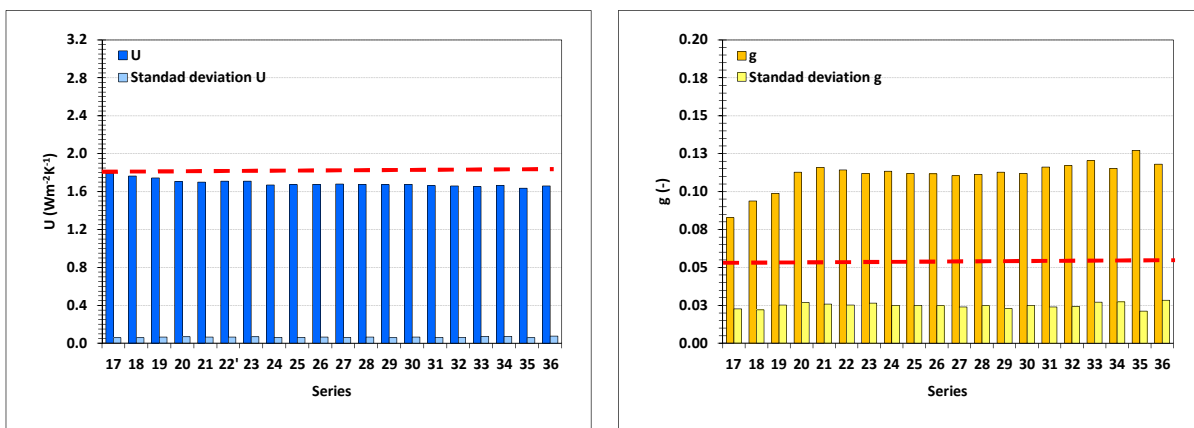
Figure 3: Average value and standard deviation of the parameter estimates. Considering heat transfer surface coefficients depending on wind speed and surface temperatures (equations (4) and (5)). Dotted red lines indicate the same parameters assuming standard constant surface resistances.

11
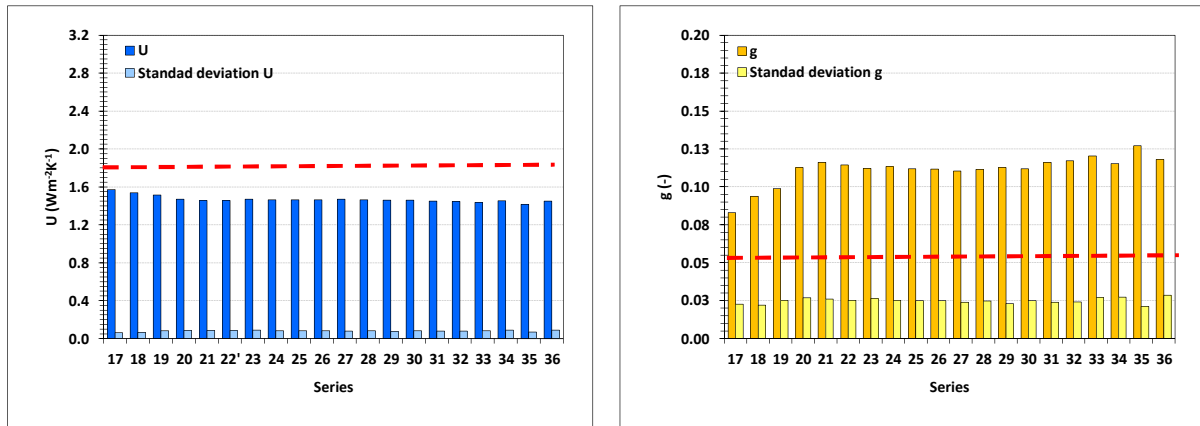
Figure 4: Average value and standard deviation of the parameter estimates. Considering heat transfer surface coefficients depending on wind speed, according to equations (2) and (3). Dotted red lines indicate the same parameters assuming standard constant surface resistances.

2.3 Test procedure

2.3.1 Boundary conditions

This wall was tested in a test cell at the LECE laboratory at Plataforma Solar de Almeria, in the South East of Spain (37.1°N, 2.4°W). The weather at this test site is dry and extremely hot in summer and cold in winter. Temperature swings largely between day and night. Global vertical solar radiation is very strong in winter, and horizontal is very strong in summer. Sky is usually very clear.

Testing is done under outdoor weather conditions. The following outdoors climate sensors installed locally near the tests component are included in the supplied data: Global vertical solar radiation, air temperature, vertical longwave radiation, wind speed, and relative humidity. Additional meteorological sensors installed at the test site, not included in the data sets, were used to check consistency of these outdoors measurements.

Indoors air is cooled in summer and heated in winter, being the temperatures respectively around 18°C and 40°C. A ventilator is used to avoid indoor air temperature stratification.

2.3.2 Measurements

The measured physical quantities have been chosen according to the following criteria (See Table 2 for nomenclature and units):

- T_i, T_e, considering T_i-T_e as one of the main driving forces to the heat flux density.
- G_v, to analyse if it affects the heat flux density and, if so, to include in the model to estimate the air to air U value.
- T_{si}, T_{se}, G_{lw}, H and WV to investigate if the non constant contribution of surface coefficients is negligible or not regarding the U value estimate. These measurements allow several different approximations for each surface effect.
- T_{si} can be used to analyse the effect of temperature on the measurement of heat flux density. Assuming that the sensitivity of the sensor depends on its temperature.
- Other effects such as influence of moisture and wall temperature on thermal conductivity could be studied.

Additionally a meteorological station is installed at the test site, including redundancies in some of the main physical quantities to guarantee their correct representation. The following sensors are installed in this meteorological station: Global, horizontal, and south vertical solar radiation, air temperature, longwave radiation, wind speed and direction, relative humidity and CO_2 concentration.

2.3.3 Measurement devices

This section describes the measurement equipment and other considerations regarding their accuracy.

The following list summarises the used measurement transducers and sensors:

- Air temperature: Platinum thermoresistance, PT100, 1/10 DIN, directly measured using a four-wire connection, with a solar radiation shield and ventilated for outdoor measurements.
- Surface temperature: Analogous sensors and connections as those used for air temperature, in this case built in the corresponding surface.
- Heat flux density: Sensor model HFP01 manufactured by Hukseflux, accuracy of sensitivity coefficient 5%, voltage measured directly by differential connection.
- Vertical global Solar Irradiance: Pyranometer, model CM11 manufactured by Kipp and Zonen, secondary standard according to ISO 9060:1990, voltage directly measured using a differential connection.
- Vertical long wave radiation on the surface of the test component: Pyranometer, model CGR-4 manufactured by Kipp and Zonen, voltage directly measured using a differential connection.
- Wind velocity: Sensor model WindSonic manufactured by GILL INSTRUMENTS LTD.
- Outdoors relative humidity. Sensor model HMP45A/D manufactured by VAISALA.

A data acquisition system with the following characteristics has been implemented: 16-bit A/D resolution, range of measurements fitting sensor output, modules distributed to minimise wiring, based in Compact Field Point modules manufactured by NATIONAL INSTRUMENTS. Particularly the following list summarises the used modules:

- cFP-RTD-124: Four-Wire RTD and Resistance inputs. Range –200 °C to 850 °C used for measurement of temperature.
- cFP-TC-125: Differential thermocouple or millivolt inputs. Range –20 mV to 80 mV used for measurement of global and long wave radiation and heat flux density.
- cFP-AI-111: Milliamp input. Range 4–20 mA used for measurement of wind velocity.
- cFP-AI-110: Voltage or current input. Range 0–1 V used for measurement of relative humidity.

Twisted pairs and grounded shield are employed to reject noise and avoid perturbations from wiring.

More information on the measurement devices is included in reference 7.

2.4 Data

The data supplied correspond to a testing period since the 1st of February 2010 to the 31st of October 2010. Data sets were deliberately oversized regarding length of testing period, sampling frequency and measured variables. These data sets include extremely different tests conditions. The usefulness of such data oversize is summarised by the following three points:

1. Usually tests don't give so much information, and issues such as length of testing period, sampling frequency, measured variables and test conditions, are decided in the phase of experimental design before testing. All these decision made in the phase of experimental design can significantly affect the accuracy of identification results. The oversizing of the data considered in this case study allows analyst to make themselves such decisions, in the sense that they can select which data are going to use for the analysis. This data selection is implicitly associated to particular length of testing period, sampling frequency, measured variables and test conditions.
2. This data oversizing also allows to carry out identification analysis, and to compare accuracy of results when different data sets are used for analysis. In practice, the differences in the data used for each case corresponds to different decisions in experimental design, so quality of the results obtained for each case give information on the influence of the different test design on the accuracy of identification results.
3. Additionally data oversizing regarding test length gives a strong support for robust validation of results.

11 data files are supplied, one for each month, except May and October that have gaps of 11 h and 10 h respectively, and have been split in two parts separated by these gaps.

Data files are text files organised in rows and columns. Each column corresponds to a variable. The first row is a head that contains the names of the recorded variables as indicated in Table 1 below. Data are read and recorded in each row every minute. Nomenclarure and units corresponding to these data are summarised in Table 2.

Table 2: Nomenclature and units

Name	Measurement	Unit
DAY	Day	DD/MM/AAAA
TIME	GMT Time	hh:mm
DAY_J	Day	Julian day
Te	Outdoors air temperature	°C
Ti	Indoors air temperature	°C
Tsi	Internal surface temperature	°C
Tse	External surface temperature	°C
Øi	Heat flux density in the internal surface.	W/m^2
Gv	Vertical global solar radiation.	W/m^2
Glw	Vertical long wave radiation	W/m^2
WV	Wind velocity near the wall	m/s
H	Relative humidity	%

2.5 Data overview

This section gives an overview of the data available in this case study. Graphical overview can help to evaluate qualitatively the data to reject data subsets if any abnormal behaviour is detected.

Data overview can help to discuss the selection of data for analysis. This selection should be done taking into account the oversizing of data sets in this particular case study described in section 2.4. This overview can help to motivate any additional analysis based on the extra data that are available.

Both aspects intrinsic quality of data, and issues related to experimental design related to data analysis and its accuracy, are briefly discussed in the following sections 2.5.1 and 2.5.2 respectively.

2.5.1 Intrinsic quality of measurements

Figure 5 to Figure 13 show an overview of the main variables recorded. Most of these graphs show normal tendencies for the considered measured variables.

However this overview reveals that outdoor surface temperature is not correct in February and March (Figure 5 and Figure 6 (d)). The symptoms pointing to this affirmation are the following: The variable recorded as external surface temperature for these months in phase with the outdoor air temperature, it is quite similar to this air temperature at night and remarkably higher in the central hours of the day. This behaviour is observed when the sensor is not properly glued to the surface and it is measuring its own temperature instead of the surface. However when the temperature sensor is properly glued and integrated in the measured surface its measurement is a bit delayed regarding the outdoor air temperature. Night measurements are also bit different (See Figure 7 to Figure 13 (d)). Consequently it is concluded that the measurement of external surface temperature must be rejected for February and March.

2.5.2 Data quality regarding identification

Two different periods can be clearly distinguished in Figure 5 to Figure 13 and Table 3. The first one, till the mid of June (Figure 9), is characterised by a relatively large positive difference between indoor and outdoor air temperatures, and also by large levels of global solar radiation measured on the external surface of the wall, Figure 5 to Figure 9 (b) and (c). The second period is characterised by a relatively small and negative difference between indoor and outdoor air temperatures, and also by lower levels of global solar radiation measured on the external surface of the wall, Figure 9 to Figure 13 (b) and (c). The absolute value of the heat flux density, which is mainly driven by these two effects, ranges in similar values in both periods as can be seen in Figure 5 to Figure 13 (a). In the first period, when thermal energy is leaving the room, the two effects are strong and opposite. In the second period the indoor temperature level is changed and thermal energy is entering the room. However, each of these main driving effects are adding but weak in the second period, and as consequence this period is more vulnerable to uncertainties, which increase difficulty in the identification process, mainly in the first part of this second period when these effects present the lowest values.

This behaviour is confirmed by the analysis reported in ref. 8. Results reported in this reference show different behaviour for series recorded in these different periods. The theoretical dependence on the boundary conditions reported in section 2.2.1 doesn't explain this different behavior. However it can be understood considering the higher level of uncertainty in the parameter estimates in the second period due to the poorer levels of the main driving variables in this period, discussed in this section.

Table 3: Summary of data. Winter in blue, summer in yellow and spring and autumn in white. The included U values for each series are the theoretical values, assuming the equations (4) and (5) as approximation to estimate the surface heat transfer coefficient depending on wind speed and surface temperatures.

Series	Dates	ΔT (ºC)	ΔT_S (ºC)	G_v (W/m^2)	W (m/s)	G_{lw} (W/m^2)	Φ (W/m^2)	U (Wm^{-2}K^{-1})
11	03/02/2010 - 12/02/2010	26.14	N/A	157.27	1.60	341.12	39.92	N/A
12	13/02/2010 - 22/02/2010	28.73	N/A	110.78	1.53	338.42	49.34	N/A
13	23/02/2010 - 04/03/2010	24.10	N/A	182.88	2.65	357.63	36.05	N/A
14	05/03/2010 - 14/03/2010	29.11	N/A	113.72	3.18	338.85	47.51	N/A
15	15/03/2010 - 24/03/2010	33.80	N/A	128.76	2.42	356.17	57.98	N/A
16	25/03/2010 - 03/04/2010	32.13	N/A	184.70	2.79	353.03	50.97	N/A
17	04/04/2010 - 13/04/2010	31.90	17.78	137.11	3.41	363.87	54.48	1.79
18	14/04/2010 - 23/04/2010	28.47	14.55	100.99	2.46	372.68	48.33	1.76
19	24/04/2010 - 03/05/2010	18.85	8.38	133.81	2.10	390.75	27.36	1.74
20	04/05/2010 - 13/05/2010	20.98	10.19	133.12	1.48	374.22	33.83	1.71
21	20/05/2010 - 29/05/2010	18.10	8.95	120.56	1.27	394.71	29.70	1.70
22	30/05/2010 - 08/06/2010	13.91	6.44	116.34	1.23	430.05	21.71	1.71
23	09/06/2010 - 18/06/2010	17.75	8.87	99.52	1.48	403.55	29.20	1.71
24	23/06/2010 - 02/07/2010	-6.96	-4.98	112.70	1.30	423.92	-17.12	1.67
25	03/07/2010 - 12/07/2010	-9.27	-6.36	113.08	1.32	440.89	-22.21	1.67
26	13/07/2010 - 22/07/2010	-9.37	-6.88	124.28	1.30	448.99	-23.85	1.68
27	23/07/2010 - 01/08/2010	-8.02	-6.37	128.75	1.35	441.48	-22.42	1.68
28	02/08/2010 - 11/08/2010	-9.06	-6.97	131.30	1.32	445.87	-24.77	1.68
29	12/08/2010 - 21/08/2010	-7.56	-6.03	131.72	1.24	436.27	-22.90	1.67
30	22/08/2010 - 31/08/2010	-10.09	-6.03	163.31	1.27	444.83	-29.32	1.68
31	01/09/2010 - 10/09/2010	-6.52	-6.04	165.33	1.09	421.65	-23.82	1.66
32	11/09/2010 - 20/09/2010	-4.75	-4.98	161.70	1.08	413.27	-20.43	1.66
33	21/09/2010 - 30/09/2010	-4.00	-4.90	186.54	1.00	406.82	-21.11	1.65
34	01/10/2010 - 10/10/2010	-3.01	-4.39	187.10	1.27	401.79	-19.45	1.66
35	11/10/2010 - 20/10/2010	1.80	-2.09	196.05	0.47	376.14	-10.94	1.64
36	21/10/2010 - 30/10/2010	3.73	-0.83	197.07	1.00	366.51	-7.61	1.66
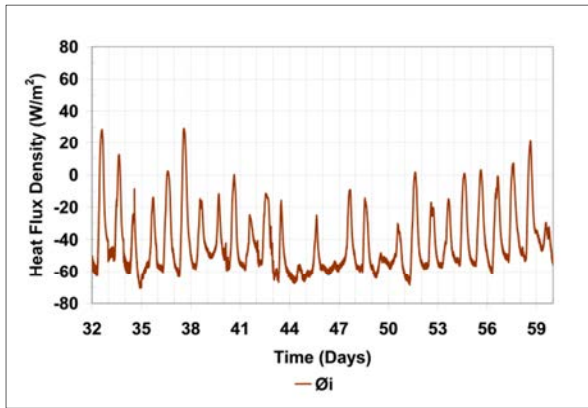
(a) Heat flux density
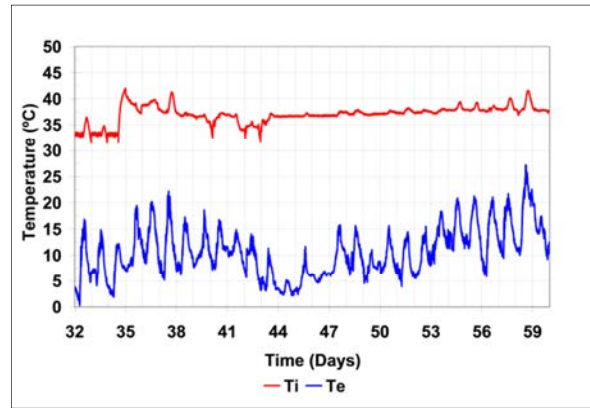
(b) Indoor and outdoor air temperatures
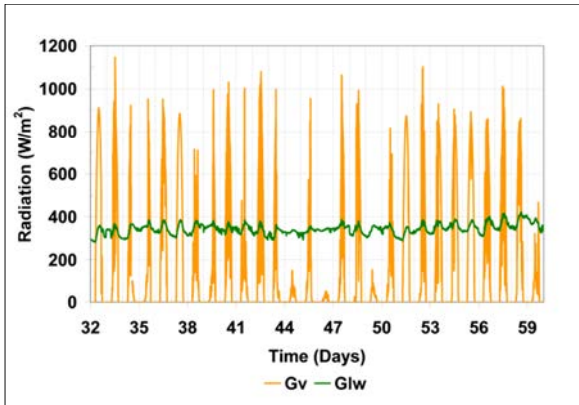
(c) Global solar and long wave vertical radiation
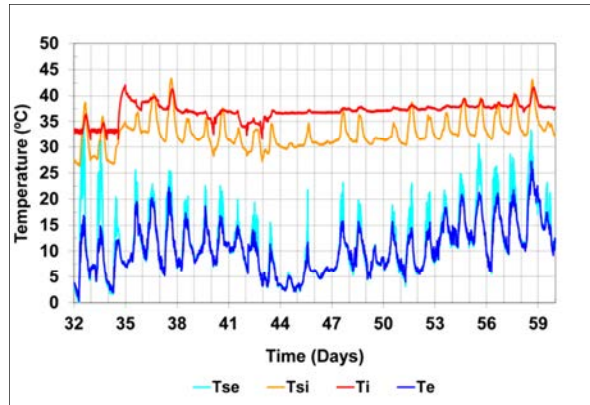
(d) Air and Surface temperatures
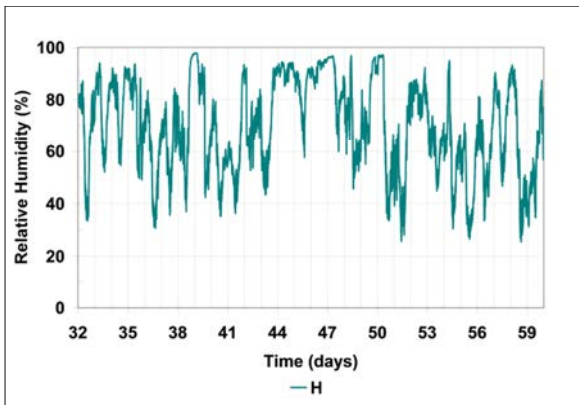
(e) Outdoor relative humidity
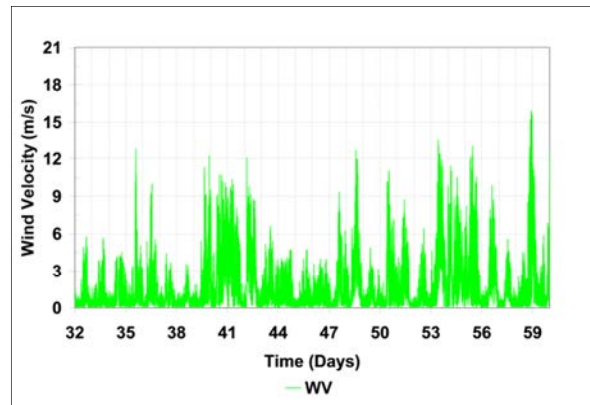
(f) Wind speed

Figure 5: Opaque wall. Data overview. February 2010.
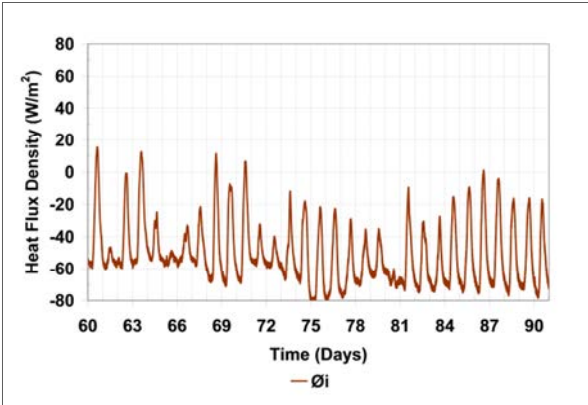
(a) Heat flux density
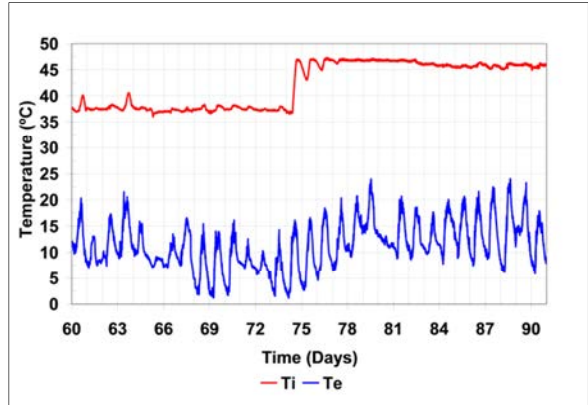
(b) Indoor and outdoor air temperatures
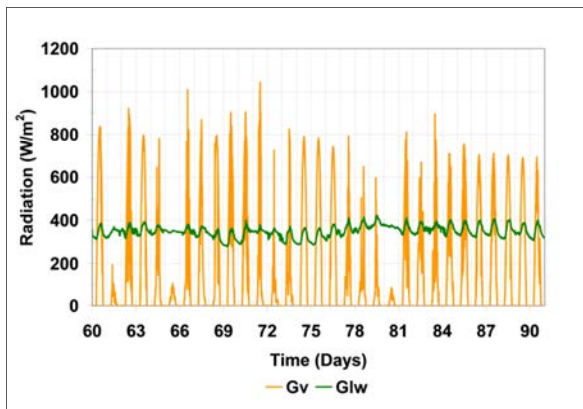
(c) Global and long wave vertical radiation
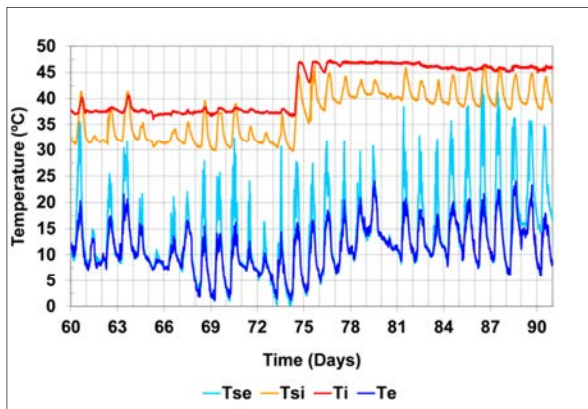
(d) Air and surface temperatures
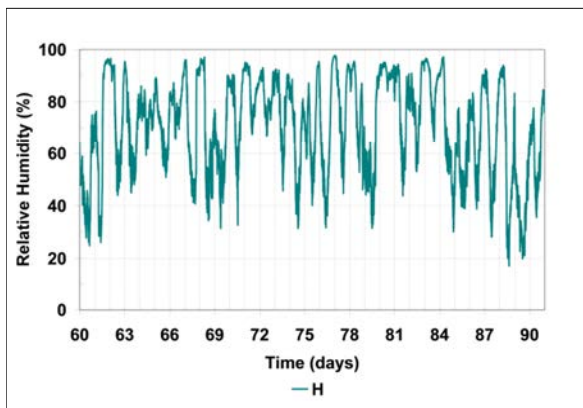
(e) Outdoor relative humidity
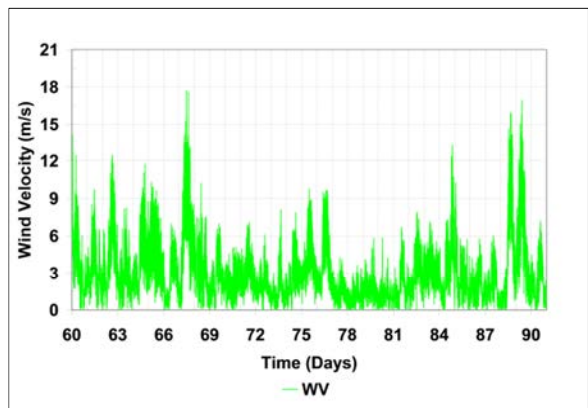
(f) Wind speed

Figure 6: Opaque wall. Data overview. March 2010.
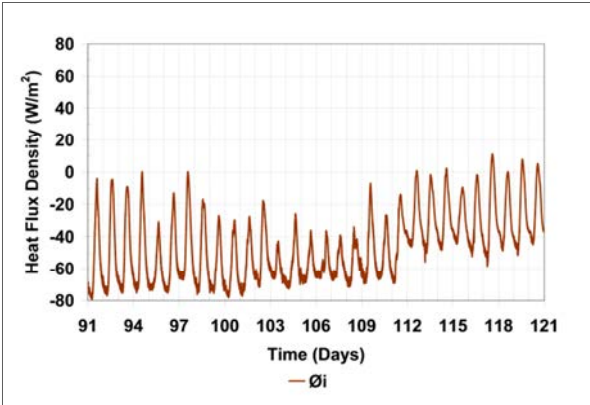
(a) Heat flux density
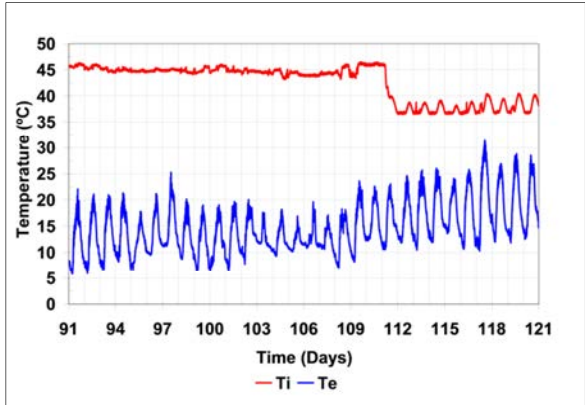
(b) Indoor and outdoor air temperatures
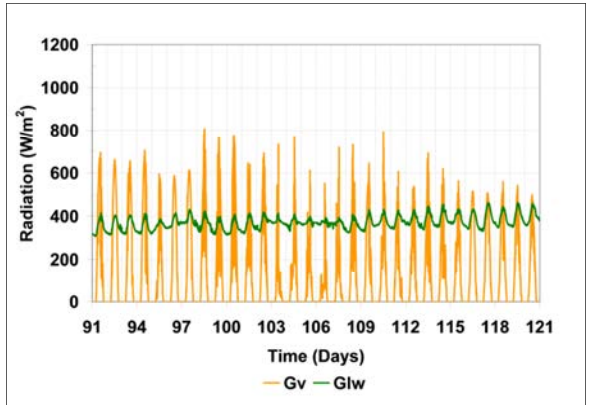
(c) Solar and long wave radiation
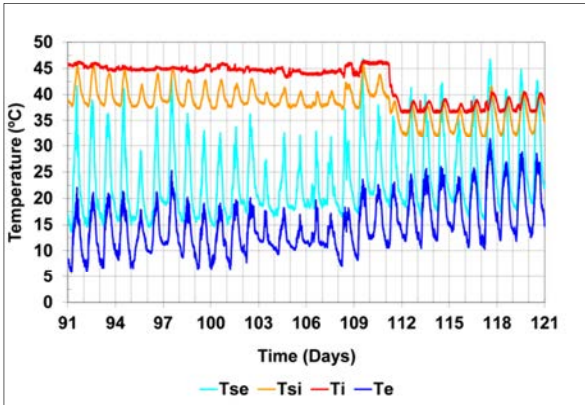
(d) Air and surface temperatures
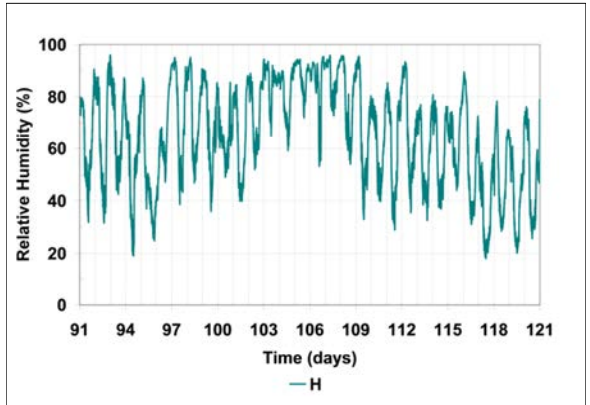
(e) Outdoor relative humidity
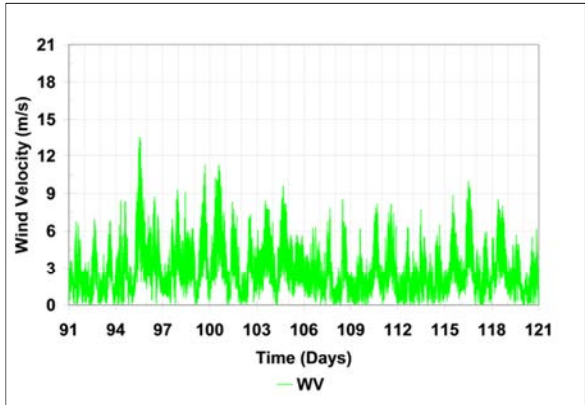
(f) Wind speed

Figure 7: Opaque wall. Data overview. April 2010.
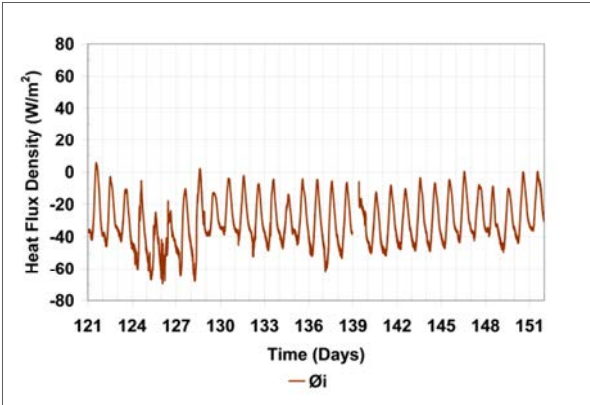
(a) Heat flux density
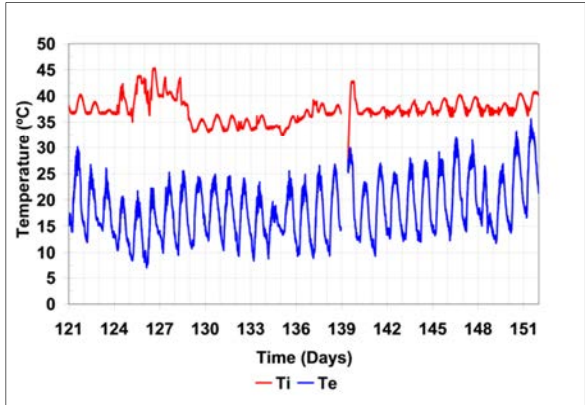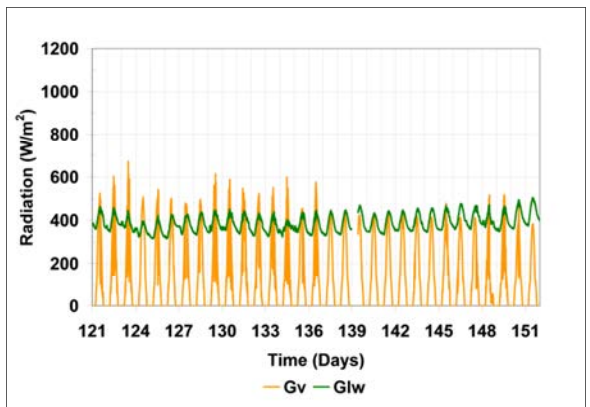
(b) Indoor and outdoor air temperatures

(c) Solar and long wave vertical radiation
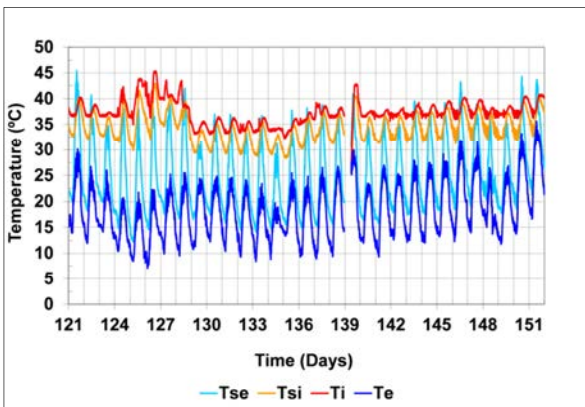
(d) Air and surface temperatures
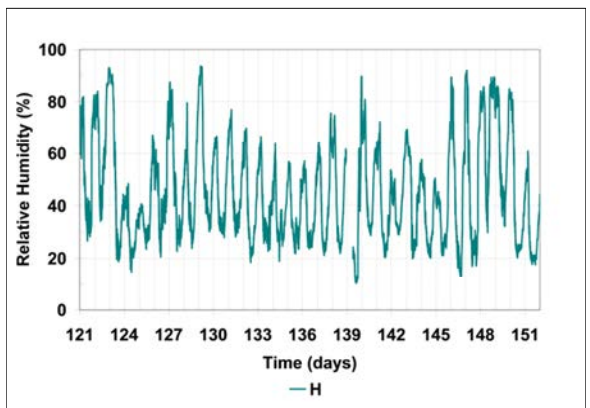
(e) Outdoor relative humidity
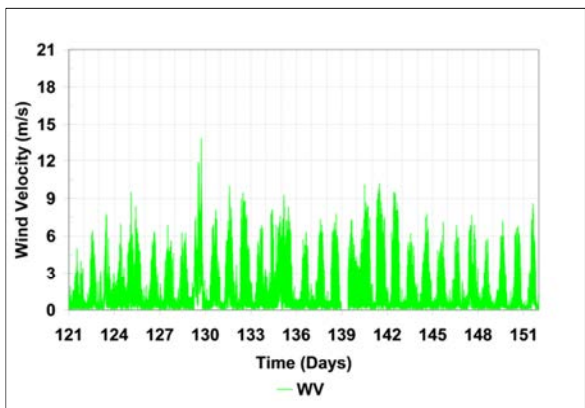
(f) wind speed

Figure 8: Opaque wall. Data overview. May 2010.
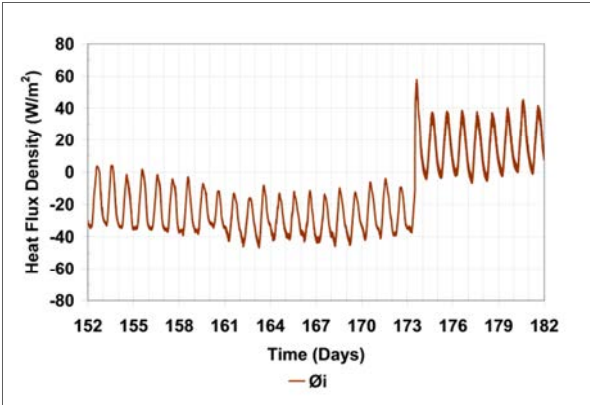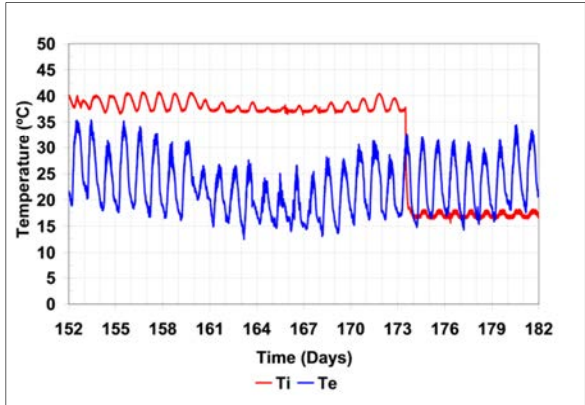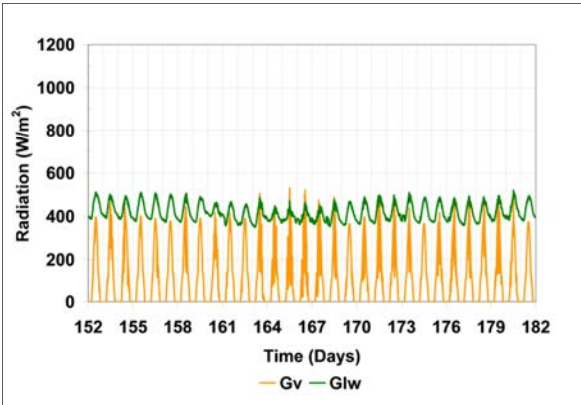
20

(a) Heat flux density

(b) Indoor and outdoor air temperatures

(c) Solar and long wave vertical radiation
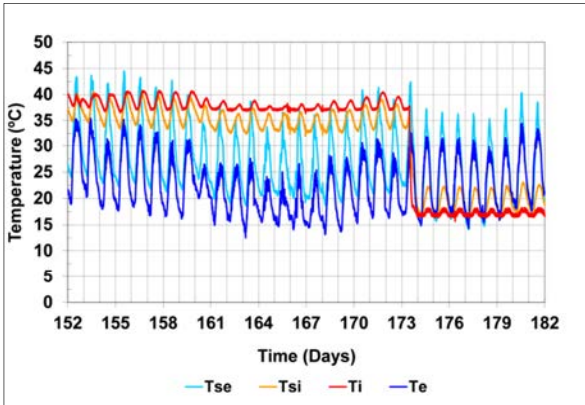
(d) Air and surface temperatures
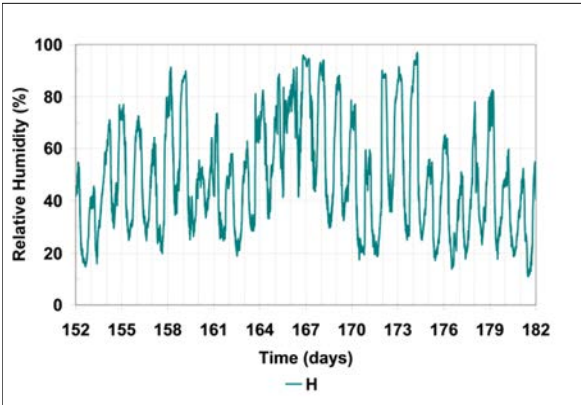
(e) Outdoor relative humidity
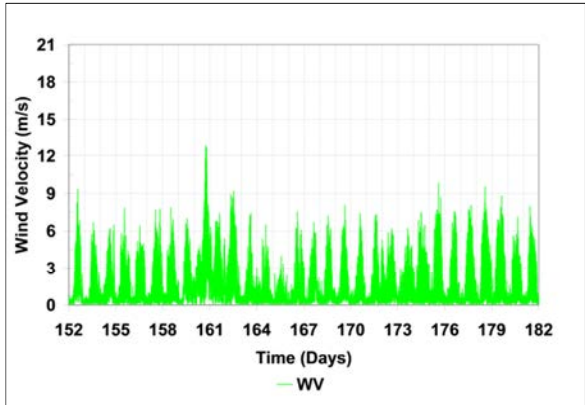
(f) Wind speed

Figure 9: Opaque wall. Data overview. June 2010.
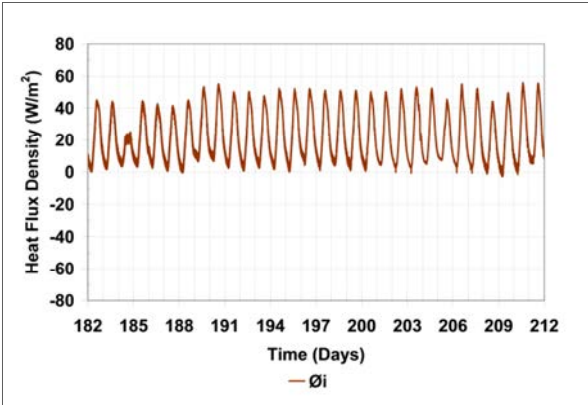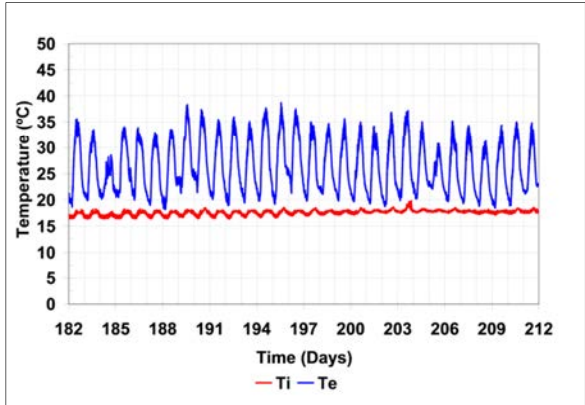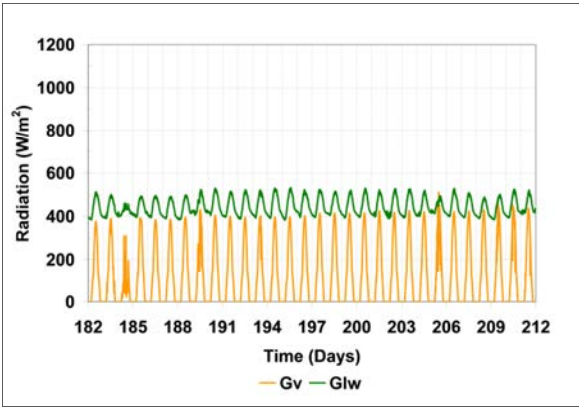
21

(a) Heat flux density

(b) Indoor and outdoor air temperatures

(c) Solar and long wave vertical radiation
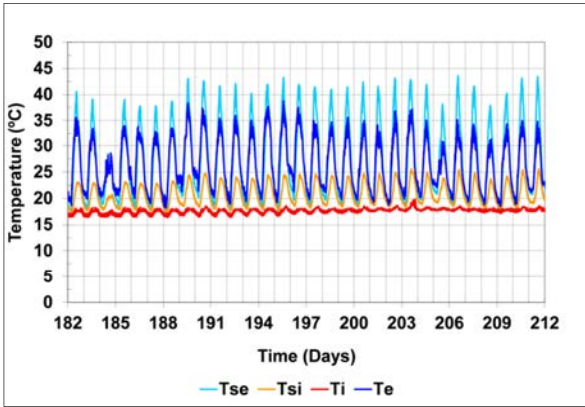
(d) Air and surface temperatures
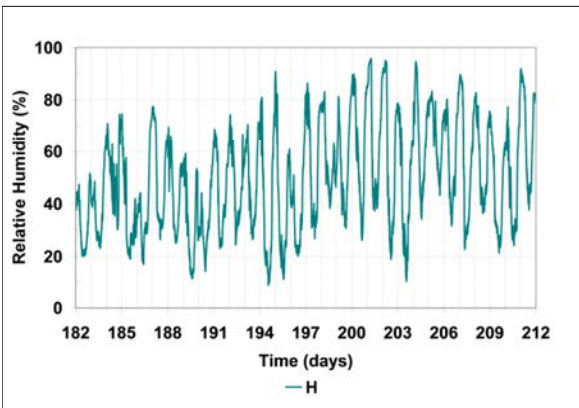
(e) Outdoor relative humidity
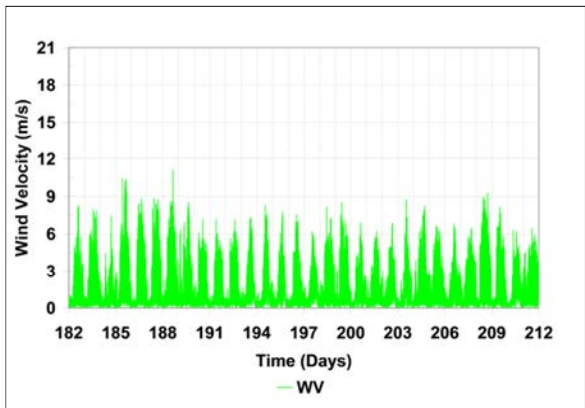
(f) Wind speed

Figure 10: Opaque wall. Data overview. July 2010.
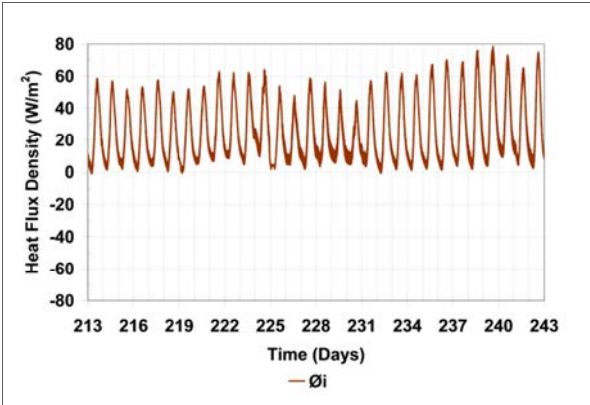
(a) Heat flux density
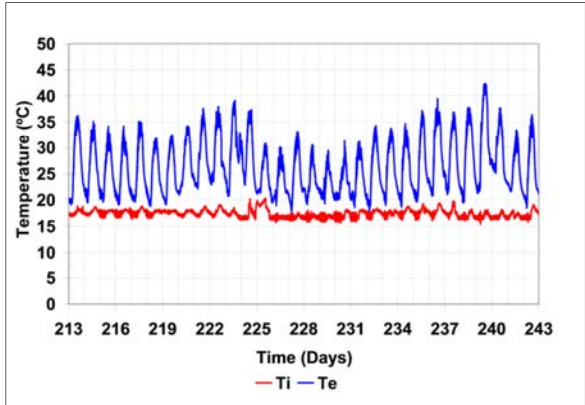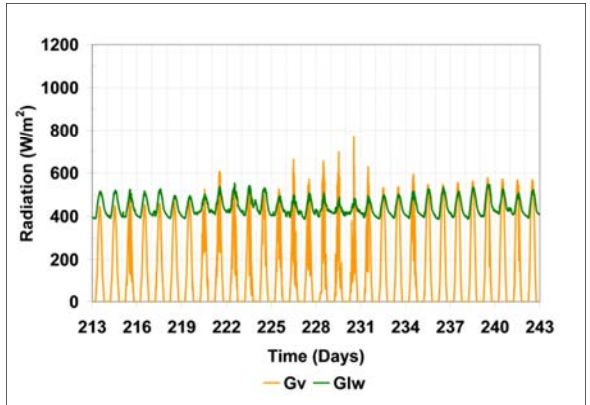
(b) Indoor and outdoor air temperatures

(c) Solar and long wave vertical radiation
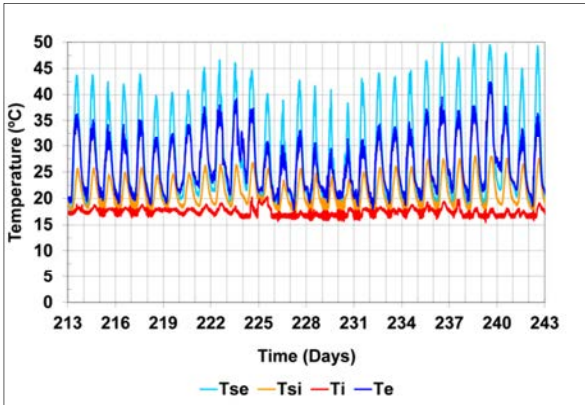
(d) Air and surface temperatures
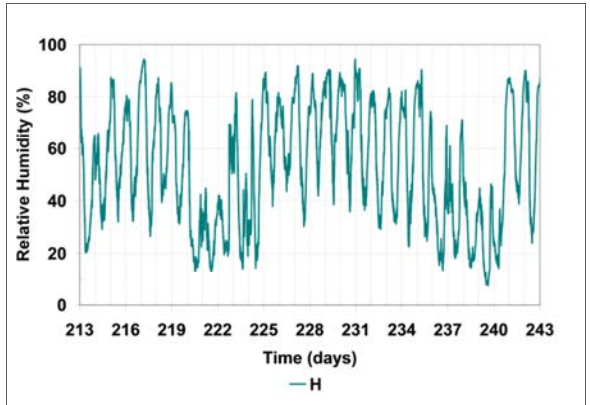
(e) Outdoor relative humidity
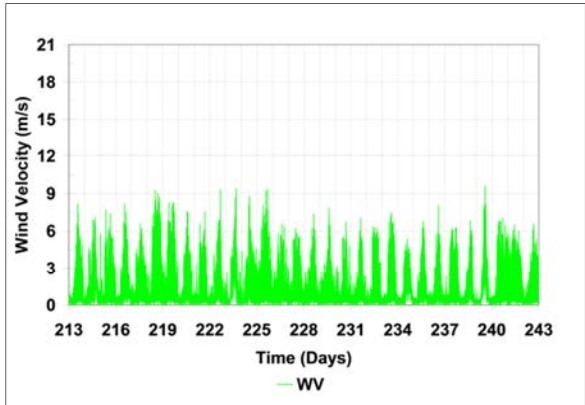
(f) Wind speed

Figure 11: Opaque wall. Data overview. August 2010.
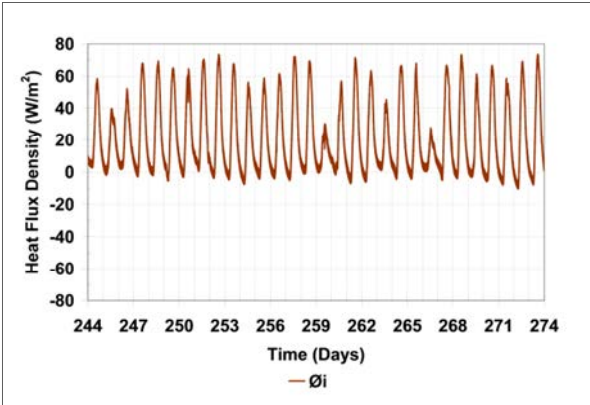
(a) Heat flux density
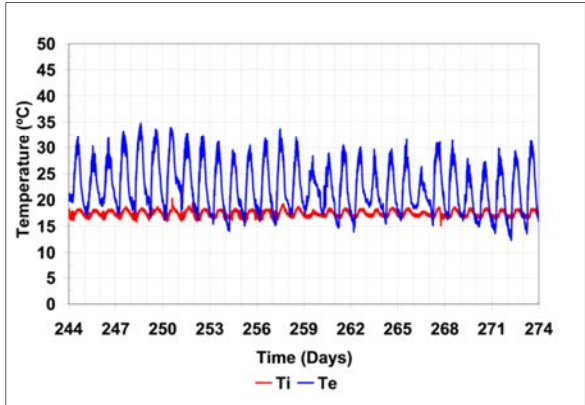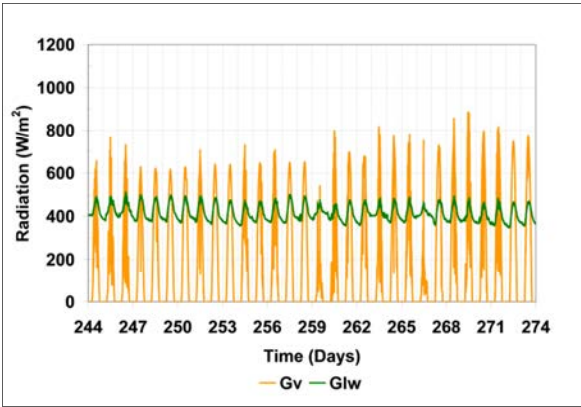
(b) Indoor and outdoor air temperatures

(c) Solar and long wave vertical radiation
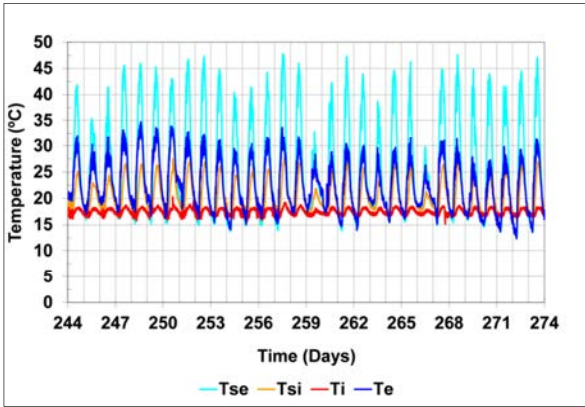
(d) Air and surface temperatures
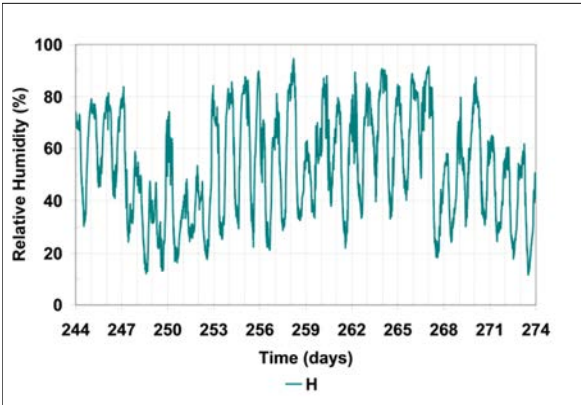
(e) Outdoor relative humidity
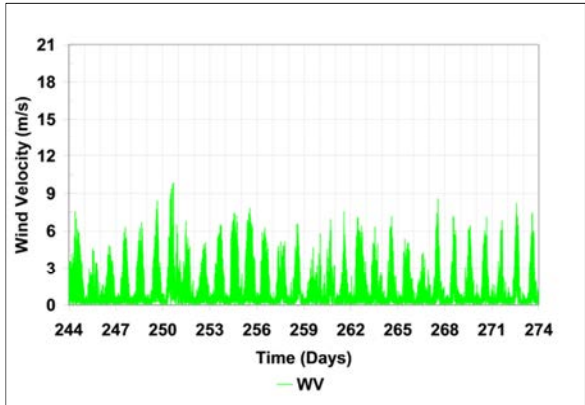
(f) Wind speed

Figure 12: Opaque wall. Data overview. September 2010.
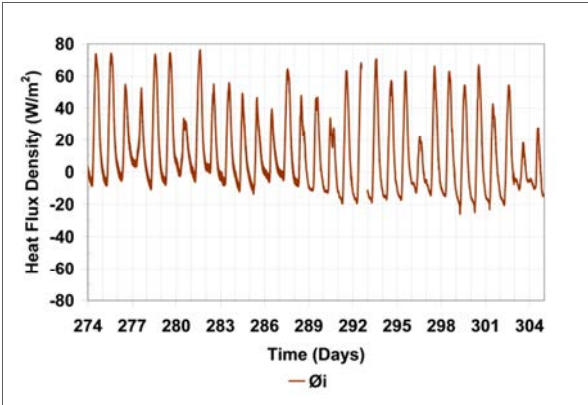
(a) Heat flux density
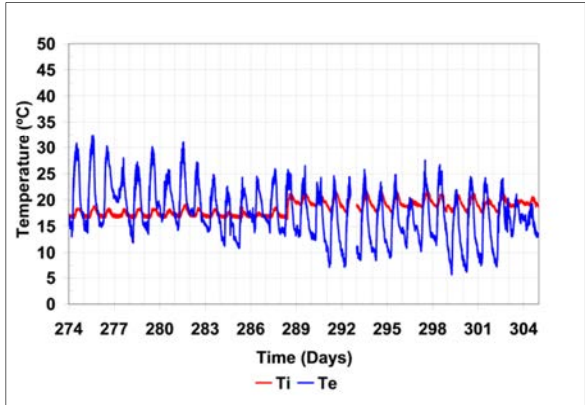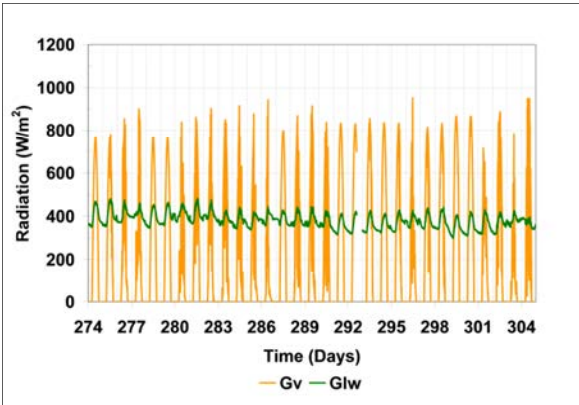
(b) Indoor and outdoor air temperatures

(c) Solar and long wave vertical radiation
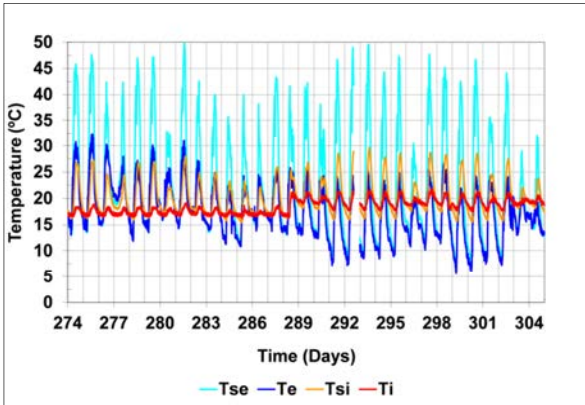
(d) Air and surface temperatures
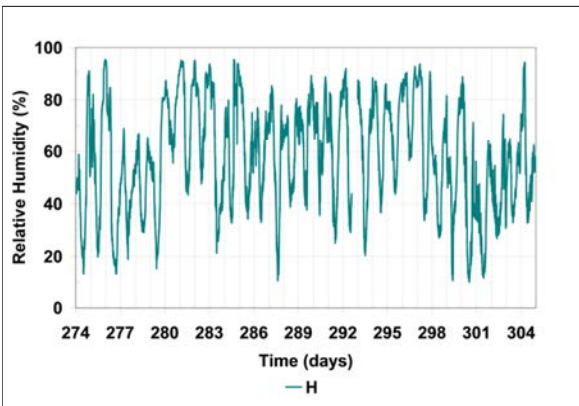
(e) Outdoor relative humidity
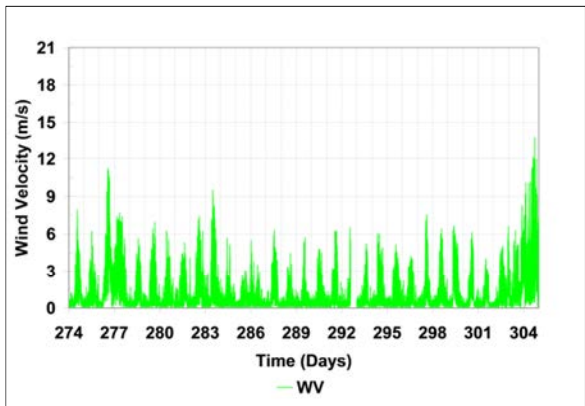
(f) Wind speed

Figure 13: Opaque wall. Data overview. October 2010.

2.6 Common exercise 1

The following requested output has been defined for this exercise:

1. U value estimate of the wall. Justifying and discussing:

    a.   The minimum subset of variables necessary for the model.

    b.   Period used for the analysis and its length.

2. Validate model by residual analysis.

3. Check consistency of results for different data sets.

4. Describe step by step the analysis and validation carried out. Try to be as clear and illustrative as possible.

2.7 Common exercise 2

The following requested output was proposed for this exercise:

1. Consider the given system as a building envelope and obtain its following parameters:

    a.   Solar heat gain.

    b.   Time constants.

    c.   Effective heat capacity.

2. Find a model describing the external surface temperature and obtain the solar absorptance of this surface.

3. Report the analysis carried out and results. This report must describe and justify step by step the analysis and validation carried out. Try to be as clear and illustrative as possible.

2.8 Summary of results of common exercises 1 and 2 – discussion of the results

Most contributions to these common exercises are exclusively considering the U value estimates. Most participants have obtained similar results for this parameter as shown in Figure 14, even using different analysis approaches and models. So even having room for improvement, at least in this simple case the results obtained for this parameter are quite good.

Very few participants gave uncertainty estimate and some of them gave a very high value for it, which is an issue that should be further improved.

In some reports results from different models were given but no one is pointed as best and no discussion is included about criteria to select the final result. In these cases all the results found in the report are included in this summary. In some cases participants apply different analysis approaches in order to compare results. In these cases all the results are also included in the summary given in Figure 14.
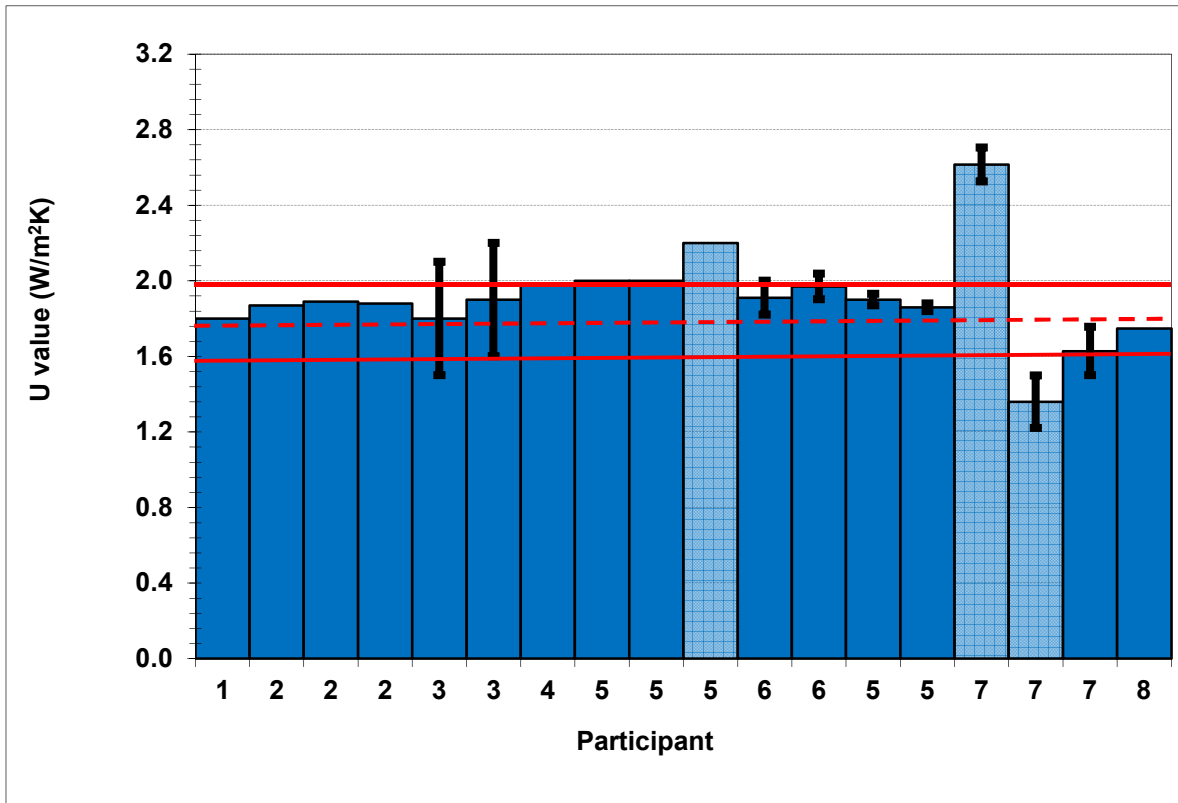
Figure 14: Summary of U value estimates. Dotted red lines indicate the theoretical U value estimated assuming standard constant surface resistances. Red line indicate ±10% of this value, taken as reference typical uncertainty derived from measurements. Marked values given by participants 5 and 7 are considered outlayers.

Other aspects requested in the common exercises such as g-value, solar heat gain, time constants, capacity, absorptance effect of data period and length etc., where not analysed by participants. However these aspects are interesting topics for further research.

Posterior work reported in Refs. 7 and 8 considered some of these issues.

Data files are available for further research and can be download from DYNASTEE web page.

27

3. Round Robin Test Box

3.1 Overall aim of the round robin experiment

The global objective of the Round Robin Experiment was to design and perform a well controlled comparative experiment on testing and data analysis. As a follow-up on the common exercise on the opaque wall (see chapter 2) and before moving to more complex (real) buildings, it was decided to perform a round robin experiment on a test box, a scale model of a simplified building. The test box has been shipped to different partners (different climatic conditions) with the aim to perform a full scale measurement of the test box under real climatic conditions. In a second step, the obtained dynamic data was distributed to different institutes who tried to characterize the test box based on the provided experimental data. In this way it was not a pure round robin experiment (inter-laboratory comparison performed independently by different institutes), but can be seen as a combination of a round robin test and data analysis comparison, the latter, somewhat comparable with e.g. the BESTEST for numerical modelling.

The overall aim of the experiment was hence to determine the state-of-the-art on experimental design, full scale measurements and dynamic data analysis: where are we as experts at the moment? Furthermore, the well-controlled experiment allows:

- investigating the capabilities, limitations and reliability of full scale testing

- investigating the capabilities, limitations and reliability of dynamic data analysis

- investigating the influence of variables such as climatic conditions on characterisation methods

and at the same time, the experiment should

- provide a well-documented data set for validation of data analysis methods.

As such, the round robin experiment (as later on other case studies in the Annex-project) linked the different subtasks of Annex 58.

The experiment itself consisted of three main parts:

a. The design of the test box experiment

A first common exercise supported the development of the test box. The needs for the measurement set-up and the errors due to non-measured phenomena or sensor accuracy have been studied. In this exercise, the test box was a virtual box, only existing on paper. But, studying the virtual box for specific climates gave insight in its energetic behaviour and helped to design the set-up and experiment.

Hence, this part strongly related to subtask 2 on optimizing full scale dynamic testing, by investigating how numerical models can be used for the design of good full scale testing. Starting from some restraints of the experimental set-up and the aimed characterization, simulations have been used to optimize the set-up by studying the influence of the experimental conditions, the positioning of sensors, the frequency and duration of the measurements,…

The objectives of this part and the specific prescriptions and outcomes can be found in appendix 3.1 of this report.

b. The full scale dynamic testing

Based on the outcome of part a), a test box has been constructed by KU Leuven, Belgium. The exact composition and fabric properties of the box were unknown to all other participants of the Annex 58-project. After construction the box has been shipped to different partners, where it was tested under real climatic conditions. Winter 2012-2013 the test box has been tested at the premises of the Belgian Building Research Institute in Limelette, Belgium. Afterwards the box has been shipped to Spain, where it was measured under summer conditions in Almeria. Thereafter the box went to Bilbao and Prague.

Each of the partners participating in the full scale dynamic testing had to decide on the specific measurement equipment (temperature, humidity, ventilation, infiltration, number and type of sensors, installation of the sensors, frequency of measuring,…) and was responsible for the handling and documenting of the obtained data. A 'do's and don't'-document was provided to the measuring teams, giving some background info on the test box – without revealing its properties – to guarantee that no changes would be introduced when installing the measurement devices (appendix 3.2). More details on the different measurement campaigns can be found in the following chapters 4, 5, 6 and 7 of this report.

c. The dynamic data analysis

The data obtained in step b) was the starting point of several common exercises within subtask 3 of Annex 58. The obtained data was sent around to different institutes for data analysis. Aim was to try to characterize the test box based on the received documented dynamic data. A cross comparison between the obtained results and a comparison with the exact composition of the box was made afterwards. Note that the exact composition of the test box (e.g. structure of the walls, roofs, floor, type of glazing) was only revealed at the end of the Annex 58-project by the institute that constructed the box.

The specific objectives, instructions and outcomes of the common exercises are described in sections 5.10 and 0 of this document.

3.2 Description and exact composition of the Test Box

Based on the numerical analysis in the first step of the round robin test experiment, a test box has been designed and constructed by KU Leuven. A schematic overview and horizontal section of the design is presented in Figure 15. The test box has a cubic form, with exterior dimensions of 120x120x120 cm³. The floor, roof and wall components of the box are all identical and have a thickness of 12cm, resulting in an inner volume of 96x96x96cm³.

One wall contains an operable wooden window with overall dimensions of 71x71 cm² and a glazed part of 52x52 cm². The double glazing (4-15-4) has a U-value of 1.1 W/m²K (EN 673, in a vertical position and with $\Delta T=15°C$) and g-value of 0.63. The air gap (15 mm) between both glass layers (4 mm) is 90% argon-filled. Solar absorptance of outer and inner glass layers are 7% and 8% respectively. The solar transmittance of the glazing system is 56%. The outdoor and indoor solar reflection coefficients are 29% and 28% respectively.

To avoid thermal bridges and local effects as much as possible, no inner structure is foreseen in the walls. To realise this, the box consists of an inner box of double layered fibre cement boards. Insulation boards are then glued to the inner box, whereupon an outer box is constructed consisting of fibre cement construction board, finished with a white coloured fibre cement cladding board. The inner walls of the box are painted in a mat black paint. After finishing the box, a steel structure is provided around the box, so that the box remains free from the thermal influence of the ground. This simplifies characterisation assumptions as the

box can be considered as floating in free air. In Figure 16 the subsequent construction steps are shown.
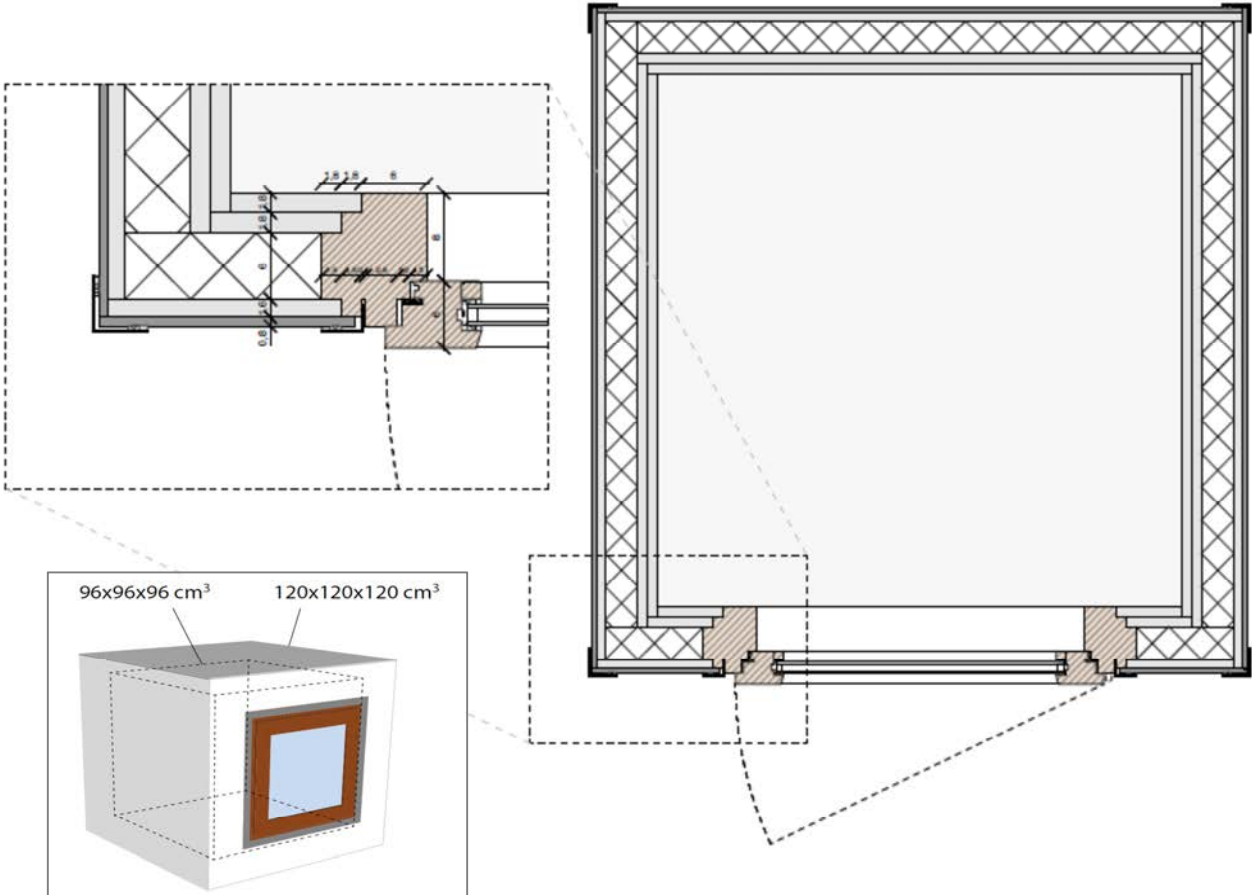
Figure 15: Schematic view and horizontal section of the design of the round robin test box.
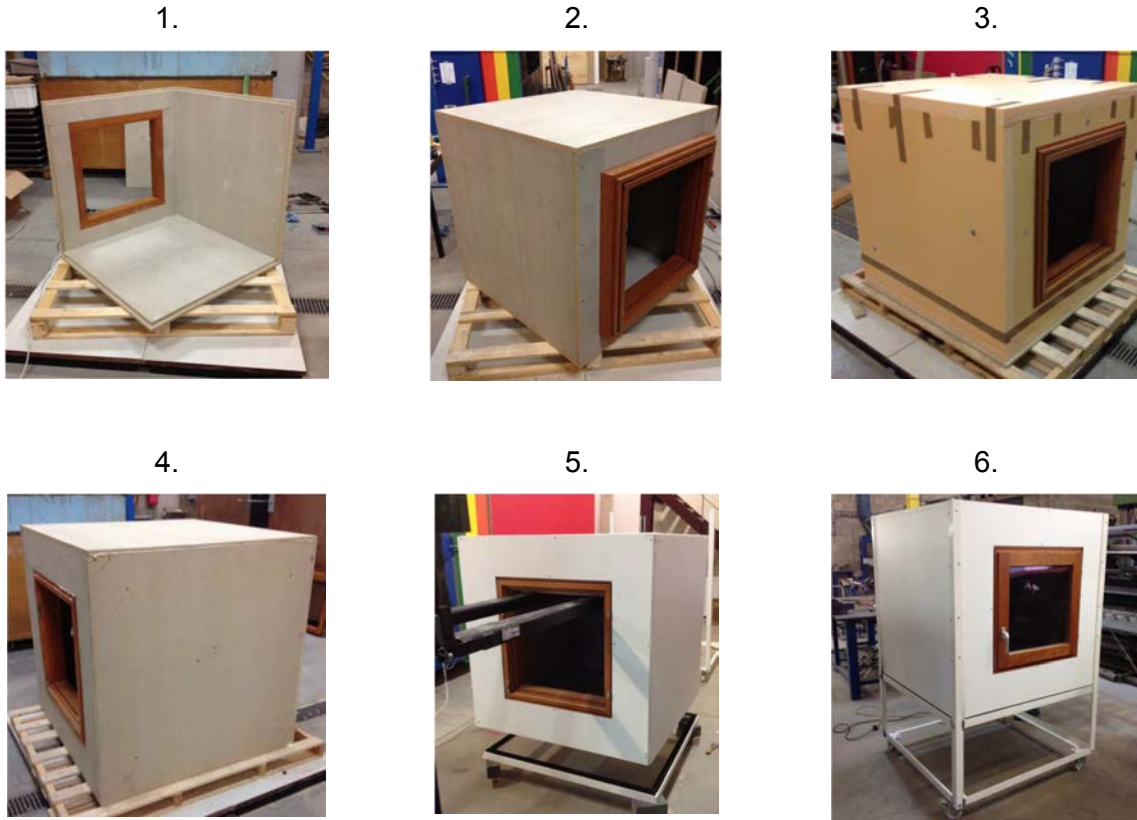
Figure 16: Subsequent steps in the construction of the round robin test box: 1. Inner box of double layered fibre cement boards, 2. Operable window in one façade, 3. Insulation glued to the inner box, 4. Outer box of fibre cement board, 5. Fibre cement finishing layer, 6. Steel structure supporting the box.

Table 4 gives the material properties of the different layers of the box, as provided by manufacturers. Based on these values the one-dimensional thermal resistance of the test box fabric is calculated as 1.927 m²K/W. Taking into account the surface resistances (corresponding ISO 6946:2007) this corresponds to a U-value of 0.476 W/(m².K). Note that this value does not take into account the possible presence of a thin air and/or glue layer between the different material layers. The presence of such a layer might slightly increase the actual thermal resistance of the fabric, and hence decrease the obtained U-value. To get an idea of the impact, let us assume a thin air layer of 2.0 mm at the interface between two layers. Knowing that the fabric contains four interfaces, the extra resistance could theoretically count up to 0.32 m²K/W, raising the overall resistance to 2.25 m²K/W. It must be taken into accounts that this increase might it be a bit different for the different opaque walls.

Table 4: material properties of the different layers of the box as provided by the manufacturer.

	thermal cond. [W/(mK)]	density [kg/m³]	heat capacity [J/(kg/K)]
Fibre cement boards (inner box)	0.35	1250	1470
XPS insulation	0.034	25	1450
Fibre cement board (outer box)	0.35	1250	1470
Fibre cement cladding	0.60	1925	1018
Window frame (wood)	0.17	700	2070

3.3 Determination of the target value of the overall HLC and solar aperture of the box

In the common exercises on the round robin test box, participants were asked to characterize the thermal characteristics and performance of the box based on the data of the full scale experiments performed at the different locations. Details of this exercises can be found in section 3. Apart from a more dynamic characterization (dynamic response, effective capacitance,…), also the basic overall heat loss coefficient (HLC) and solar aperture (g.A) were one of the requirements. As a kind of reference, the current section determines the target value for this overall HLC based on, on the one hand, numerical simulations, and on the other hand on dedicated experiments under well-controlled conditions. The obtained values will be compared with the results obtained by the participants in section 5.10.

3.3.1 Theoretical value for the HLC based on numerical simulation

To determine the theoretical goal value of the overall heat loss coefficient of the round robin test box, a 3D-simulation has been performed with TRISCO, a 3D steady state heat transfer model for the thermal analysis of building components (www.physibel.be). By imposing different indoor and outdoor temperatures the overall heat loss through the fabric of the box can be calculated. Figure 17 presents a vertical and horizontal section through the box, showing the isotherms when an indoor temperature of 25°C and outdoor temperature of 0°C is imposed. On the contour plots the edge effects and thermal bridging at the window façade junction is clearly visible.
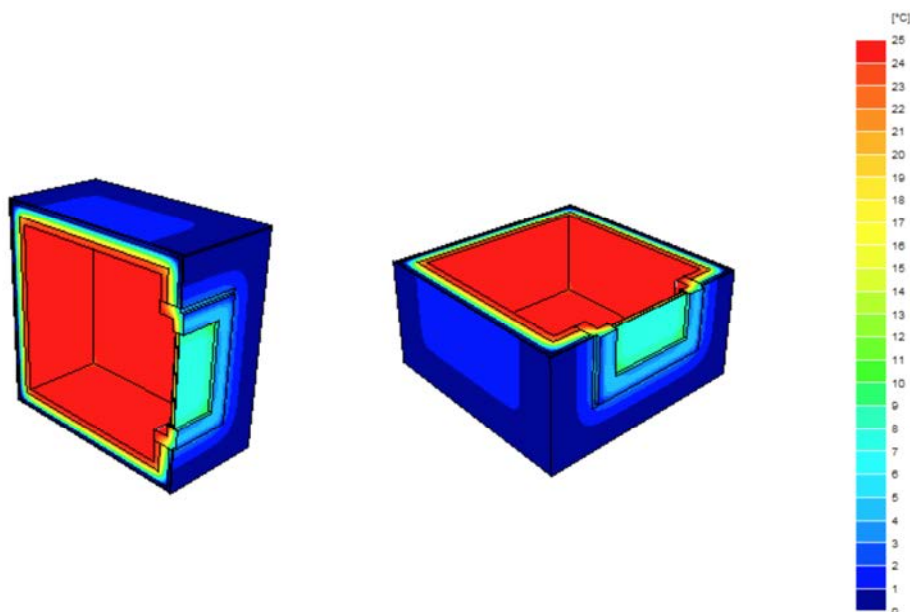
Figure 17: Temperature plots as obtained in the numerical simulation of the thermal performance of the round robin box. The edge effects and thermal bridging at the window perimeter are clearly visible.

Taking standard surface thermal resistances (R_{si}=0.13; R_{se}=0.04 m²K/W) into account (ISO 6946:2007) a simulated overall heat loss coefficient of 4.08 W/K is obtained.

A detailed analysis of the measured surface temperatures and heat fluxes during a co-heating campaign at the test site of BBRI (see chapter 4), however, revealed that the thermal

resistances based on the on-site measured data were slightly higher than the theoretical calculated ones (Deconinck and Roels, 2014). Analysing the on-site measured data with the averaging method (ISO 9869), linear regression method or state space models, all revealed a thermal resistance of the fabric between 2.0 and 2.3 m²K/W. As an example, Figure 19 compares the theoretical reference value with the results obtained for the different walls with a first order state space model. The used state space model is depicted in Figure 18 and uses the measured surface temperatures of the wall as inputs and has the internal heat flux through the wall as output. Note that the observation in Figure 19 is in line with the remark mentioned above that the glue and/or air layer between the different layers is not taken into account in the theoretical reference R-value of the fabric components and that a higher thermal resistance can be expected in reality.

Additionally, it must be kept in mind that the thermal conductivity of the material properties as listed in Table 4, are no constant values, but will vary with temperature. Hence, the determined overall heat loss coefficient will anyway be boundary condition dependent.
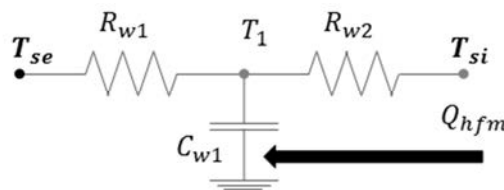
Figure 18: First order state space model with T_{se} the external surface temperature, T_{si} the internal surface temperature, T_1 the state temperature, R_{w1} and R_{w2} the model resistances , C_{w1} the model capacitance and Q_{hfm} the internal heat flux through the wall. The total thermal resistance of the wall equals the sum of model resistances R_{w1} and R_{w2}.
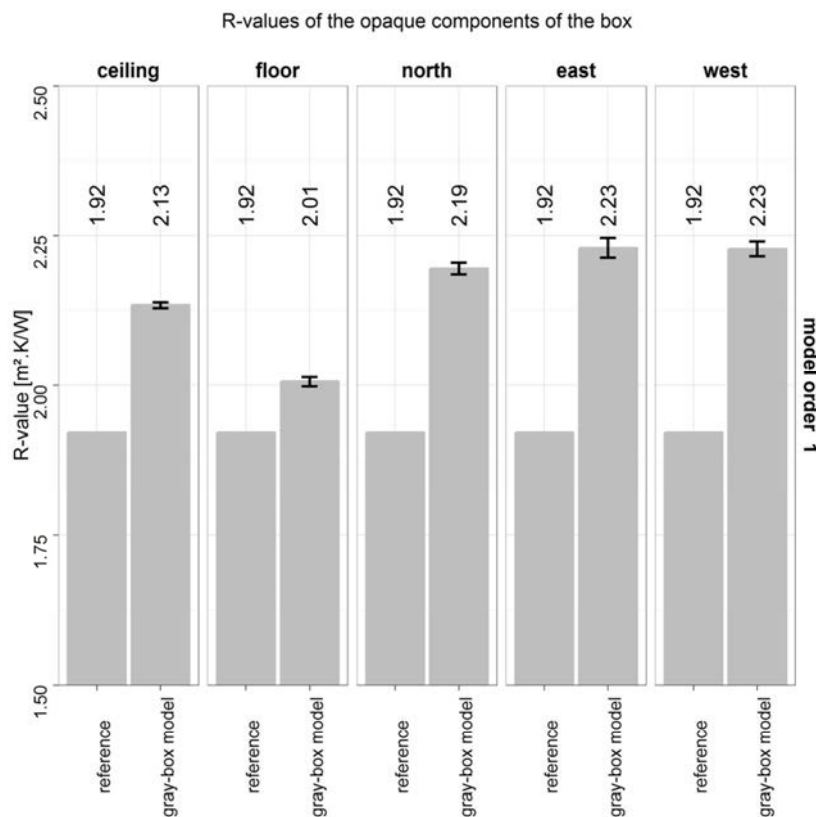
Figure 19: Comparing the theoretical thermal resistance of the opaque elements with the values obtained with a first order state space model applied to the measurement data of the first measuring campaign at BBRI.

Taking into account a thermal resistance for the opaque elements of 2.22 m²K/W (instead of the theoretical value of 1.927 m²K/W) results in a calculated overall heat loss coefficient of 3.75 W/K.

Apart from the uncertainty on the actual thermal resistance of the individual components of the round robin fabric, also the local surface heat transfer coefficients might introduce an uncertainty on the obtained results. At the outside, for instance, low wind speeds may reduce the transfer coefficients compared to the standard value, while higher wind speeds will have the opposite effect. (Hens, 2012) proposes the following dependency for the convective part of the heat transfer coefficient:

$$v < 5 \text{ m/s} \qquad h_c = 5.6 + 3.9*v \qquad\qquad (7)$$

$$v > 5 \text{ m/s} \qquad h_c = 7.2*v^{0.78} \qquad\qquad (8)$$

with v the wind speed measured at the closest weather station. Taking into account the radiative part, this results in outside surface coefficients, ranging between 10 and 30 W/(m²K).

Also at the inside of the box, buoyancy effects and indoor surface temperatures may result in a deviation from the standard value.

To account for both phenomena, the surface transfer coefficients have been varied as parameter in the TRISCO-simulations. It was found that the surface coefficient introduces an additional uncertainty of up to 10% for the obtained heat loss coefficient. Figure 20 summarises the effect of both uncertainty on the fabric resistance as well as uncertainty on the surface transfer coefficients.

Figure 20 give estimated ranges of variations of the HLC depending on generic variations of surface heat transfer coefficients, etc. Section 0 in chapter 5 analyses this variation of the same parameter for the actual measurements of the climatic boundary conditions given in the particular tests carried out. The aim of this analysis is to narrow the intervals of expected values given Figure 20, according the actual measurements in the data series used for the common exercises.

Figure 20: Effect on the calculated overall heat loss coefficient of the round robin box of both uncertainty on the fabric resistance as well as on the surface heat transfer coefficient.

3.3.2 Target value for the solar aperture of the box

Apart from the HLC, the determination of the solar aperture of the box was one of the requested outcomes in most of the common exercises on the box. In reality the solar aperture will be a kind of aggregated value taking into account solar gains both through window and opaque elements. In most cases one can assume, though, that the window will be the most important fabric element with respect to solar gains. Therefore, a rough estimate and target value can be determined based on the g-value of the window. For the current glass, the g-value is 0.63. Taking into account a correction for clarity of the window (0.95) and the current glass surface of 0.2704 m² results in a solar aperture of 0.162 m².

As said, this value is only a rough estimate as it does not take into account shading (nor of the window frame, nor of the environment), assumes a constant g-value mainly corresponding to perpendicular incidence and does not cover solar gains through the opaque elements.

Further analysis of the target g value taking into account the actual measurements of climatic boundary conditions, and transmission through the opaque walls, is reported in section 0 in chapter 5.

Appendix 3.1: Design of test box experiment

Reliable Building Energy Performance Characterisation
Based on Full Scale Dynamic Measurements

ROUND ROBIN EXPERIMENT

COMMON EXERCISE 1 – DESIGN OF THE TEST BOX EXPERIMENT
INSTRUCTION DOCUMENT
STAF ROELS / HANS BLOEM / DIRK SAELENS, NOVEMBER 2011

COMMON EXERCISE 1: DESIGN OF TEST BOX EXPERIMENT
– INSTRUCTION DOCUMENT –
Staf Roels, Hans Bloem, Dirk Saelens - November 2011

1. General objectives of the round robin experiment

The global objective of the Round Robin Experiment is to design and perform a well controlled comparative experiment on testing and data analysis. The main idea is that a test box (a scale model of a simplified building) is shipped to different partners (different climatic conditions) with the aim to perform a full scale measurement of the test box under real climatic conditions. In a second step, the obtained dynamic data is distributed to different institutes who will try to characterize the test box based on the provided experimental data. In this way it is not a pure round robin experiment (inter-laboratory comparison performed independently by different institutes), but it is more a combination of a round robin test and data analysis comparison, somewhat comparable with e.g. the BESTEST for numerical modeling.
The aim of the experiment is first of all, at the start of Annex 58, to

-   determine the state-of-the-art on experimental design, full scale measurements and dynamic data analysis: where are we as experts at the moment?

It can be seen as a first step before moving to more complex (real) buildings. Furthermore, the well-controlled experiment allows:

-   investigating the capabilities, limitations and reliability of full scale testing
-   investigating the capabilities, limitations and reliability of dynamic data analysis
-   investigating the influence of variables such as climatic conditions on characterisation tools

and at the same time, the experiment should

-   provide a well documented data set for validation of data analysis tools.

As such, the round robin experiment (as later on other case studies in the Annex-project) links the different subtasks. The experiment itself will consist of three main parts, each performed as a separate common exercise (CE):

1.   **The design of the test box experiment (CE1)**
     This first CE will support the development of the test box (scale model of a building). The needs for the measurement set-up and the errors due to non-measured phenomena or sensor accuracy have to be studied. In this exercise, the test box is a virtual box that exists on paper only. But, studying the virtual box for specific climates will give insight in its energetic behaviour and will help to design the set-up and experiment.

Hence, CE1 strongly relates to ST2 on optimizing full scale dynamic testing, by investigating how numerical models can be used for the design of good full scale testing. Starting from some restraints of the experimental set-up and the aimed characterization, simulations will be used to optimize the set-up by studying the influence of the experimental conditions, the positioning of sensors, the frequency and duration of the measurements,…

The objectives of CE1 and the specific prescriptions can be found in this instruction document.

2. **The full scale dynamic testing (CE2)**
   Based on the outcome of CE1, a test box will be constructed by one of the institutes. After construction the box will be shipped to different partners, where it will be tested under real climatic conditions. Each of the partners participating in CE2 has to decide on the specific measurement equipment (temperature, humidity, ventilation, infiltration, number and type of sensors, installation of the sensors, frequency of measuring,…) and is responsible for the handling and documenting of the obtained data (one of the topics within ST2.2).
   The specific objectives and instructions will be prescribed in a specific instruction document of CE2.

3. **The dynamic data analysis (CE3)**
   The data obtained in CE2 will be sent around to different institutes for data analysis. Aim is to try to characterize the test box based on the received documented dynamic data. A cross comparison between the obtained results and a comparison with the exact composition of the box is made afterwards. Note that the exact composition of the test box (e.g. structure of the walls, roofs, floor, type of glazing) is only revealed at this point by the institute that constructed the box.
   This CE strongly relates to ST3 on dynamic data analysis and performance characterization. The specific prescription for CE3 will be provided in a separated instruction document.

2. Objectives of CE 1: Design of test box experiment

First of all it has to be clarified that the aim of this common exercise is not to design the test box itself (so e.g. no construction drawings are asked for), but that **the aim is to support the design of the experimental set-up** to characterise the energy performance and dynamic energy processes of the test box. Hence the virtual box described in this document has to be considered as a scale model of a building that you receive at your institute, requested to characterise the energy performance of it for your climatic conditions.

This means that the overall geometry is assumed to be known (in reality this can be measured when you receive the box and is for this exercise provided in section 3 of this document), but that – keeping in mind the aimed characterisation – you have to decide on the possible measurement steps, the measurement equipment (type and number of sensors, positioning), on the frequency of data acquisition and you have to investigate the expected accuracy and reliability of the results (possible causes of errors, uncertainties,..).

The tool you want to use to design the experiment, is completely free. It can range from a simple hand calculation method to advanced dynamic numerical simulations with BES-models. To reduce the step to participate in CE1, the exercise consist of three phases: a base case, which has to be seen as a more fictitious case and allows applying both simple calculation tools as well as advanced BES-models, a more realistic base case and an extended case increasing the complexity of the problem statement. The tool used, the applied boundary conditions and the issues investigated have to be described in a short document (see section 6: requested output) and each participant of the CE will have the opportunity to present his approach at the next working meeting in Bilbao.

The main aims of Common Exercise 1 are hence to introduce design methods for dynamic experiments, and to explore approaches to evaluate (and increase?) the expected reliability when designing experiments. The choice of methods is free for both aspects, and CE 1 generally targets an overview of different methods applied to design test experiments (onset for state of the art on experimental design) and a comparison of their outcomes. At the same time the results of this common exercise is important information for the participants of CE2, who will perform the full scale dynamic testing of the test box at their institute.

3. Description of the virtual box

3.1. Overall geometry

As the test box later on has to be shipped to different partners and a simple well-controlled experiment is aimed at, some constraints such as geometry, overall dimensions,… of the box are put forward that have to be taken into account.

The test box is a cubic box, with overall dimension 120x120x120 cm³. Floor, roof and three of the four walls are opaque, one wall contains a window with opening frame. The thickness of all façade elements is 12 cm, creating an inner volume of approximately 96x96x96 cm³. A support with a height of 50 cm is provided to put the test box on, so that the box remains free from the ground during the experiments. So the box can be considered free in space (50 cm from the ground) to allow air flowing freely around the box. Details of the overall geometry with the exact dimensions can be found in Figure 1.
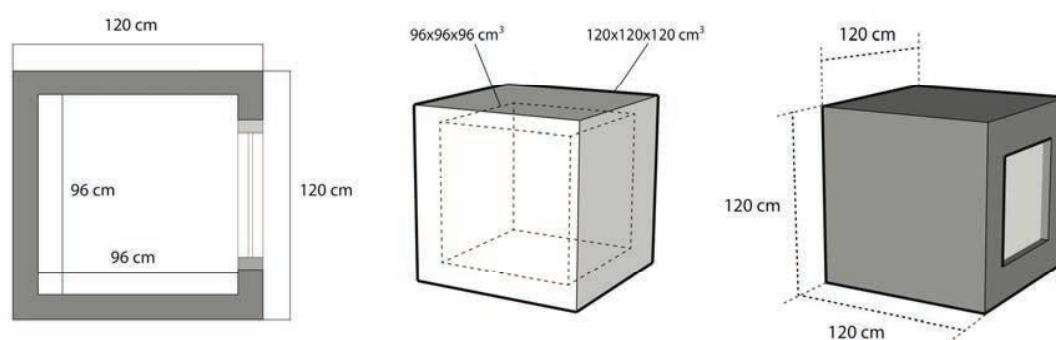
Figure 1. Overview of the test box, with overall dimensions.

3.2. Base case 1: Closed box – no window

In a first step (base case 1) floor, roof and all four walls are identical and opaque - so no window is present. Apart from the geometrical thermal bridges (outer corners), no structural thermal bridges are present. So it may be assumed that no other material than the façade material is used at the junctions of the façade elements, neither within one of the elements and that all elements consist of the same materials. This means that in the model used to design the experiment, each façade element (and further simplified eventually all façade elements together) can be represented by a resistance/capacity model. Furthermore the test box itself has no heating or cooling system (note that a heating or cooling system can of course be simulated as measuring element to characterise the box).

Two additional parameters are incorporated. The first one is the <u>number of layers</u> within each façade element. In a first step it is assumed that each façade element consists of one single material layer of 12 cm thick. For the façade material two alternatives have to be evaluated: a light weight material with low capacity and a heavy weight material with high capacity. In a second step, all façade elements are again identical, but now made up of a combination of three layers. From outside to inside the composition consists of a layer of heavy weight material (3 cm), a layer of light weight material (5 cm) and again a layer of heavy weight material (4 cm). The most relevant material properties of both materials are given in Table 1.

The second parameter is the <u>ventilation of the box</u>. Two cases have to be considered: 1) the box is perfectly airtight and no ventilation is foreseen ACH=0.0, and 2) the box has a fixed (virtual) ventilation rate of 1.0 ACH.

Table 1. Relevant material properties of façade materials

	light weight material	heavy weight material
thermal conductivity λ (W/mK)	0.03	2.9
density ρ (kg/m³)	50.0	2750
heat capacity c (J/kg.K)	1450	1000
solar absorption coefficient $a_{k\,(-)}$	0.4	0.8
long wave emission coefficient e_l (-)	0.93	0.97

.

3.3. Base case 2: Test box with window

Compared to base case 1, now in one façade a window system is placed (see Figure 1). This will have its impact on the indoor temperature. The window consists of a fixed frame and glass unit. A detail of the dimensions of the window and the installation in the test box can be found in Figure 2. The relevant material properties of the window frame can be found in Table 2. For the glass unit the overall properties according to CEN can be used, resulting in an overall U-value of 1.39 W/m²K and a solar heat gain coefficient (SHGC) of 0.65. Instead of the overall values, the detailed values of tables 3 and 4 (detailed properties of the different layers and angle dependent properties) can be used.

The same parameters as in base case 1 (number of layers within each façade element and type of material as well as the ventilation rate) have to be considered, with in addition the impact of the orientation of the test box.
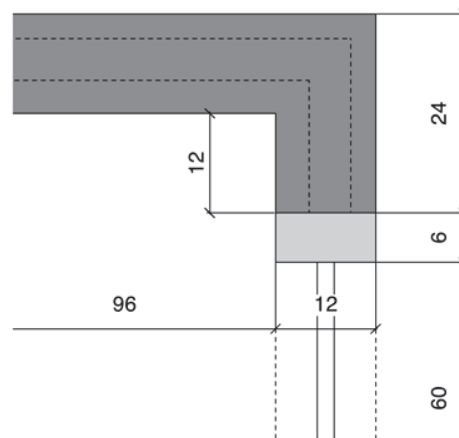
Figure 2. Fixing of the window frame in the test box. The window frame may be considered as a monolithic wood part (12x6 cm²), the glass unit as two glass panes with a cavity in between, positioned in the middle of the window frame. Note that the glass spacers are neglected.

Table 2. Relevant material properties of window frame

	window frame
thermal conductivity λ (W/mK)	0.16
density ρ (kg/m³)	650.0
heat capacity c (J/kg.K)	1880
solar absorption coefficient $a_{k\,(-)}$	0.35
long wave emission coefficient $e_{l}\,(-)$	0.9

Table 3. Composition and overall window properties and detailed properties of different layers
(surface 1 corresponds to surface facing outside, surface 2 facing inside)

layer	thickness (mm)	transmission	reflection surface 1	reflection surface 2	emission surface 1	emission surface 2	thermal conductivity (W/mK)
outside pane	3.8	0.845	0.074	0.074	0.84	0.84	1.0
cavity	12.0	(mixture of 10% air, 90% argon)					0.022
inside pane	3.8	0.644	0.241	0.197	0.065	0.84	1.0

Table 4. Angle dependent solar properties of glass unit

angle	0	10	20	30	40	50	60	70	80	90	hemispheric
total solar transmission	0.557	0.560	0.552	0.541	0.526	0.498	0.435	0.317	0.146	0.000	0.463
reflection outside	0.245	0.240	0.238	0.240	0.249	0.268	0.313	0.420	0.632	1.000	0.299
reflection inside	0.234	0.227	0.225	0.228	0.238	0.258	0.297	0.387	0.587	0.999	0.282
absorption outside	0.102	0.102	0.104	0.107	0.111	0.117	0.122	0.127	0.126	0.000	0.113
absorption inside	0.096	0.098	0.106	0.112	0.113	0.117	0.129	0.135	0.095	0.000	0.115
SHGC	0.647	0.651	0.649	0.644	0.631	0.606	0.554	0.441	0.238	0.000	0.569

3.4. Extended case 3: Unknown composition

Compared to the base case 1 and base case 2, it is assumed that each façade element now consists of different material layers parallel to the façade surface. The thickness of each layer and its material properties however are unknown. Furthermore the material layers within roof and floor can be different from the ones in the walls. Also other parameters can be varied. Hence, this extended case gives participants the possibility to elaborate further on different issues regarding reliability of the measurement set-up for the same box but with unknown composition.

4. Aimed characterisation of test box

The measuring experiment has to be designed in such a way that at least the following performances can be analysed/characterised:

- overall heat loss (W/K) of the test box

- solar gains

- dynamic behaviour of the test box

4.1. Overall heat loss (W/K) of the test box

The overall heat losses of the box can be seen as a steady state performance. For a dynamic experiment under real climatic conditions this mainly corresponds to a kind of averaged performance. Important aspects to take into account when designing the measuring experiment are e.g. duration of the experiments, averaging intervals, disturbance by dynamic responses,…. So the main aim is to investigate whether it is possible to recalculate the input parameters by simulating the dynamic behaviour of the test box and the virtually measured data of the experiment.

4.2. Solar gains

The performance of the box with respect to solar gains should be characterised. No further prescriptions are given, so the performance can be described by a kind of averaged value (typical $g_{window}.A_{window}$) or a more dynamic value based on orientation and time, and this for the specific climatic conditions of your country. Again, the main aim is to investigate whether it is possible to recalculate the input parameters by simulating the dynamic behaviour of the test box and the virtually measured data of the experiment.
Note that, solar gains can be considered for both set-ups, e.g. with and without window system.

4.3. Dynamic behaviour

Apart from the overall heat losses and the solar gains, a characterisation of the dynamic behaviour of the box is aimed at. This means response of the box to changing boundary conditions (typical daily cycli of temperature, solar gains,…), capacity of the box,….

Preferably, characterisation of the test box is done at least for base case 1 and 2 and this for the three requested performances (overall heat loss, solar gains, dynamic behaviour). Remember that the global aim of this common exercise is to support the design of the experimental set-up. So, the influence of the experimental conditions, of the positioning of the sensors, of the frequency and duration of the measurements, of ventilation and infiltration rate… on the obtained characterisation should be analysed in a way that the measurements can be optimised to obtain reliable results.

5. Typical measurement equipment that can be used

For those who are not familiar with measuring campaigns, but want to show their capabilities in simulating and designing experiments a short overview of the typical measurements that can be used is given:

- climatic boundary conditions: it may be assumed that the measuring campaign is performed at a location where a weather station is present, providing the typical weather data such as outdoor temperature and relative humidity, diffuse and direct solar radiation, wind speed and wind direction

- typical equipment in the test box: at different positions on the inner and outer surfaces of the test box measurements of surface temperature (°C) and heat fluxes (W/m²) can be performed. In addition also the air temperature within the box can be measured.

- Simplified co-heating test: it is possible to maintain a constant indoor temperature in the test box by means of a simple electric heating system (e.g. infrared bulb) and measure the power supply to maintain this temperature.

6. Requested output

As the Common Exercise is very free concerning applied methodology and tools, participants are requested to deliver a word-document describing at least the applied methodology to design the test box experiment, the proposed measurement equipment and measurement steps, the items taken into account (such as required frequency of data acquisition,…) and obtained results. The document will be named *RR_CE1_country_institute.doc (e.g. RR_CE1_Belgium_KUL.doc).*In addition all participants will have the opportunity to give a short presentation on their approach on the next working meeting in Bilbao.

Note that it is not necessary to complete the whole exercise, but results of part of the Common Exercise could already be relevant (e.g. only the Base Case 1 and 2 and not the Extended case or characterisation of only one or two of the required performances).

Results of Common Exercise 1 can be sent to staf.roels@bwk.kuleuven.be before February 24th 2012.

Appendix 3.2: Do's and don'ts Round Robin Experiment

Reliable Building Energy Performance Characterisation Based on Full Scale Dynamic Measurements

Do's and don'ts Round Robin Experiments

Dear Annex 58 participants,

This short instruction document serves to provide a set of guidelines for the institutes participating in the Round Robin Experiment. Evidently, as the goal of this exercise is to learn from each other's experience in performing experiments to characterise building energy performance, participants are encouraged to use their own particular test methodologies. Apart from the proposal to include a common part in the measurement campaign, this document gives a short explanation on what is delivered with the box and the provisions that have been made to install logging equipment and sensor connection wires.

Do's

Installing measurement equipment

Underneath the box, a platform is provided to install measurement equipment. The participants are expected to provide their own measures to protect measurement equipment against rain and wind. Recall that this protection needs to be made in such a way that the outdoor weather conditions underneath the box are not significantly disturbed (primarily the convective part of outside heat transfer coefficient).

In order to facilitate drawing sensor wires from inside to outside of the Round Robin Test Box, an opening has been made in the bottom part of the fabric. This opening is surrounded by a fixed tube. The flexible tube, delivered with the box, has dimensions that allow it to be fit through this opening. Sensor wires can then be fit through, after which the whole is sealed by e.g. spray foam inside the flexible tube and airtight taping of edges between flexible and fixed tubes.

Common part in measurement campaign:

In order to promote comparison between the measurement campaigns performed by different institutes and in different climates, the following experiments should be included:
- <u>Co-heating in outdoor climate:</u>
  elevated steady-state indoor temperature of 25°C during at least 2 weeks.
- <u>Free-floating-temperatures in outdoor climate:</u>
  no heating power during at least 2 weeks.

Don'ts

The Round Robin Test Box is precious!

The Round Robin Test Box has been built by very skilled workers and with a lot of love. Therefore, and in order to avoid the fabric of the box to change over time, it is at all times prohibited to:
- put nails/screws in and/or through the envelope,
- make holes in the envelope,
- not position it in the most evident way: on its four wheels and in upright position,
- submerge the box in water,
- ... to perform any action that would possibly compromise the box fabric condition.
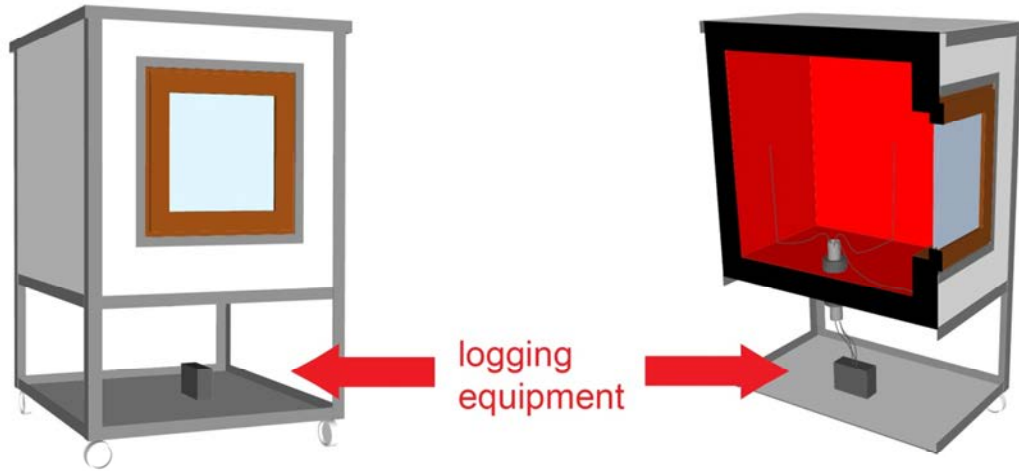
Sensors can be connected to logger through built-in opening

flexible
tube
fitted into
opening

sensor wires
+ air tightning with
e.g. spray foam

box
fabric

taping of edges
between flexible
and fixed tubes
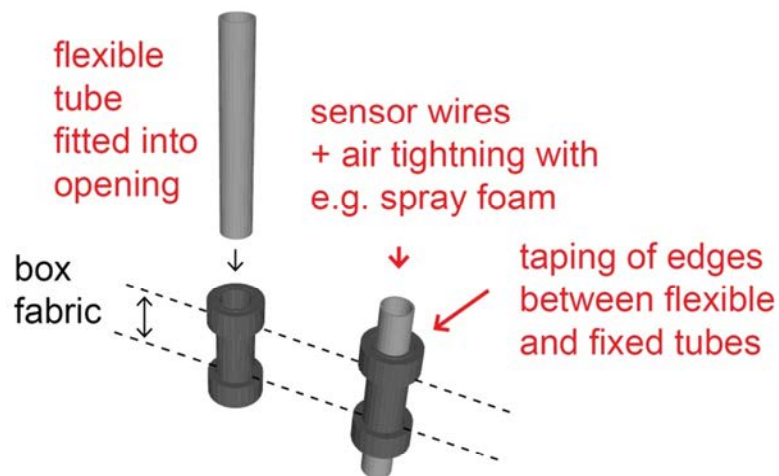
Flexible tube end is delivered with the box to fit through the opening. Sensor wires can be drawn through, after which it is tightened by e.g. spray foam inside the flexible tube and taping of edges between flexible and fixed opening tubes

4. Round Robin Tests: Outdoors Tests at BBRI

4.1 Preliminary experiment at BBRI

Before performing the 'official' experiment on the test box under real outdoor conditions (see §0), a preliminary experiment has been made in order to check the good functioning of the data acquisition system and to obtain a first estimate of the unknown thermal properties of the test box.

4.1.1 Boundary conditions

The RR Test Box was tested at the premises of BBRI (Belgian Building Research Institute) in Limelette, Belgium. It has been placed in a non-heated storage hall, in the lee of wind, sun and longwave radiation to the sky. The air temperature in the storage hall was relatively constant during the whole testing period (~15 days, in December 2012).

4.1.2 Measurement devices

Thermocouples Type T (copper-constantan) were taped at the center of each external and internal face of the test box.

Other thermocouples Type T have been also used to measure the air temperature in the non-heated storage hall on one hand and the air temperature in the center of the test box on the other hand.

4.1.3 Heating devices

The heating power is supplied by 4 electrical resistances (tubes with fins, see Figure 25) of 66.5 Ohm (760W at 225V) connected in series, yielding a total maximum power of 188W. The delivered energy is measured via a counter with a resolution of 1 Wh/pulse and the power supplied during each timestep is given as a back-calculated value.

The heating system is PID-controlled in time (cut-in/cut-out) such that the heating power is always balancing from the low and high power levels and can virtually reach any power between these limits when integration is done for a certain period of time.

4.1.4 Test sequences

The experiments consisted in performing a co-heating test with three different indoor air temperature setpoints:

- Test 1: constant indoor air temperature of 26°C during about 5 days
- Test 2: constant indoor air temperature of 21°C during about 5 days
- Test 3: constant indoor air temperature of 31°C during about 5 days

The air temperature in the storage hall was relatively constant during the whole testing period, ranging from 8°C to 10°C.
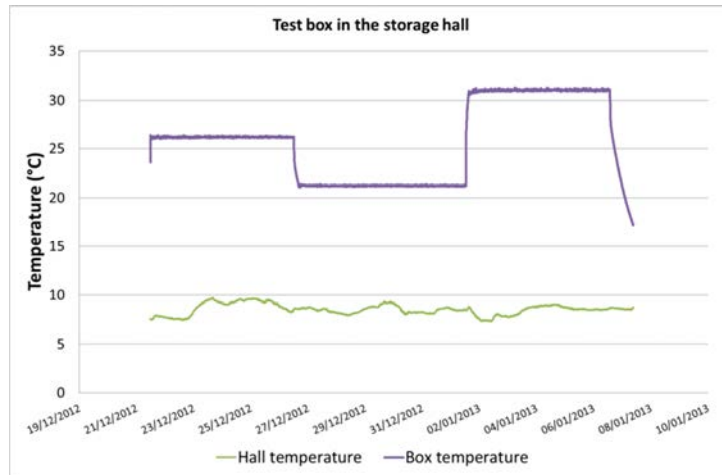
Figure 21

4.1.5 Data analysis

By applying a simple linear regression between the heating power and the temperature difference (box temperature minus hall temperature), a first estimate of the heat loss coefficient (HLC) has been obtained, using the 15 minutes centered-average data. It ranges between 3.4 and 3.5 W/K.
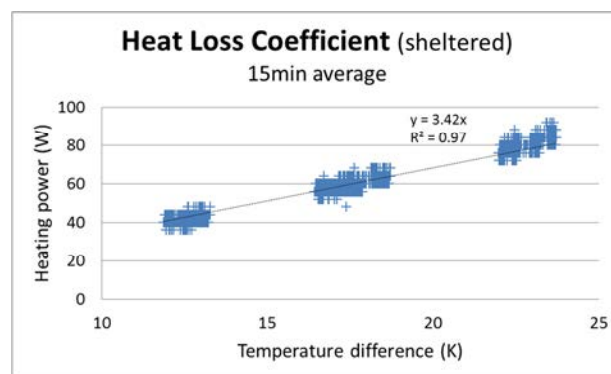
Figure 22 : linear regression for the estimation of the HLC (W/K)

4.2 Outdoors tests at BBRI

4.2.1 Boundary conditions

The RR Test Box was tested at the premises of BBRI (Belgian Building Research Institute) in Limelette, Belgium (Lat. 50°41' N, Long. 4°31' E), at 30 km from Brussels. In general, the weather climate at this test site is maritime temperate, consisting of mild winters and rather cool summers. It is usually rainy, humid and cloudy.

The experiments extended over a period of one month, starting the 25th of January 2013 and ending the 28th of February 2013.

Testing is done under real outdoor weather conditions.

48

The following outdoor climate sensors installed near the test box are included in the supplied data:

- air temperature (with a solar radiation shield and ventilated),
- vertical global solar radiation (parallel and next to the glazing),
- horizontal long wave radiation from the sky.

Additional meteorological sensors installed at the test site (200 m from the test box) are also included in the data sets:

- horizontal global solar radiation,
- horizontal diffuse solar radiation,
- vertical long wave radiation (from the South direction),
- wind velocity,
- wind direction (North 0°, East 90°),
- relative humidity.

Figure 23 : location of the test box (red triangle) and the main weather station (blue square) at the experimental station of the BBRI (Limelette).

4.2.2 Measurement devices

On each face of the test box (5 opaque faces and 1 glazing), the following sensors have been installed:

- Internal surface temperature (in the center of the face),
- External surface temperature (in the center of the face),
- Heat flux at the internal face (in the center of the face).

Figure 24: test box measured at the experimental station of the BBRI (Limelette).

The indoor air temperature has been measured along the vertical symmetry axis of the box at 1/3 and 2/3 of the total height of the box.

Table 5 gives information on all installed sensors. More detailed information on the transducers and sensors used during the experiments is given below:

- Surface temperature: type T thermocouple (copper-constantan), temperature at the cold junction measured by a Pt100 sensor. Taped in the center of the internal and external faces of the test box.

- Air temperature: type T thermocouple (copper-constantan), temperature at the cold junction measured by a Pt100 sensor. Shielded and naturally ventilated.

- Horizontal and vertical solar irradiance: pyranometer, model CM11 manufactured by Kipp and Zonen. The diffuse horizontal solar irradiance is measured by means of a shadow ring. The vertical pyranometer is fixed to the test box frame in alignment to the plane of the window.

- Horizontal and vertical long wave radiation: pyrgeometer, model PIR, manufactured by Eppley. The sensor for the measurement of the horizontal long wave radiation is placed on the back-left corner of the ceiling of the test box and is mechanically ventilated.

- Heat flux density: sensor (thermopile), model HFP01 manufactured by Hukseflux, thickness 5mm, total size diameter 80mm, calibration constant supplied with each individual sensor, accuracy +- 5%.

- Heating power: measured via an energy meter (Finder module (7E.13)) and then with a DAS composed by an ADAM module (model 4080, pulses). It has been rapidly noticed that the resolution of this electric energy meter (1 pulse per Wh consumed, fine enough for a conventional use) was rather coarse for an experiment with this test box. Unhappily, no time was left at this point to order and install a finer energy meter and it was decided to proceed with this known limitation. 15 minute averages are required in order to find continuous heating power values, where the raw data (one recording every 5 minutes) yield quite discrete heating power values. This means that the identification of parameters related to short time constants is not compromised, but their estimation uncertainty is larger. The assessment of lower frequency behavior is expected to be unaffected.

50

Table 5 : measurement transducers and sensors used during the experiments

n°	Name		Measurement	Unit	sensor type	Acquisition System
	Time		Time	DD/MM/AAAA hh:mm		
1	Tsi glazing			°C	thermocouple type T	Agilent 34970A
2	Tsi left			°C	thermocouple type T	Agilent 34970A
3	Tsi back		Internal surface temperature	°C	thermocouple type T	Agilent 34970A
4	Tsi right			°C	thermocouple type T	Agilent 34970A
5	Tsi ceiling			°C	thermocouple type T	Agilent 34970A
6	Tsi floor			°C	thermocouple type T	Agilent 34970A
7	Ti down		Indoor air temperature (1/3 height of the box)	°C	thermocouple type T	Agilent 34970A
8	Ti up		Indoor air temperature (2/3 height of the box)	°C	thermocouple type T	Agilent 34970A
9	Tse glazing			°C	thermocouple type T	Agilent 34970A
10	Tse left			°C	thermocouple type T	Agilent 34970A
11	Tse back		External surface temperature	°C	thermocouple type T	Agilent 34970A
12	Tse right			°C	thermocouple type T	Agilent 34970A
13	Tse ceiling			°C	thermocouple type T	Agilent 34970A
14	Tse floor			°C	thermocouple type T	Agilent 34970A
15	Te		Outdoor air temperature, shielded and ventilated	°C	thermocouple type T	Agilent 34970A
16	Øi glazing			W/m²	Huksflux HFP01	Agilent 34970A
17	Øi left			W/m²	Huksflux HFP01	Agilent 34970A
18	Øi back		Heat flux density at the internal face	W/m²	Huksflux HFP01	Agilent 34970A
19	Øi right			W/m²	Huksflux HFP01	Agilent 34970A
20	Øi ceiling			W/m²	Huksflux HFP01	Agilent 34970A
21	Øi floor			W/m²	Huksflux HFP01	Agilent 34970A
22	Qi (W)		Heating delivered power (Wh/h)	W	Finder Type 7E.13	Adv. ADAM 4080
23	Gv		Vertical global solar radiation (plane of the glazing)	W/m²	Kipp & Zonen CM11	Agilent 34970A
24	Gh		Horizontal global solar radiation	W/m²	Kipp & Zonen CM11	HP3852A
25	Gh, dif		Horizontal diffuse solar radiation	W/m²	Kipp & Zonen CM11	HP3852A
26	Glw-h		Horizontal long wave radiation from the sky	W/m²	Eppley PIR	Agilent 34970A
27	Glw-v		Vertical long wave radiation from the sky	W/m²	Eppley PIR	HP3852A
28	WD		Wind direction	°	Thies Clima 4.3129	HP3852A
29	WV		Wind velocity	m/s	Thies Clima 4.3519	HP3852A
30	RH		Relative humidity	%	Vaisala type HM70	HP3852A

4.2.3 Data acquisition system

A data acquisition system 'Agilent 34970A', manufactured by Agilent Technologies, has been used for the acquisition of all temperatures and heat flux densities, together with the vertical global solar radiation (in the plane of the glazing) and the horizontal long wave radiation.

Another data acquisition system is used to acquire all others weather datasets, at about 200m away from the testbox: HP3852A, manufactured by Hewlett Packard.

4.2.4 Heating and cooling devices

The heating power is supplied by 4 electrical resistances (tubes with fins, see Figure 25) of 66.5 Ohm (760W at 225V) connected in series, yielding a total maximum power of 188W. The delivered energy is measured via a counter with a resolution of 1 Wh/pulse and the power supplied during each timestep is given as a back-calculated value.

The installed power allowed reaching a temperature gradient higher than 40K, which is expected to be able to keep the inside temperature close to 25°C even when outside temperatures reach -15°C.

Figure 25: one of the four serial component resistances providing 188W all together.

The heating system is PID-controlled in time (cut-in/cut-out) such that the heating power is always balancing from the low and high power levels and can virtually reach any power between these limits when integration is done for a certain period of time.

In order to reduce the temperature stratification within the box, a small fan (8.3W) blowing in the top-down direction was added inside the box.

There was no cooling device.
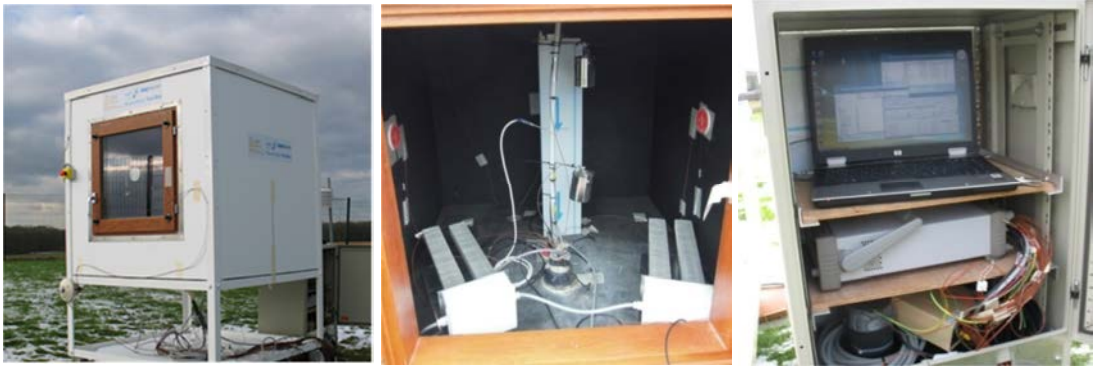
Figure 26: the South-facing window of the test box (left), the inside equipment (middle) and part of the acquisition system (right).

4.2.5 Test sequences

The following experiments have been carried out:

- Test 1 : co-heating test with constant indoor temperature (25°C during 2 weeks)
- Test 2 : free-floating indoor air temperature (no heating power during 2 weeks)
- Test 3 : dynamic heating test sequence (ROLBS) (3.5 days)

Table 6

	Fan status	Min. Power	Max. Power
Co-heating	On	8.3W	~198W
Free floating	Off	0W	0W
ROLBS	On	8.3W	~106W

The actual instantaneous power depends on the network voltage which is expected to be close to 225W (values in the Table 6 above are based on that assumption).

The ROLBS experiment (see Figure 27) has been run after the free floating sequence. It is composed of the following symmetric number of segments arranged randomly at both the power levels: 0.5h (2*16 occurrences), 1h (2*6 occurrences), 2.5h (2*2 occurrences), 6.5h (2*1 occurrence), 16.5h (2*1 occurrences). No extra validation sequence of the ROLBS type is available. Nevertheless, the two other data sets could also be used for validation.
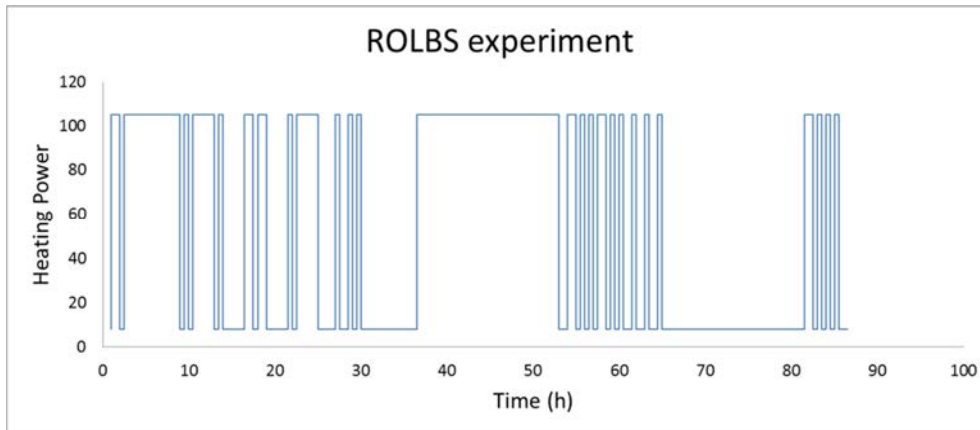
Figure 27 : Heating power, oscillating between low and high power levels, during the ROLBS experiment (3.5 days)

Because of the low resolution of the energymeter, and in order to facilitate the inter-comparison of results, synthetic data is supplied for the heating power of the ROLBS experiment. Low and high power levels have been assumed to be constant (stable network voltage assumed) and are determined based on the average power during the two sequences of 16.5h. The Low level power is set to 8.3W and the High power level to 105.8W.

During the measurements, power cuts at the main weather station unfortunately occurred at the beginning of the co-heating set and at the beginning of the ROLBS set. This has been left as it is since main variables are still available from the test box acquisition (global vertical solar radiation in the plane of the glazing of the Testbox and the horizontal long wave radiation).

4.2.6 Data

Three data files are supplied, one for each test. They correspond to the testing periods extending:

- Test 1: from the 25th of January 2013 to the 8th of February 2013.
- Test 2: from 8th of February 2013 to the 22th of February 2013
- Test 3: from 25th of February 2013 to 28th of February 2013

Important to note is that, as mentioned before, there has been a problem (power cut) with the data acquisition of the main weather station at the beginning of the co-heating period (Test 1, on the 27th of January 2013) and at the beginning of the ROLBS period (Test 3, on 25-26th of February 2013). Hence these lines are empty in the file for the channels related to the above mentioned additional meteorological sensors.

The recording of the acquisition system Agilent 34970A (near the test box) occurs punctually every 5 minutes only. Data have been corrected to GMT timeframe. The energy consumption is measured by means of a cumulative counter that is incremented each time 1Wh is consumed. In the provided data files, this consumption is converted to Watts. The other data (temperatures, heat fluxes, solar vertical radiation, long wave horizontal radiation) are recorded in parallel.

The recording of the main weather station (acquisition system HP3852A) is every minute in the GMT timeframe. In order to consolidate the data, the weather station data have been averaged with a 5 minutes interval. The averaging for the wind direction is done in a vectorial form such that no loss of accuracy occurs if the wind is oscillating around the 0-360° (North) orientation.

The data files are text files organized in rows and columns. Each column corresponds to a variable. The first row represents the headers of the respective columns and refers to the recorded variables as indicated in Table 5. Data are read and recorded in each row every 5 minutes.

The data is made available on the DYNASTEE website.
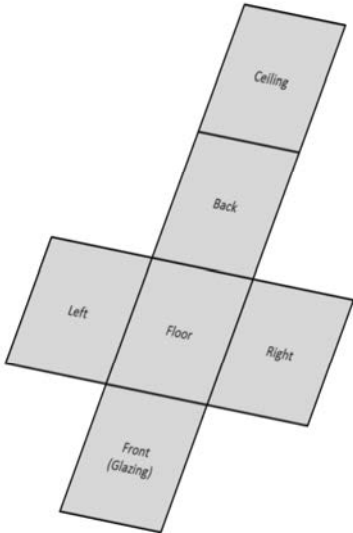
Figure 28: Identification of the faces of the test box

5. Round Robin Tests: Outdoors Tests at CIEMAT

5.1 Introduction

This first series of experiments carried out at CIEMAT-PSA has been designed taking as reference the previous set of experiments carried out at BBRI described in chapter 4. Particular measurement devices and test conditions in these new tests are described in the following.

5.2 Boundary conditions

The RR test box was tested at the LECE laboratory at Plataforma Solar de Almeria, in the South East of Spain (37.1°N, 2.4°W). The weather at this test site is dry and extremely hot in summer and cold in winter. Temperature swings largely between day and night. Global solar radiation on the south vertical surfaces is very strong in winter, and on the horizontal surfaces it is very strong in summer. Sky is usually very clear.

The experiments extended over a period of 44 days, starting the 28th of May 2013 and ending the 10th of July 2013.

Testing is done under real outdoor weather conditions.

The following outdoor climate sensors installed near the test box are included in the supplied data:

- air temperature (with a solar radiation shield and ventilated),
- vertical global solar radiation (parallel and next to the glazing)
- wind speed
- wind direction (North 0°, East 90°)

Additional meteorological sensors installed at the test site (80 m east from the test box) are also included in the data sets:

If you want to list something, proceed as follows:

- horizontal global solar radiation
- beam solar radiation.
- diffuse solar radiation.
- vertical long wave radiation.
- relative humidity.

Other sensors installed at the test site (325 m north from the test box):

- horizontal long wave radiation from the sky.
- vertical global solar radiation facing north

5.3 Measurement devices

This section describes the measurement equipment and other considerations regarding their accuracy.

The following list summarises the used measurement transducers and sensors:

- Air temperature: Platinum thermoresistance, PT100, 1/10 DIN, directly measured using a four-wire connection, with a solar radiation shield and ventilated for outdoor measurements. (Figure 39 and Figure 42).
- Surface temperature: Analogous sensors and connections as those used for air temperature. The used sensor consists in a very small sensing element embedded in a very slim semi-transparent substrate. These devices have been glued to the measured surfaces in their centre and covered with a tape of same colour of the surface, to integrate them as much as possible with the corresponding surface. (Figure 40 and Figure 41).

  The internal temperature of the glass has been measured using the same device and two additional sensors: One using other type of PT100 with a very small and slim white substrate (named as Tsi glaz-ing2), and other using a type T thermocouple (named as Tsi glazing3).

- Average surface temperature: Type T thermocouples class 1 according to IEC-584-1982, voltage directly measured using a differential connection, Nine sensors have been matrix distributed and glued in each internal face of the Test Box. The average of the corresponding nine sensors is given for each face.
- Heat flux density: Sensor model HFP01 manufactured by Hukseflux, accuracy of sensitivity coefficient 5%, voltage measured directly by differential connection. One of these devices has been glued to the centre of each internal face of the Box and covered with a tape of the same colour of the surface (Figure 40).
- Horizontal and vertical global solar irradiance on the horizontal and south vertical surfaces respectively: Pyranometers, model CM11 manufactured by Kipp and Zonen, secondary standard according to ISO 9060:1990, voltage directly measured using a differential connection. (Figure 42 and Figure 43).

  Analogous devices used for diffuse solar irradiance but installed in a two-axis sun tracker SOLYS 2. (Figure 43).

- Beam solar irradiance: Pyrheliometer, model CHP1 manufactured by Kipp and Zonen, First Class ac-cording to ISO 9060:1990, installed in a two-axis sun tracker SOLYS 2 (Figure 43). Voltage directly measured using a differential connection.
- Horizontal and vertical long wave radiation on the horizontal and south vertical surfaces respectively: Pyrgeometers, model CGR-4 manufactured by Kipp and Zonen, voltage directly measured using a dif-ferential connection.
- Heating power: Power transducer, model SINEAX DME 440 manufactured by Camille Bauer Ltd. 4..20mA current loop directly measured.
- Wind velocity: Sensor model WindSonic manufactured by GILL INSTRUMENTS LTD. 4..20mA current loop directly measured. (Figure 42).
- Outdoors relative humidity. Sensor model HMP45A/D manufactured by VAISALA. 4..20mA current loop directly measured.

A data acquisition system with the following characteristics has been implemented: 16-bit A/D resolution, range of measurements fitting sensor output, modules distributed to minimise wiring, based in Compact Field Point modules manufactured by NATIONAL INSTRUMENTS. Particularly the following list summarises the used modules (Figure 44):

- cFP-RTD-124: Four-Wire RTD and Resistance inputs. Range –200 °C to 850 °C used for measurement of temperature.
- cFP-TC-125: Differential thermocouple or millivolt inputs. Range –20 mV to 80 mV used for measurement of global and long wave radiation and heat flux density.
- cFP-AI-111: Milliamp input. Range 4–20 mA used for measurement of wind velocity.

- cFP-AI-110: Voltage or current input. Range 0–1 V used for measurement of relative humidity.

Twisted pairs and grounded shield are employed to reject noise and avoid perturbations from wiring.

5.4 Data acquisition

All data are read and recorded every minute in the GMT timeframe.

The measurements corresponding sensors in the test box and near it and in meteo 1 are collected using the same distributed data acquisition system. Measurements corresponding to Meteo 2 are recorded using an independent data acquisition system with the same characteristics as the one used for the test box. Both data acquisition systems are synchronised to the main time server at PSA.

5.5 Initial preparation of the test box

5.5.1 Heating power and its measurement

Heating power is necessary to produce a delta T high enough to produce a heat flux through walls that allow to see the phenomena to characterize.

Taking as reference the heat flux observed through opaque wall in co-heating test at BBRI (about $10W/m^2$), a set point of at least 40°C is necessary to achieve an equivalent heat flux in Almeria at this time. Higher indoor air temperatures are avoided for security.

Several actions have been taken to improve the accuracy and resolution in amplitude and time of the measurement of heating power regarding previous test as explained below.

In order to improve the resolution in amplitude a very accurate measurement device, which accuracy is 0.25% of reading, has been used.

Even using a so accurate device time resolution can be very poor if temperature control is very accurate and the switching frequency is higher than the sampling frequency (Figure 31).

Switching frequency depends highly on the control dead band: dead band must be low enough to maintain stable indoor air temperature and high enough to avoid high frequency switching that can lead to low resolution measurement of heating power.

Power supplied by the heating device must be high enough to maintain the indoor air temperature set point taking into account that outdoor air temperature can vary from day to night (differences up to 20°C between day and night), and not too high to avoid indoor air stratification and also to avoid fast switching (see Figure 29 and Figure 30).

Taking all these conditions into account, several heating devices, dead bands and set points for indoor air temperature have been examined, with the final goal of achieving the following (see Figure 29 to Figure 34):

- A heat flux through the opaque walls high enough for identification.
- Switching frequency low enough to allow enough time resolution for accurate power measurement.
- Indoor air temperature that is stable enough and at the same time avoiding stratification.

Finally a 100W incandescent lamp has been used as heating device, with 40°C as set point and 0.5°C dead band. Indoor air temperature shows acceptable stability and low stratification, measurement of heating power has enough resolution, and heat flux through the opaque walls is high enough for identification.

For the test using a ROLBS power sequence a 60W incandescent lamp has been used to avoid indoor air temperature increase above 40°C.
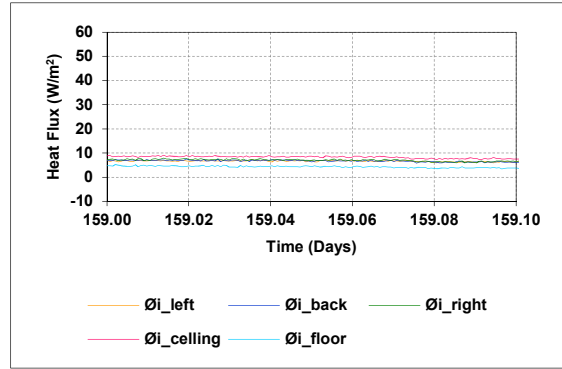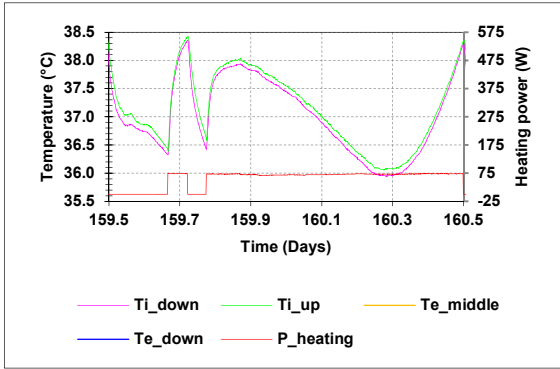
Figure 29: Indoors air temperatures, heating power and heat flux through opaque walls using a 60W incandescent lamp. Indoors air temperature decrease at night below the set point (left) and very low heat flux through the opaque walls (right). Day 159 is 8th of June.
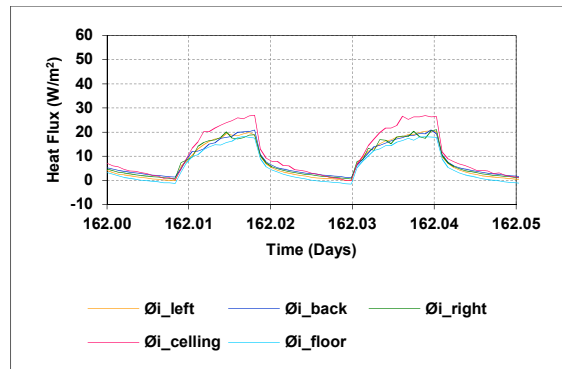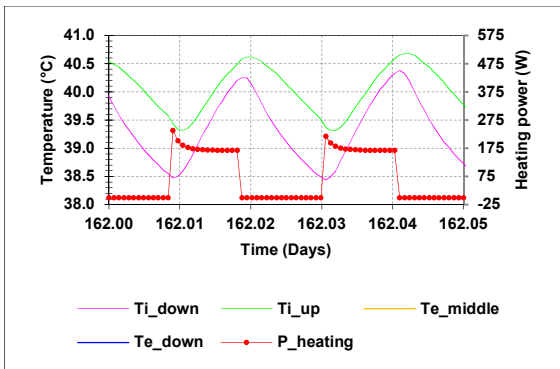
Figure 30: *Indoors air temperatures, heating power and heat flux through opaque walls using a 100W resistance, 40°C set point and 2°C dead band. Indoors air temperature is oscillating and shows a high stratification (left). Heat flux through the opaque walls is high enough when power is on (right). Day 162 is 11st of June.*
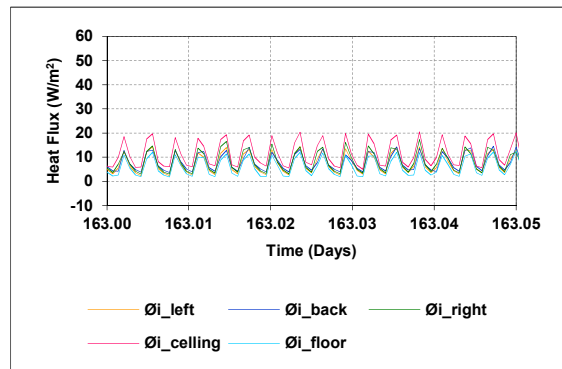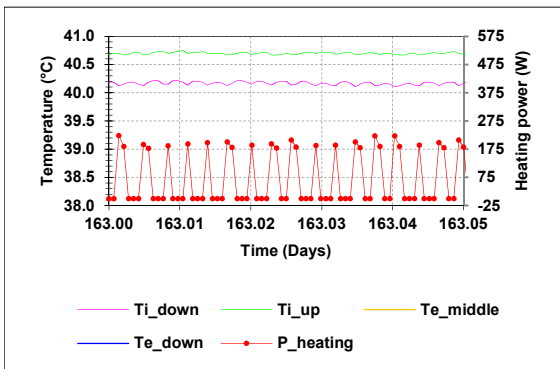
Figure 31: Indoors air temperatures, heating power and heat flux through opaque walls using a 100W resistance, 40°C set point and 0.5°C dead band. Indoors air temperature shows better stability and lower stratification, but measurement of heating power has low resolution due to the fast switching frequency (left). Heat flux through the opaque walls is high enough when power is on (right). Day 163 is 12th of June.
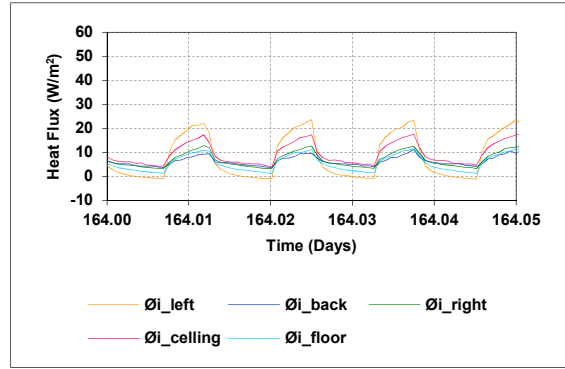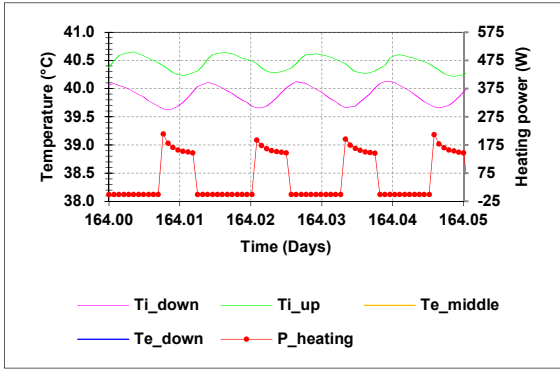
Figure 32: Indoors air temperatures, heating power and heat flux through opaque walls using a 100W resistance, 40°C set point and 0.8°C dead band. Indoors air temperature shows worse stability and too high stratification, measurement of heating power has enough resolution (left). Heat flux through the opaque walls is high enough when power is on (right). Day 164 is 13th of June.
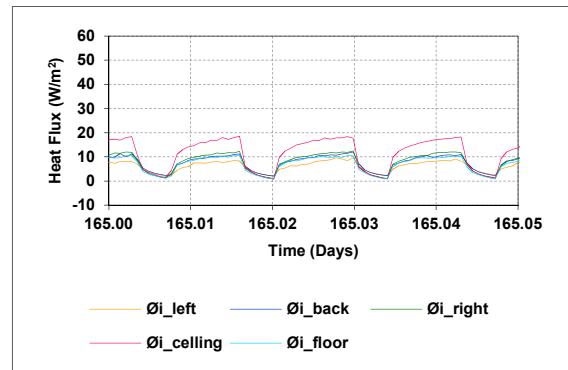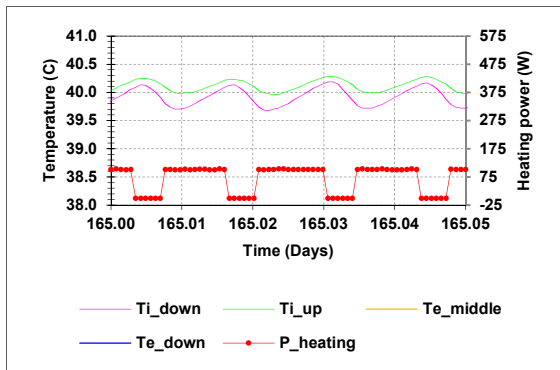
Figure 33: Indoors air temperatures, heating power and heat flux through opaque walls using a 100W incandescent lamp, 40°C set point and 0.8°C dead band. Indoors air temperature shows acceptable stability and low stratification, measurement of heating power has enough resolution (left). Heat flux through the opaque walls is high enough when power is on (right). Day 165 is 14th of June.
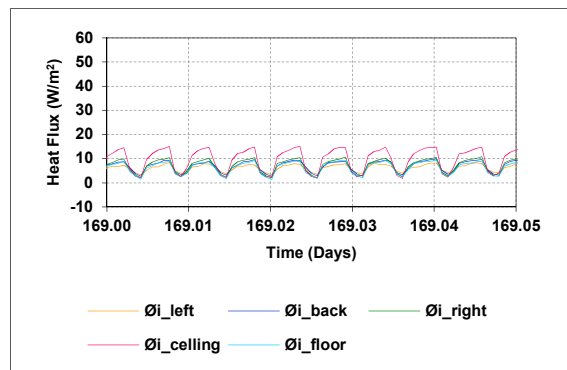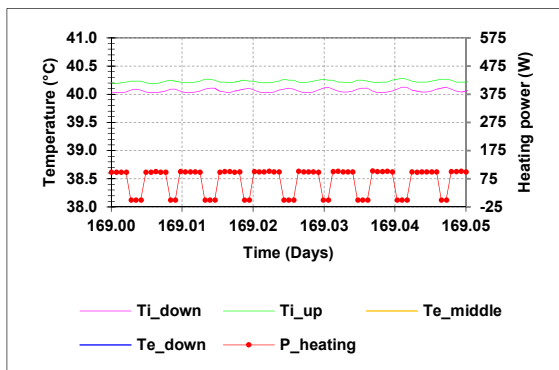
Figure 34: Indoors air temperatures, heating power and heat flux through opaque walls using a 100W incandescent lamp, 40°C set point and 0.5°C dead band. Indoors air temperature shows acceptable stability and low stratification, measurement of heating power has enough resolution (left). Heat flux through the opaque walls is high enough when power is on (right). Day 169 is 18th of June.

5.6 Performed experiments

5.6.1 Common Exercise 4

Data recording started once all the sensors and measurement instruments were installed and fully operative.

At first, 3 data series identified as series 1 to 3 in the following, were recorded in parallel to the process followed to optimise the tests conditions. In this phase measurements are considered reliable but test conditions are not considered fully optimised for analysis.

Afterwards, 3 series identified as series 4 to 6 in the following were generated. These series correspond to constant indoor air temperature set point, ROLBS power sequence and free running test respectively. These data series were optimised as possible regarding analysis and under the given meteorological conditions.

The list below summarises the main distinctive characteristics of all the mentioned data series:

- Series 1: 31/05/2013 to 05/06/2013. One step of heating the first day, two days free running and the rest with constant heating using a 60W incandescent lamp. Missing: Tse_left, Tse_back.
- Series 2: 5/06/2013 to 10/06/2013. Controlled heating power using a 60W incandescent lamp. First day indoor air temperature set point is 40°C, afterwards it is 38°C, and dead band is 2°C.
- Series 3: 10/06/2013 to 17/06/2013: Controlled heating power using a 100W resistance. Indoor air temperature set point is 40°C, dead band is 2°C, 0.5°C and 0.8°C the first, second and third days respectively..
- Series 4: 17/06/2013 to 26/06/2013: Controlled heating power using a 100W incandescent lamp. Indoor air temperature set point is 40°C, dead band is 0.8°C the first day and 0.5°C afterwards.
- Series 5: 28/06/2013-1/07/2013: ROLBS power sequence. Heating power using a 60W incandescent lamp.
- Series 6: 2/07/2013-10/07/2013: Free floating temperature.

5.6.2 Other tests

Once finished the experiments used for the common exercises, additional test based on the same measurement equipment, were carried out in Almería. A total test period was 8 month taking into account the data used for the common exercises and these additional data.

The objectives of these additional tests were:

- To incorporate features which are present in real life test. These features bring physical effects that increase complexity to the analysis, but it is still somehow simplified as far as the round robin test box is relatively simple.
- To have additional data series recorded under different test condition to analyse robustness of analysis approaches, support validation of results and analyse the influence of the different test conditions on accuracy of results.

Different tests with the following characteristics were carried out:

- Test allowing ventilation in summer: Window is 1cm opened and orifice for cables is not sealed.

- Test with arbitrary orientation: window facing East.
- Several test sequences adding PCM tiles in summer and autumn: Free running, ROLBS power sequence, and constant power steps alternated with free running.
- Equivalent sequences to summer tests used for the common exercises but in sunny cold winter: ROLBS power sequence, Co-heating (two sequences. Set points to 35°C and 21°C respectively), and free running

Additionally, infrared pictures were taken to check the homogeneity of the construction.

5.7 Initial preparation of the test box

For all these tests, the face of the box equipped with the glazing is oriented to the South.

On each face of the box (5 opaque faces and 1 glazing), the following sensors have been installed:

- Heat flux at the internal face (in the centre of the face)
- External surface temperature (in the centre of the face)
- Internal surface temperature (in the centre of the face)
- Average of the internal surface temperature (from a matrix of nine measurement points, only in opaque faces)

The indoor temperature has been measured along the vertical symmetry axis of the box at 1/3 and 2/3 of the total height of the box.

In the initial test phase, different electrical resistances and incandescent lamps have been tried as heating device, with the objective of finding one which allows to maintain stable indoor air temperatures and at the same time exhibiting a switching frequency lower than the sampling interval to allow for accurate monitoring of heating power. Finally, a 100W incandescent lamp has been chosen.

Six data files are supplied, one for each test. The data files are text files organized in rows and columns. Each column corresponds to a variable. The first row represents the headers of the respective columns and refers to the recorded variables. Data are read and recorded in each row every minute.

Nomenclature used is the same as in the previous test by BBRI (see instructions for participants in section 5.10). The text "_1" and "_2" has been added at the end of the name of variables to indicate that these measurements correspond to Meteo 1 or Meteo 2 respectively (see Figure 36).

The text "N/A" has been used in the data files in records for which the corresponding measurement are not available.

The data is made available on DYNASTEE website.

Table 7: Nomenclature and units. Variables in common to the previous experiments at BBRI.

Name	Measurement	Unit
TIME	GMT Time	DD/MM/AAAA hh:mm
Tsi glazing		°C
Tsi left		°C
Tsi back	Internal surface temperature	°C
Tsi right		°C
Tsi ceiling		°C
Tsi floor		°C
Ti down	Indoors air temperature (1/3 height of the box)	°C
Ti up	Indoors air temperature (2/3 height of the box)	°C
Tse glazing		°C
Tse left		°C
Tse back	External surface temperature	°C
Tse right		°C
Tse ceiling		°C
Tse floor		°C
Te down	Outdoors air temperature se figure below the box (Figure 35)	
Te middle	Outdoors air temperature se figure mid height of the box (Figure 35)	
Øi glazing		W/m²
Øi left		W/m²
Øi back	Heat flux density in the internal surface.	W/m²
Øi right		W/m²
Øi ceiling		W/m²
Øi floor		W/m²
P heating	Heating power	W
Gv	Vertical south global solar radiation (plane of the glazing).	W/m²
Gh_1	Horizontal global solar radiation.	W/m²
Gh, dif_1	Diffuse solar radiation	W/m²
Glw-h_2	Horizontal long wave radiation	W/m²
Glw-v_1	ertical south long wave radiation	W/m²
WD	Wind direction	°
WV	Wind speed	m/s
H_1	Relative humidity	%

Table 8: Nomenclature and units. Added variables regarding the previous experiments at BBRI.

Name	Measurement	Unit
Tsi glazing2	Internal glass surface temperature (small size PT100).	°C
Tsi glazing3	Internal glass surface temperature. (type T thermocouple).	°C
Tsi left avg		°C
Tsi back avg		°C
Tsi right avg		°C
Tsi ceiling avg	Average of the internal surface temperature	°C
Tsi floor avg		°C
Tsi frame avg		°C
Tsi front avg		°C
Gb_1	Beam solar radiation	W/m^2
Ggr_1	Ground reflected solar radiation	W/m^2
Gvn_2	Vertical north global solar radiation	W/m^2
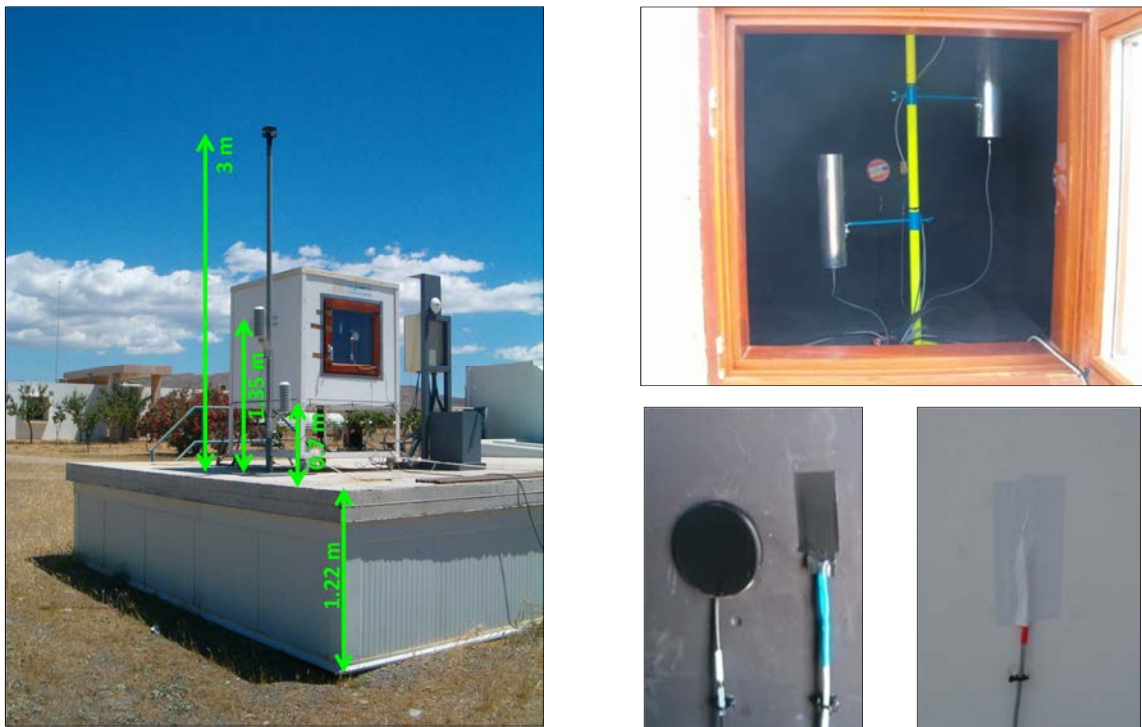
Figure 35: the test box and meteorological devices near to it (left), indoor air temperature (right-top), heat flux and internal and external surface temperature sensors (right-bottom).

Figure 36: Location of the test box and the other meteorological devices at Plataforma Solar de Almería (PSA).

Figure 37: Placement. Facing south in an open area.

Figure 38: Anchoring additional to the brakes, to prevent damage due to strong winds which are very frequent in the test site

Figure 39: Indoors air temperature and shielding devices

Figure 40: Installation of internal heat flux density and surface temperature sensors. First glued to the internal surfaces and then covered with a tape of same colour of the internal surface.
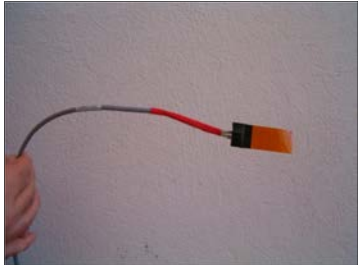
Figure 41: Installation of external surface temperature. First glued to the external surfaces and then covered with a tape of same colour of the external surface.

Figure 42: Meteorological sensors near the test box: Outdoors air temperature, global vertical solar radiation, wind speed and direction.

Figure 43: The test box and meteorological devices near to it (left), meteorological devices at meteo 1 (right)

Figure 44: Data acquisition modules

5.8 Expected range of parameters estimated for the actual tests boundary conditions

The design values of the constructive material were presented in chapter 3, which also gave estimates ranges of variations of the characteristic parameters depending on the boundary climate conditions.

This section analyses this variation of the same characteristic parameters for the actual measurements of the climatic boundary conditions given in the particular tests carried out. The aim of this analysis is to narrow the intervals of expected values for each data series regarding the intervals given chapter 3.

The parameter estimates of the Round Robin Box have been calculated according to different expression taken from the literature frequently used in practice. The differences observed in the results given by these expressions give an approximated idea of the range of variability that can be obtained from the identification analysis among the different data series due to boundary conditions and other sources of uncertainty. The results obtained in this calculation can be used to carry out external validation to reject models giving results showing any of these behaviours:

- Being too far from these estimated reference values.

- Showing variability in the U and g values in a range that is remarkably higher that the range of variability theoretically calculated.

The U values and g value of the opaque wall have been calculated according to the same expressions (1) to (6) used in chapter 2, section 2.2.1.

The g value of the glassing has been calculated according to the following expression (ASHRAE , 1999):

$$g = \tau + \alpha_1 \frac{U}{h_e} + \alpha_2 \frac{h_e - U}{h_e} \qquad (9)$$

Where τ is the solar transmittance of the glazing system, α_1 and α_2 are the absorptances of outer and inner glass layers respectively, and h_e is the external surface heat transfer coefficient. The values τ = 0.56, α_1 = 0.07, α_2 = 0.08, and U = 1.1 $Wm^{-2}K^{-1}$ have been used according to the technical characteristics given by the manufacturer of the window, to estimate its theoretical g value (section 3.2). Different approximations have been studied, according to the same three different approximations considered for the surface heat transfer coefficients used to calculate the U value.

The parameter estimates obtained in chapter 3 have been considered as starting point, particularly the following R, and HLC assuming constant standard heat transfer surface coefficients:

- Thermal resistance value of the opaque walls (R), from 1.927 to 2.2 m^2K/W.

- HLC value of the whole wall from 3.75 to 4.08 W/K that correspond inversely to the R values of the opaque wall from 1.927 to 2.2 m^2K/W.

These variations on R value from 1.927 to 2.2 m^2K/W and HLC from 3.75 to 4.08 W/K, take into account some slight increase of the actual thermal resistance of the fabric due to the possible presence of a thin air and/or glue layer between the different material layers. Consequently it must be taken into account that this uncertainty source in R and HLC,

doesn't depend on the boundary climatic condition, so it must be un-dependent on the data set used for the identification.

Taking into account the mentioned R and HLC basis ranges, the following parameters have been estimated for the different climatic boundary conditions given in the data series corresponding to the tests in Limelette (Belgium) and Almería (Spain).

- U and g values of the opaque walls and glassing.

- HLC and solar aperture of the whole Round Robin Box.

Figure 45, Figure 47 and Figure 48, show the parameter estimates averaged for each data series according the different approximations. Figure 46 focus on the U and g values of the opaque walls, obtained considering heat transfer surface coefficients depending on wind speed and surface temperatures. This figure shows the average value and standard deviation of the parameter estimates obtained applying this approximation in each data series.

These figures reveal low differences among the **U value of opaque walls, U value of glassing, g value of the glassing and UA of whole wall** obtained for the different boundary conditions. The main differences are derived from the assumptions related to the constructive details of the walls (such as the possible presence of a thin air and/or glue layer between the different material layers of the opaque walls and it thickness), and also the formulation used to estimate the surface heat transfer coefficients. Once adopted any of these assumptions, the results are very similar for the different boundary conditions as explained in the following.

- Assuming the equations (4) and (5) as approximation to estimate the surface heat transfer coefficient depending on wind speed and surface temperatures, the standard deviation among all the average values for all the data series is 0.7%, 1.7%, 0.01% and 0.7%, and the standard deviation for the instantaneous values in each data series is in the range 0.4-1.3%, 1.1-3.0%, 0.01-0.04% and 0.5-1.3%, for U value of opaque walls, U value of glassing, g value of the glassing and UA of whole wall respectively (see Figure 45 to Figure 48).

- Assuming the equations (2) and (3) as approximation to estimate the surface heat transfer coefficient depending on wind speed, the standard deviation among all the average values for all the data series is 0.3%, 0.6%, 0.2% and 0.3% and the standard deviation for the instantaneous values in each data series is in the range 0.4-1.9%, 1.1-4.0%, 0.003-0.05 and 0.5%-1.9%, for U value of opaque walls, U value of glassing, g value of glassing and UA of whole wall respectively (see Figure 45 to Figure 48).

It is concluded that the variation detected by these theoretical calculations due to wind speed and surface temperatures are considered very low and undetectable in the U values of walls and glassing, g values of the glassing, ad UA value of the whole wall, estimated by identification, taking into account typical measurement uncertainties (around to 10%).

However the differences observed in these figures among the **g values of the opaque walls** obtained for the different boundary conditions are relatively higher.

- Considering surface heat transfer coefficient depending on wind speed and surface temperatures according to equations (4) and (5), the standard deviation among all the average values for all the data series is 8.7-7.4% and the standard deviation for the instantaneous values in each data series is in the range 11.8-41.5%. See Figure 46.

- Considering surface heat transfer coefficient depending just on wind speed according to equations (2) and (3), the standard deviation among all the average values for all

the data series is 8.5% and the standard deviation for the instantaneous values in each data series is in the range 15.0-58.3%.

The variation detected by these theoretical calculations due to wind speed and surface temperatures might be not negligible in the g values estimated by identification. See Figure 46. However taking into account that the absolute value of this g value is extremely low, its contribution is not detectable in the energy balance of the internal surface of the opaque walls so it is negligible and consequently its relatively high uncertainty is not relevant in practice.
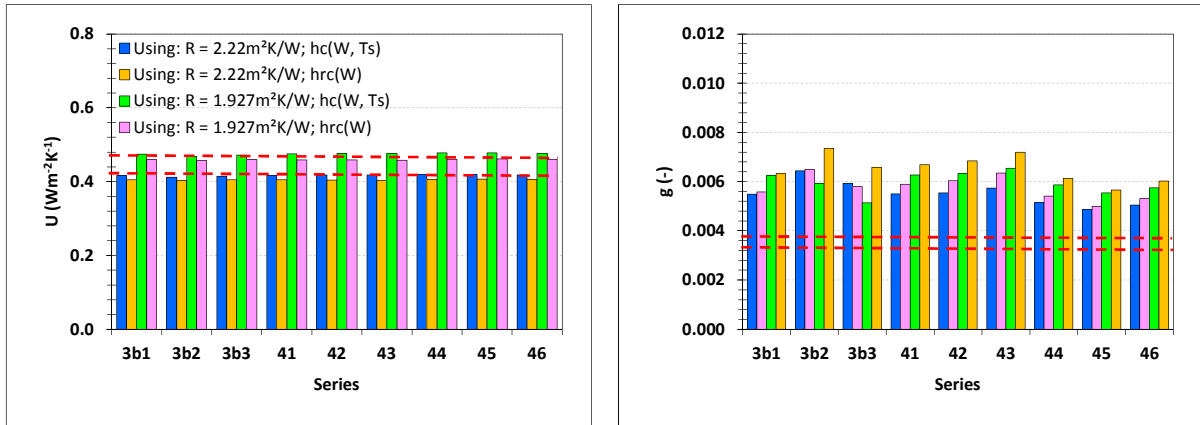
Figure 45 : Theoretical U and g values for the opaque walls using different forms of non-constant surface heat transfer coefficients, corresponding to wind speeds and surface temperatures measured in series 3b1, 3b2, 3b3 (in Limelette, Belgium) and 41, 42, 43, 44, 45 and 46 (in Almería, Spain). Dotted red lines indicate the same parameters assuming standard constant surface resistances, where U value is 0.418 or 0.477 $Wm^{-2}K^{-1}$ and g value is 0.0033 or 0.0038, depending whether or not a thin air and/or glue layer between the different material layers is considered.
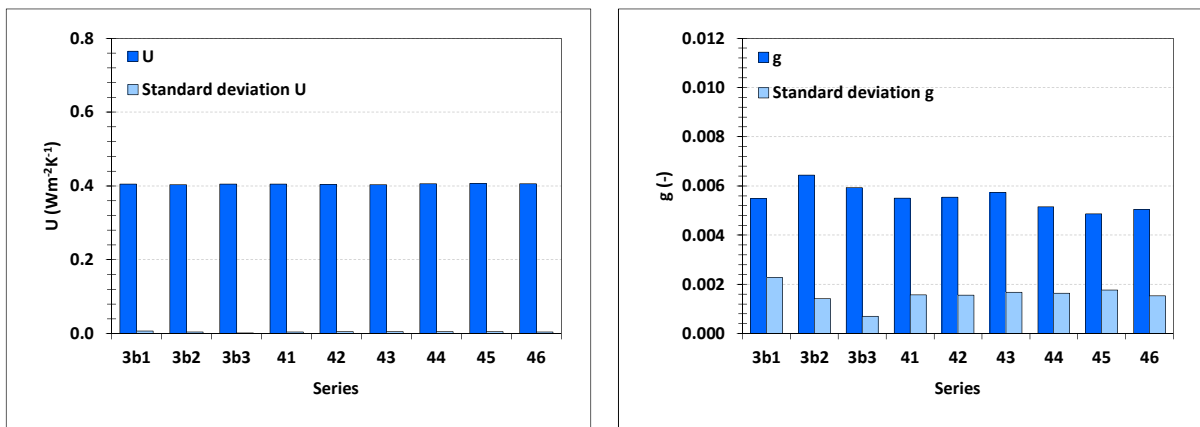
Figure 46 : Average value and standard deviation of the U and g values of the opaque walls. Considering heat transfer surface coefficients depending on wind speed and surface temperatures.
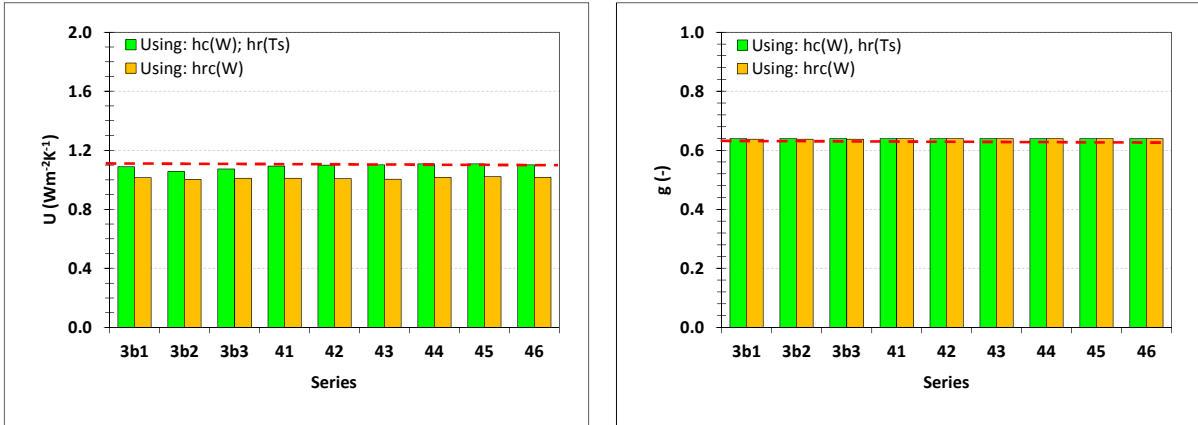
Figure 47 : U and g values of the glassing. Considering heat transfer surface coefficients depending on wind speed and surface temperatures. Dotted red lines indicate the same parameters assuming standard constant surface resistances.
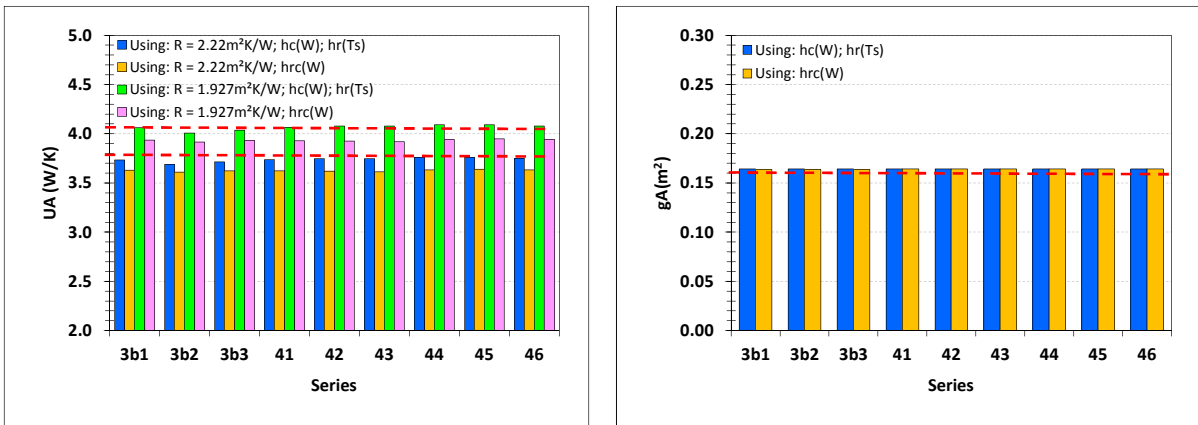
Figure 48: Overall HLC and solar aperture of the whole box. Considering heat transfer surface coefficients depending on wind speed and surface temperatures. Dotted red lines indicate the same parameters assuming standard constant surface resistances, where UA value is 3.75 or 4.08 W/K, depending whether or not a thin air and/or glue layer between the different material layers is considered.

5.9 Data overview

Figure 49 indicates a significant difference between the levels of horizontal solar radiation, which is significantly higher in summer in Spain than in winter in Belgium.
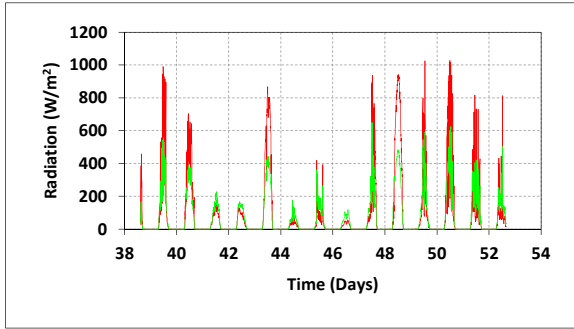
(a) Winter Belgium. Series 3b.2 in sections 4.2.5 and 4.2.6.
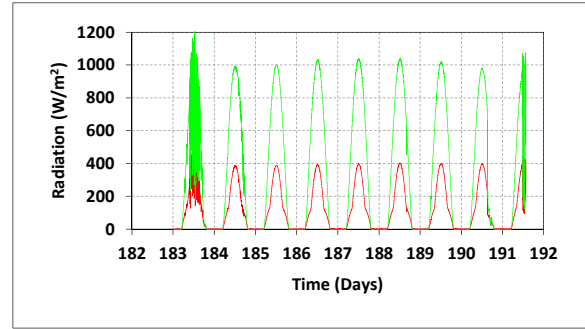
(b) Summer Spain. Series 4.6 in section 5.6.1.

Figure 49: Global vertical (red) and horizontal (green) solar radiation. Winter and summer.

Observation of heat flux through the opaque walls in Figure 50 gives relevant information to model the influence of solar radiation. Figure 50c and d show that heat flux through the different opaque walls, are quite similar in summer in Spain. It must be taken into account that differences lower than the uncertainty in the measurement of heat flux sensor cannot be interpreted as actual differences. The minimum uncertainty in this measurement is 5%.

However mayor differences are seen in Figure 50a and b among the different walls in winter in Belgium. Heat flux through the roof lower than heat flux trough the floor may be because solar gain reduces the net heat losses through the roof. But taking into account that this behaviour is not seen in summer in Spain when horizontal radiation is much higher, it is concluded that it is due to solar radiation through the window and incident in the internal surfaces. This makes sense taking into account sun position. Similar considerations are done for east and west walls.
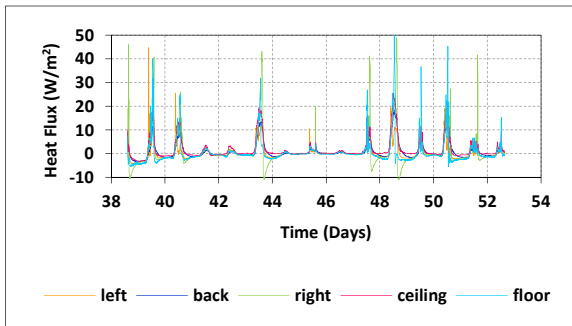
(a) Heat flux through each opaque wall. Winter Belgium.
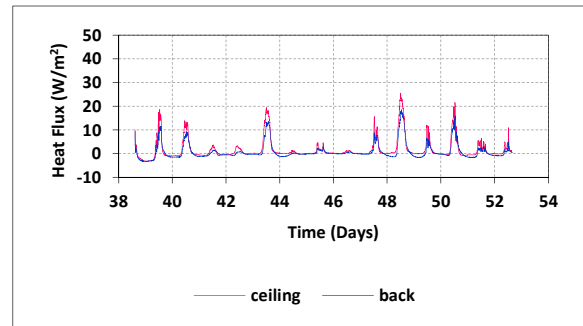
(b) Heat flux through ceiling and back wall. Winter Belgium.
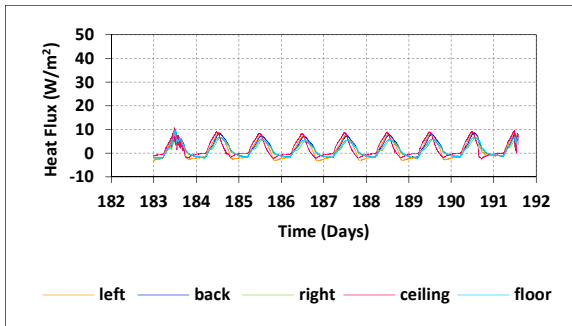
(c) Heat flux through each opaque wall. Summer Spain.
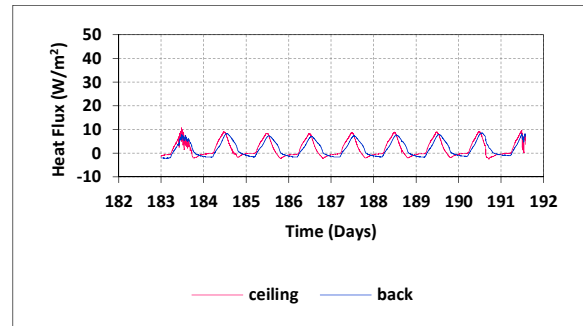
(d) Heat flux through ceiling and back wall. Summer Spain.

Figure 50: Heat flux through the opaque walls in different free running tests in winter and summer. Series 3b.2 and 4.6 respectively in sections 4.2.5, 4.2.6. and 5.6.1.

72

5.10 Common exercises 3b and 4

Common exercise 4 (CE4) consists of two independent parts. Contributions can be to either one or both. Common exercise 3b (CE3b) is identical to part 1 of CE4.

Series 1 to 3 from at BBRI and series 1 to 5 from at CIEMAT can be used for part 1 and series 6 from at CIEMAT must be used for part 2. It must be taken into account that some of the provided data may not be necessary.

5.10.1 Part 1: Obtain the energy performance indicators

The aim of this part is to obtain the energy performance indicators using the data recorded at CIEMAT-PSA.

As in previous exercises, participants are given the freedom to choose which physical characteristics (overall heat loss coefficient, solar aperture, effective heat capacities, time constants, …) of the RR Box to assess. However, at least one of the following performances should be extracted from the analysis:

- U value (W/m^2K) of each opaque wall of the test box
- overall heat loss (W/K) of the test box
- solar gains (m^2)
- dynamic behaviour of the test box

Use data series 1 to 5. The suitability of each data set to fit the objective must be discussed.

5.10.2 Part 2: Cross validation of identified models

The aim of this part is to analyse the capability of a model identified on the basis of one data set to predict the box's behaviour during another period, for which only the inputs are available. Two possibilities come forward:

- Using models identified on the basis of measurement campaigns performed by BBRI, predict the output on the basis of input data recorded at CIEMAT-PSA.
- Using models identified on the basis of data recorded at CIEMAT-PSA, predict the output during a measurement period different from the one used to identify model.

Discuss difference between predicted and simulated output in both cases.

Use data series 6.

5.10.3 Reporting

The submitted reports need to comprise a detailed description of the applied analysis and validation carried out. Report must be concise and as clear and illustrative as possible in all steps.

The report must consider at least the following items:

- Pre-processing (Data overview, discussion about quality of data and suitability to fit objectives, etc.)

- Modelling (Hypotheses and approximation about the physics behind the model used, statistical and mathematical approach, software tools, etc.)

- Validation (statistical criteria and physical consistency).

- Clear indication of results and uncertainty in each parameter estimate
- Conclusions (about results themselves, about the experiment set up and measurement campaign, etc).

Participants are requested to:

- complete the provided .xls-file of CIEMAT data series 6 (CE4_series6.xls) with the predicted output (based on models fitted to experiment data collected by BBRI and/or CIEMAT). Rename the .xls-file to *CE4_series6_country_institute.xls*.
- provide full analysis report in a .doc-file or .pdf-file (CE4_country_institute.doc/pdf).

Note that *CE4_series6_country_institute.xls* and *CE4_country_institute.doc/pdf* need to be renamed to the participant's actual country and institute name, as e.g. *CE4_Belgium_KUL.xls*.

5.11 Summary of results of common exercises 3b and 4 – discussion of the results

Table 9 and Table 10 and Figure 51 to Figure 53, summarise the results received since July 2013 till April 2014. As some of the methods are only able to determine the stationary properties of the box, Table 1 compares the obtained overall heat loss coefficient as determined by different participants.

Considering the heat loss coefficient (Figure 51 and Figure 52), some spread is observed in the results based on each data set. Note that some of the participants used different methods to determine the overall heat loss coefficient.

Comparing the results, it can be seen that most methods result in an overall heat loss coefficient around 4 W/K. Observing all reported results, the most deviating ones (assumed more inaccurate) are those given by models not considering dynamics, or just applying formulas which are far from accomplishing their hypotheses of validity.

Results following the average tendency, have been reported using different methods such as stochastic state space, ARX, ARMAX, linear regression models, and average methods. Differences are observed not only in the mathematical modelling approach but also in the physical assumptions used to build the models and concerning pre-processing issues. So, some of the differences can be attributed to the different level in analysis skills of participants. Hints to avoid mistakes that lead to results far from theoretical values are given in physical and statistical guidelines (Chapter 11 of this document and ref. 19 respectively).

Most participants that have analysed both cases, give slightly higher values of the heat loss coefficient for the data recorded in Spain (Figure 52). The dependencies of the HLC on the boundary conditions reported in section 5.8, don't explain this tendency. This increasing tendency could be qualitatively explained taking into account the different temperatures of the building fabric along both tests and the temperature dependency of its thermal conductivity. However information to carry out a theoretical study of this dependence is not available. Section 7.3.5 in chapter 7 reports the HLC obtained from tests carried out in a climatic chamber, using different set points for indoors and outdoors air temperatures. Highest results observed in those tests when indoor air temperature set point is around 50°C, must be considered as upper limits of this parameter, because this indoor air temperature was never reached in the tests used for the common exercises. Taking into account that the values obtained overlap if their uncertainty is taken into account, it is difficult to discern if these differences observed in Figure 52 correspond to a typical experimental spread around the true value, or if it is following a systematic tendency.

Some participants have detected problems modelling the effect of solar radiation and have studied different models considering different assumptions and approximations aiming to improve models. Different physical and statistical approaches have been studied but no clear improvement has been demonstrated yet, although this is an interesting topic for consideration in further works. The explanation for this could be a wrong interpretation of residuals with a frequency of 24 hours: In a first approach a non negligible correlation between the model residuals and solar radiation could lead to suggest a more detailed description of the solar radiation in the model for further improvements. However, if levels of solar radiation are high, many variables can show a relevant correlation with it, so any other effect depending on these variables and not properly modelled can show problems in the residuals in the same frequency as the solar radiation (further discussion and examples are included in the physical guidelines (chapter 11).

Some participants using models apparently logical from a physical point of view present results which are far from the average tendency. This behaviour is for instance observed when participants are trying to identify purely deterministic models using short testing periods. The outcome change radically when stochastic models are considered, incorporating the possibility of modelling errors giving more accurate parameter estimates.

Although state space models have a very high potential to represent a wide variety of physical systems governed by more general differential equations, all reported grey box state space models are relatively simple. Most applied models are limited to the RC-type, but do produce acceptable results.

Table 9: Determined overall heat loss coefficient (W/K) of the round robin test box by different modelling teams and making use of different data analysis methods.

Team		Winter data Belgium	Summer data Spain
1	Averaging method	3.77-3.92	
	State space model (RC using LORD)	3.07-3.42	
2	Averaging method	2.86-4.15	
	Linear regression (5'-data)	2.84-4.11	
	Linear regression (daily averaged data)	3.68-4.12	4.32-4.48
	AR(MA)X-models	3.79-4.06	4.07-4.20
	State space models (RC using LORD)	3.93	4.23
3	Multiple linear regression (hourly data)	4.77-5.24	
	Multiple linear regression (daily data)	3.73-4.39	
4	State space models	4.27-4.56	
5	Linear regression (daily averaged data)	3.99-4.08	
	State space models (RC using CTSM-R)	3.99	
6	State space models (RC using Matlab)	3.97	4.1-4.46
7	ARX-models	3.95	4.05-4.10
	State space models (RC using CTSM-R)	3.84	3.96
8	Averaging method	3.72-3.99	
	Linear regression (5'-data)	2.98-3.94	
	AR(MA)X-models	4.01-4.08	
	State space models (RC using CTSM-R)	4.48	
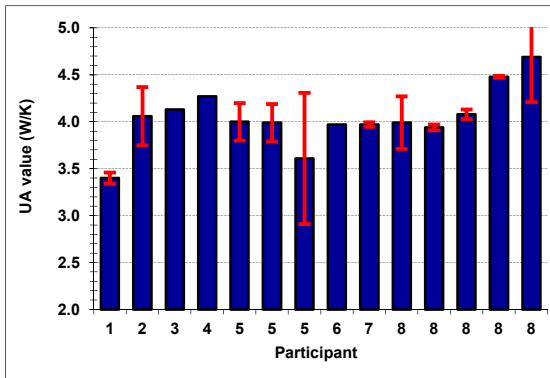
Figure 51: Summary of results from all participants using Winter Belgian data.
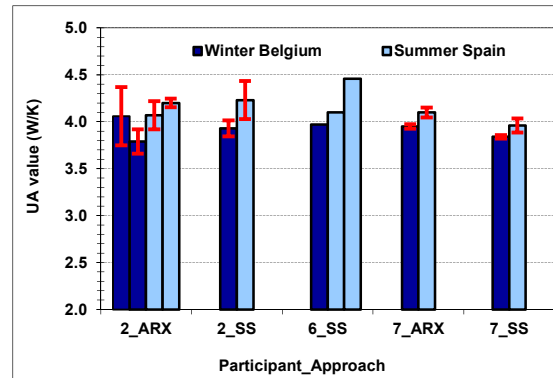
Figure 52: Results from participants that applied dynamic models to winter and summer data.

Some participants report results from different models. Results included in Figure 51 and Figure 52 are those identified as best results according to the discussion included in the report handled by participants. In other cases participants apply different analysis approaches in order to compare results. In these cases all the results are also included in the summary given in Figure 51 and Figure 52.

Apart from the overall heat loss coefficient, also the indoor air temperature has been predicted. Models identified on the basis of data corresponding to different test periods in Belgium and Spain have been used. Indoor temperature are predicted for a test carried out in Spain in Summer, which is different from the one used for identification. Note, that the measured indoor air temperatures in the predicted period was not available for the participants. The agreement between measured and predicted values is presented in Figure 53.

Taking into account the tendencies shown in Figure 53 and the average and standard deviations of the differences between predicted and measured values summarised in Table 10, it can be concluded that models identified using summer data perform better for the current case. This is attributed to the improved time resolution and accuracy on the measurement of heating power in the data used to identify this model.
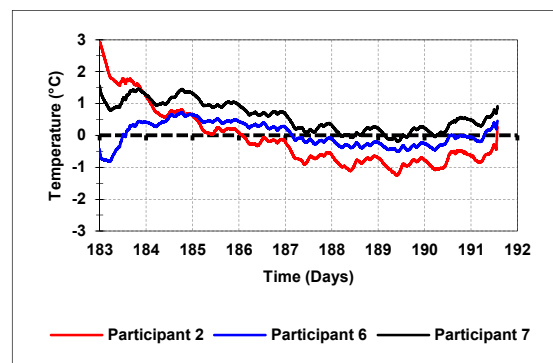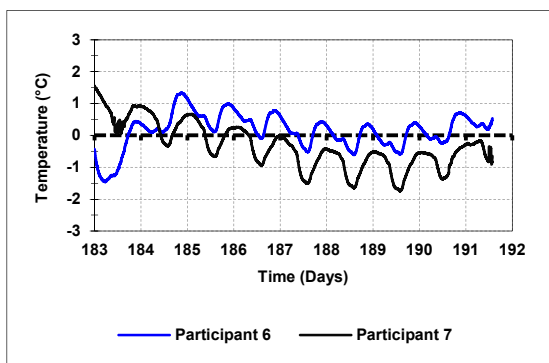
Figure 53: Difference between predicted and measured indoor air temperature, reported by participants. Left, using models based on Winter data. Right, using models based on Summer data. Predicted indoors temperature corresponds to a test carried out in Spain in Summer, which is different from the one used for identification.

Table 10: Averages and standard deviations of the difference between measured and predicted indoor air temperature reported by participants, using models based on Belgian and Spanish data. Predicted indoors temperature corresponds to a test carried out in Spain in Summer.

Participant	Model based on Summer Spanish data		Model based on Winter Belgian data	
	Mean (°C)	Stdv (°C)	Mean (°C)	Stdv (°C)
2	-0.108	0.896		
2	-0.435	0.471		
6	0.025	0.372	0.149	0.549
7	0.590	0.458	-0317	0.712

Further details on the analysis of this case study are reported in refs. 20 and 21.

6. Round Robin Tests: Tests at Laboratory for the Quality Control in Buildings of the Basque Government. Spain

6.1 Boundary conditions

6.1.1 Geographical location and coordinates

The Round Robin Test took place in the facilities of the Laboratory for the Quality Control in Building of the Basque Government, which is placed in Vitoria-Gasteiz (Spain). The coordinates of the test site are latitude: 42.868317, longitude: -2.675580. In Figure 54 it can be appreciated the placement of the sample.

Figure 54: Location of the sample.

For the test periods, the face of the test box with the window is placed to the South.
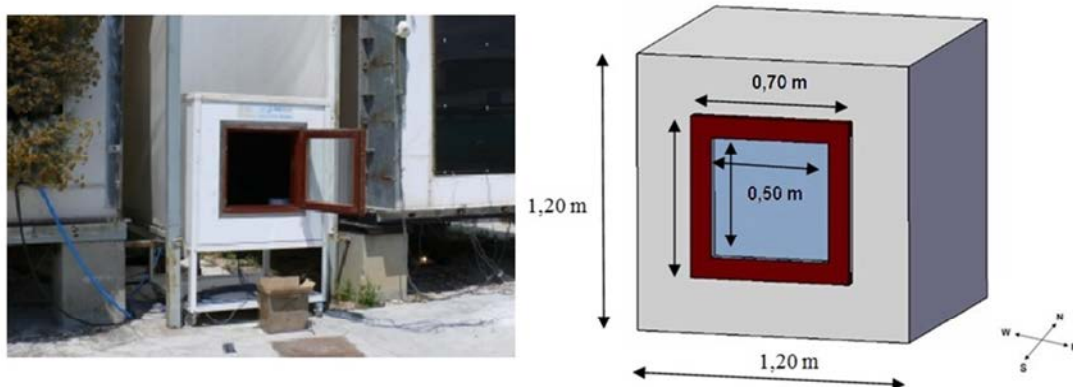
Figure 55: Installation of the Test Box (left) and dimensions of the box (right)

6.1.2 Periods of tests

Several tests have been carried out, including as in the previous test sites the following sequences:

1- FREE RUNNING TEST: There is no power generation inside the box. The test starts the 5th of August and finishes the 18th of August.

2- INDOORS AIR TEMPERATURE CONTANT SET POINT: a heat routine is produced inside the box with an infrared bulb achieving a constant temperature (40°C) inside the box. Test starts the 23th of August and finishes the 12th of September.

3- ROLBS POWER SEQUENCE. ROLBS Routine is produced inside the test box. It starts the 13th of September and finishes the 23th of September. ROLBS is a heating routine introduced in the interior of the sample to homogenize temperatures and disengage the behaviour of the sample to the environmental conditions. For security reasons, above 40°C internal energy generation turns off to prevent overheating. For more information on ROLBS see ref. 22 (Baker, 2008).

6.1.3 Measured meteorological variables

With the goal of having every point of the test under control, meteorological variables have been also recorded.

The Table 11 shows the instrumentation used with their technical characteristics.

Table 11: Technical characteristics of the instrumentation used to measure meteorological variables

Measured variable	Units	Type of Sensor	Uncertainty
Temperature	°C	PT100, A class, 4 wire connection	± 0.2 °C
Vertical Solar Radiation	W/m^2	Kipp and Zonen CMP11	± 3 %
Air speed	m/s	Ahlborn FVA-615-2 / Meteo Multi FMA510	± 0.5/± 0.3 m/s
Air Pressure	bar	Meteo Multi FMA510	± 0.5 mbar
Humidity	% rH	Meteo Multi FMA510	± 3 %
Rainfall	mm	Meteo Multi FMA510	± 5 %

As an example, some of the parameters are shown in the next images. All of them belong to the ROLBS test period. In Figure 56 it can be observed some meteorological data like the air pressure, rainfall and humidity during the test period (11 days).
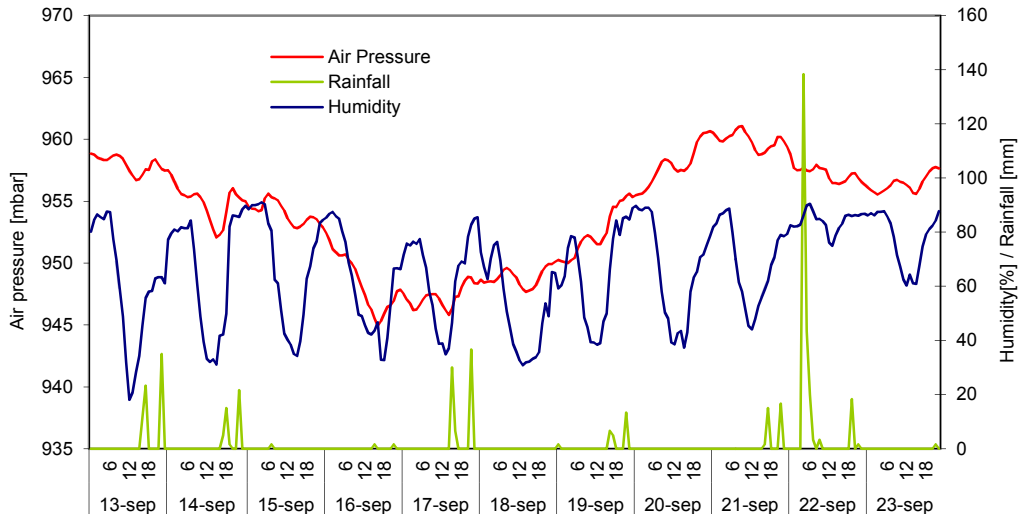
Figure 56: Meteorological data during ROLBS test period

Air speed has also been verified during the test period, having data from 2 different points at different heights (Figure 57).
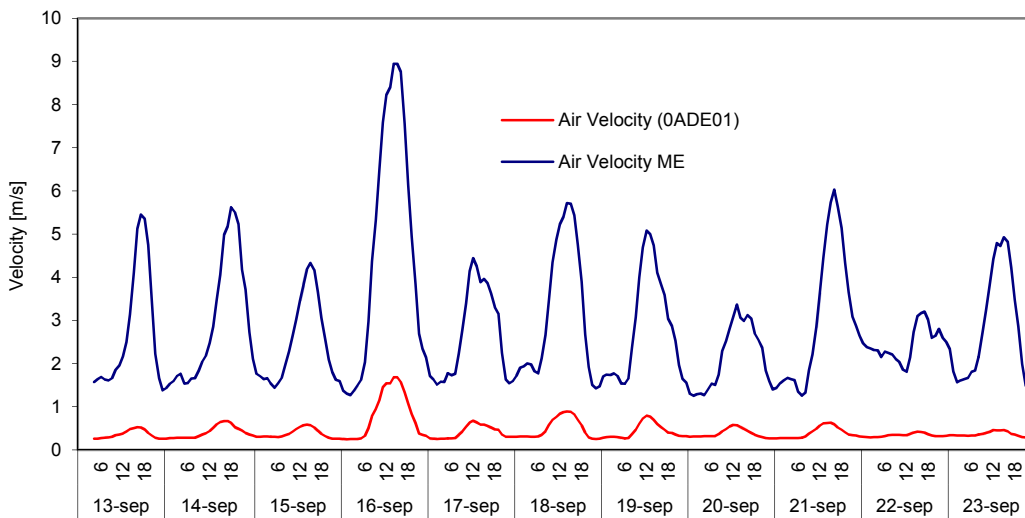
Figure 57: Air speed at different heights during ROLBS test period. 0ADE01 measured in front of the sample, ME measured at 10 m high.

Global solar radiation (both horizontal and vertical) is the next important parameter to keep an eye on. They are represented in the Figure 58.
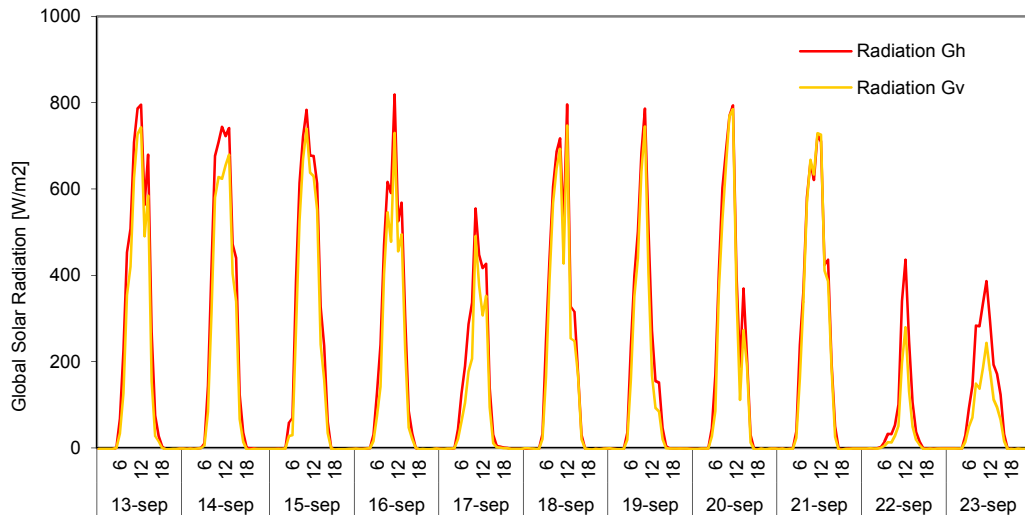
Figure 58: Global solar radiation during ROLBS test period

6.2 Measurements in the test box

6.2.1 Type, manufacturer, model and accuracy of each sensor

Suitable instrumentation has been installed for the proper thermal characterization of the sample. Temperature sensors and the heat flux meters have been calibrated in the facilities of the Laboratory.

To calculate the main parameters of the box, UA and gA, the instrumentation used with their technical characteristics is shown in the following table:

Table 2: Technical characteristics of the instrumentation used to measure test box variables

Measured variable	Units	Type of Sensor	Uncertainty
Surface Temperature	°C	PT100, A class, 4 wire connection	± 0.2 °C
Heat Flux	W/m^2	Ahlborn FQA-0801-H	± 5 %
Power Generation	W	Wattmeter SINEAX 536	± 0.2 %

6.2.2 Number of sensors, placement and nomenclature

The measured variables and the assigned names to each of them in the tests are listed below. The most important environmental conditions during the test period which have an effect in the thermal behaviour of the sample have been collected.

81

Table 12: Meteorological variables with their nomenclature

Name of the sensor	Measured variable
Gv	Global Vertical Radiation
H	Humidity
PR	Air Pressure
RF	Rainfall
Te	Outdoor Temperature
AV1	Wind speed at 2 meters height
AV2	Wind speed at 10 meters height

In the interior of the box the following instrumentation has been installed: 7 surface temperature sensors, 2 air temperature sensors, 2 heat flux meters and 1 wattmeter.

Table 13: Interior test box instrumentation with their nomenclature and placement

Name of the sensor	Measured variable
IST1	Interior Surface Temperature - East
IST2	Interior Surface Temperature - North
IST3	Interior Surface Temperature - West
IST4	Interior Surface Temperature - Ceiling
IST5	Interior Surface Temperature - Bottom
IST6	Interior Surface Temperature - Window frame
IST7	Interior Surface Temperature - Window Glass
IAT1	Interior air Temperature 1/3 height
IAT2	Interior Air Temperature 2/3 height
HF1	Heat Flux West
HF2	Heat Flux North
PG	Power Generation

Figure 59: Assembly of the instrumentation in the interior of the test box

There are 6 surface temperature sensors and 2 air temperature sensors in the exterior of the Test Box.

Table 14: Exterior test box instrumentation with their nomenclature and placement

Name of the sensor	Measured variable
EST1	Exterior Surface Temperature - North
EST2	Exterior Surface Temperature - West
EST3	Exterior Surface Temperature - East
EST4	Exterior Surface Temperature - Ceiling
EST5	Exterior Surface Temperature - Window Frame
EST6	Exterior Surface Temperature - Window glass
EAT1	Exterior Air Temperature - West
EAT2	Exterior Air Temperature - North

Figure 60: Assembly of the instrumentation in the exterior of the test box

6.2.3   Protection of sensors to improve the quality of measurements

In order to improve the quality of measurements, the following actions have been taken into account:

1. Recover with Low emissivity tape every temperature sensors which are receiving direct solar influence. See section 11.1 of chapter 11 for further information of measurement temperatures of surfaces hit by solar radiation.

Figure 61: Detail of the recovering of the temperature sensors

2. Use of Uninterruptible Power Supply (UPS) to avoid the electronic devices stop working when disturbances on the grid happen. The UPS model used is CEGASA DANUBIO 700.

Figure 62: CEGASA DANUBIO 700 UPS

6.3 Data acquisition system

6.3.1 Type, manufacturer, model, range of measurement and resolution

Type, manufacturer, model, range of measurement and resolution

It is used a multimeter Agilent 34980A, with multiplexer cards 34921A and connection terminals 34921T. Its technical characteristics are shown in the next table.

Table 15: Technical characteristics of the data acquisition system

Measured variable	RANGE	Resolution	Error
Voltage DC	100 mV	0.1 μV	4 μV
	1 V	1 μV	7 μV
	10 V	0.01 mV	0.05 mV
	100 V	0.1 mV	0.6 mV
	300 V	0.1 mV	9 mV
Intensity DC	10 mA	0.01 μA	2 μA
	100 mA	0.1 μA	5 μA
	1 A	1 μA	100 μA
Resistance	100 kΩ/1mA	0.0005 Ω	0.005 Ω
	1 MΩ/1mA	0.0001 Ω	0.005 Ω
	10 MΩ/100μA	0.0001 Ω	0.005 Ω

Figure 63: Data Acquisition system (Agilent 34980A)

6.4 Heating device and sequences

It is necessary to introduce, in some way, heat in the interior of the box, to generate the heat sequences that will generate enough temperature differences between the interior and the exterior so as to produce reliable data sets for data analysis.

A wattmeter let us know the power generation provided by an infrared bulb inside the box, achieving high temperature differences between the interior and the exterior of the box.

It is used a programmable multi-transducer SINEAX M562 (Figure 64) to measure the heat generation.

Figure 64: Programmable multi-transducer SINEAX M562

The used element to provide heat is an infrared bulb, model OSRAM SICCATHERM 150W. The bulb was placed inside of a little box, avoiding the bulb to provide direct radiation to the walls of the test box. The little box had holes in the inferior part letting the hot air scape to the interior of the sample. The bulb is shown in Figure 65.

Figure 65: Infrared bulb (OSRAM SICCATHERM 150W)

As an example, in the next Figure 66 it can be observed the heating routine, with a random profile.

Figure 66: Power generation by infrared bulb inside the box during ROLBS test period. See section 11.6.1 of chapter 11 for further information on averaging and filtering.

6.5 Data files

All the recorded data is saved in ".csv" files. Every day is generated one ".csv" file and it contains data of all the parameters from every minute of the day. The next Figure 67 shows how it is the file structured.

	A	B	C	D	E	F	G	H	I	J	K	L	M	N	O	P
1	DATA	TIME	Te	H	PR	AV2	RF	Gv	AV1	IST1	IST2	IST3	IST4	IST5	IST6	IST7
2	13/09/2014	0.5	15.1	80.2	958.9	1.3	0	0	0.25	34.85	34.75	33.92	34.67	34.72	34.4	31.51
3	13/09/2014	1.5	14.3	84.4	958.8	1.6	0	0	0.25	34.07	33.97	33.22	33.84	33.88	33.54	30.67
4	13/09/2014	2.5	13.4	86.5	958.5	1.7	0	0	0.26	33.28	33.19	32.5	33.03	33.06	32.69	29.85
5	13/09/2014	3.5	13.2	85.6	958.4	1.7	0	0	0.26	32.48	32.4	31.75	32.24	32.25	31.85	29.15
6	13/09/2014	4.5	12.1	84.8	958.3	1.6	0	0	0.26	31.69	31.62	31.01	31.45	31.44	31.03	28.36
7	13/09/2014	5.5	9.6	87.6	958.3	1.7	0	0	0.25	30.91	30.84	30.26	30.7	30.65	30.23	27.6
8	13/09/2014	6.5	11.6	87.4	958.5	1.8	0	34.44	0.33	30.17	30.1	29.56	29.95	29.92	29.45	27.29
9	13/09/2014	7.5	12.7	77.3	958.7	1.4	0	126.99	0.3	29.53	29.45	28.95	29.35	29.32	28.73	28
10	13/09/2014	8.5	15.5	69.5	958.8	1.6	0	353.71	0.32	29.16	29.04	28.53	29.11	28.99	28.24	32.83
11	13/09/2014	9.5	18	59.2	958.7	1.8	0	420.11	0.35	29.07	28.92	28.45	29.3	28.91	28.15	35.44
12	13/09/2014	10.5	20.6	48.9	958.4	2.7	0	625.49	0.41	29.37	29.19	28.6	30.02	29.07	28.61	39.32
13	13/09/2014	11.5	22.8	31.9	958	2.3	0	727.04	0.42	30.19	29.91	28.98	31.42	30.47	29.52	42.63
14	13/09/2014	12.5	24.4	18.1	957.5	2.5	0	742.45	0.41	31.29	30.88	29.6	32.89	33.32	30.66	44.64
15	13/09/2014	13.5	26.2	20.8	957.1	3.3	0	490.21	0.5	32.27	31.82	30.32	34.1	34.32	31.8	43.39
16	13/09/2014	14.5	25.8	28.4	956.7	5	0	584.68	0.66	32.97	32.53	31.1	34.9	34.53	32.78	43.61
17	13/09/2014	15.5	23.3	34.2	956.8	7.5	0	155.19	0.55	33.5	33.1	31.66	35.32	34.62	33.62	38.95
18	13/09/2014	16.5	23.7	45.6	957.2	7.4	11.7	27.66	0.53	33.61	33.23	31.81	35.05	34.37	34.07	34.21

Day of the test — *Nomenclature of the parameter*

Time treated hourly — *Data*

Figure 67: Information contained in ".csv" files

87

7. Measurements in climatic chamber at CTU

7.1 Introduction

CTU Prague performed experiments when the outdoor climate was created artificially by climatic chamber. All the tests were performed at University Centre for Energy Efficient Buildings (UCEEB) in Buštěhrad during winter and spring 2015.

Figure 68: RRTB in the climatic chamber at UCEEB

7.2 Measurement description

7.2.1 Experiments

The round robin test box was exhibited to a series of steps in the external temperature and power of the internal heat source according to Table 16. The internal temperature was approximately kept identical by replacing the bulbs inside the heat source. Each temperature step should end up in steady state situation. The steady state theoretically occurs after infinitely long time. The reasonable duration of one experiment was 4 days - see further explanation in section 7.3.2.

Internal heat source was built from steel pipe (diameter 200 mm, length 650 mm). The pipe wall was painted matt black colour. The heat was released from three electric bulbs hanging inside the pipe. The nominal power of three bulbs (25, 40, 60, 100 W) was combined so that the desired value of heat flow was set. The top of the pipe was equipped with small electric fan so that the air was blown from top to bottom. The bottom of the pipe was finished by diffusor made of circular OSB plates. The heat from such a heat source is released radiatively and convectively from the pipe wall and convectively due to the forced convection between the internal air and the air inside the pipe.

Step	T_i (°C)	Φ_p (W)	T_e (°C)	T_m (°C)	Start time	End time	Duration
1	28.8	172	-17.1	5.8	19.01.2015 14:30	26.01.2015 11:55	≈ 7 days
2	27.8	148	-11.5	8.1	29.01.2015 09:59	02.02.2015 11:34	≈ 4 days
3	26.9	104	-0.5	13.2	03.02.2015 15:37	09.02.2015 14:53	≈ 6 days
4	26.9	89	3.3	15.1	11.02.2015 12:02	17.02.2015 15:18	≈ 6 days
5	28.5	130	-6.2	11.2	25.02.2015 09:18	03.03.2015 14:29	≈ 6 days
6	51.1	168	11.0	31.1	12.03.2015 14:12	16.03.2015 10:00	≈ 4 days
7	49.7	150	14.0	31.8	16.03.2015 15:00	21.03.2015 12:45	≈ 5 days
8	50.2	207	0.3	25.3	02.04.2015 10:25	08.04.2015 07:44	≈ 6 days

Figure 69: Setup of the internal heat source

7.2.2 Sensors

A list of sensors is included in Table 17. All air temperature sensors were shielded against radiation. The surface temperature sensor was a very small element closed in transparent cover. The surface temperature sensors were attached by black tape. Only one sensor for each surface was used (attached near the centre of each surface). Heat flux sensors were attached by double side tape and tape stripes over sensor sides.

Table 17: List of sensors

Group	Name	Unit	Type
Internal air	Tai_75cm	°C	Sensit TG3B Pt1000 A 4-wire
	Tai_30cm	°C	
	Tai_08cm	°C	
	Tai_51cm	°C	Rotronic HygroClip HC2-S
	Rhai_51cm	%	
Internal surfaces	Tsi_floor	°C	Sensit TR097 Pt1000 A 4-wire
	Tsi_window	°C	
	Tsi_wall_right	°C	
	Tsi_wall_left	°C	
	Tsi_ceiling	°C	
	Tsi_wall_rear	°C	
	q_floor	W/m^2	Hukseflux HFP01-05
	q_wall_left	W/m^2	
	q_wall_right	W/m^2	
	q_window	W/m^2	
Surface of heat source	Tsi_source_up	°C	Sensit TR097 Pt1000 A 4-wire
	Tsi_source_bottom	°C	
External environment	Tae_140 cm	°C	Rotronic HygroClip HC2-S
	RHae_140 cm	%	
	Tse_floor	°C	Sensit TR097 Pt1000 A 4-wire
	Tse_wall_left	°C	
	Tse_wall_right	°C	
	Tae_leftside	°C	Sensit TG3B Pt1000 A 4-wire
	Tae_rear	°C	
	Tae_rightside	°C	
	Tae_roof	°C	
	Tae_bottom_sheet	°C	
Wattmeter	Qp	W	Hameg HM 8115

Accuracy according to manufacturer information is listed hereafter in Table 18.

Sensor	Accuracy	Manufacturer
Temperature sensors	± 0.15 °C + 0.002|T|, T in degrees of Celsius	Sensit s.r.o.
Combined temperature and relative humidity sensors	±0.1 °C, ±0.8 % from measured value of relative humidity, at 23 °C ± 5°C	Rotronic
Heat flux sensors	±5% from measured value	Hukseflux
Wattmeter*	±0.5% from measured value + 10digits	Hameg

*A small systematic error is caused by AC/DC adapter for electric fan. The adapter is plugged so that the power is registered by power meter, but waste heat from adapter is not released inside RRTB. The estimated effect of this bypassing is less than 0.3W.

7.2.3 Data acquisition system

Data acquisition system was Datataker DT85 (http://www.datataker.com).

7.3 Data analysis

7.3.1 Measured data

Some of the measured data are depicted in Figure 70 to Figure 73. Grey areas indicate the steps in external temperature and heat flow. Periods from which data were further used in the calculation of HLC are marked by red rectangles (see Table 19).
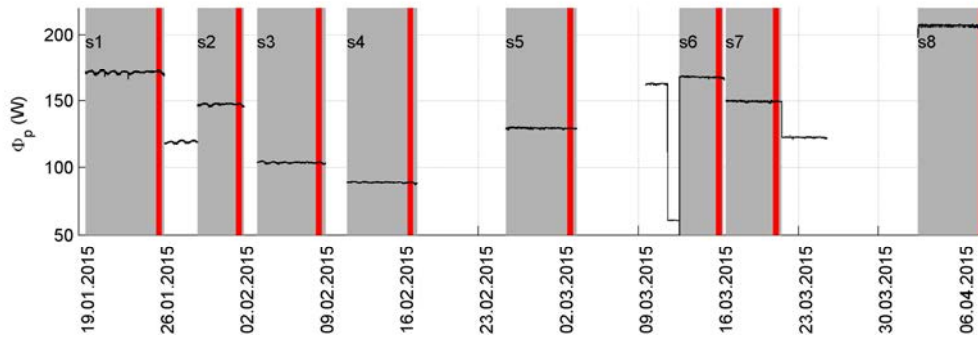
Figure 70: Heat flow
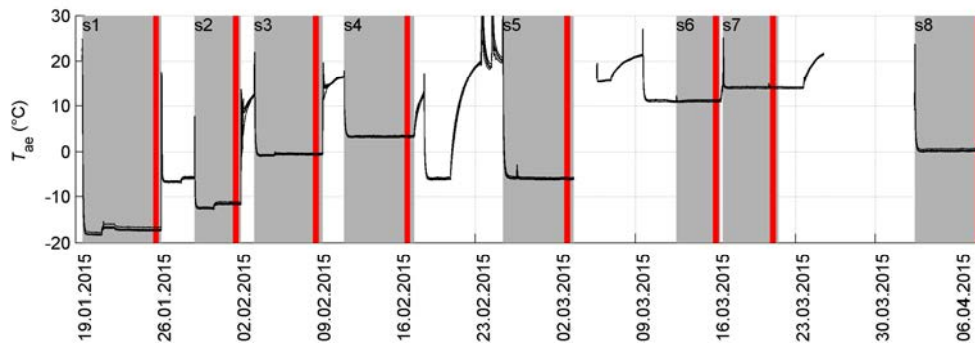
Figure 71: External air temperatures
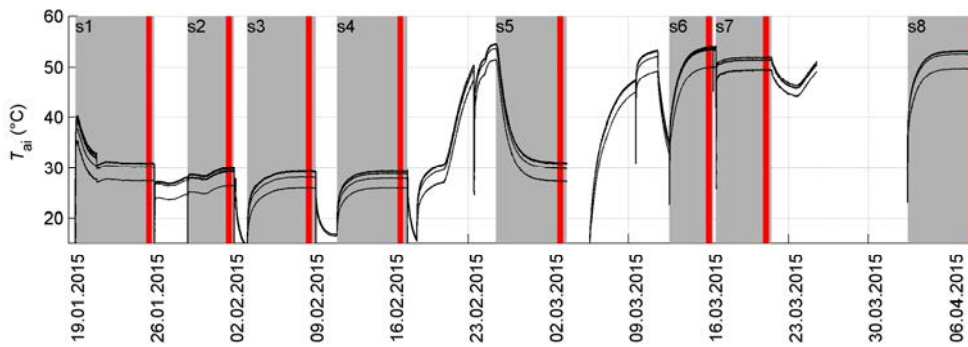
Figure 72: Internal air temperatures
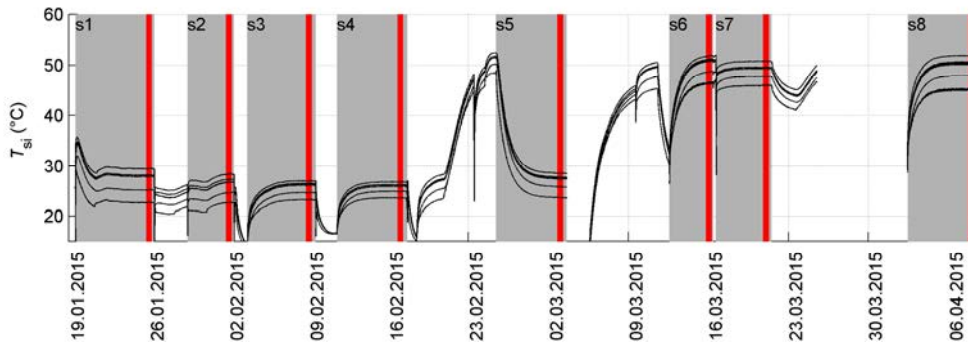
Figure 73: Internal surface temperatures

Table 19: Data used for calculation of HLC

Step	Start time	End time
1	2015.01.25;19:00:00	2015.01.26;06:59:00
2	2015.02.01;19:00:00	2015.02.02;06:59:00
3	2015.02.08;19:00:00	2015.02.09;06:59:00
4	2015.02.16;19:00:00	2015.02.17;06:59:00
5	2015.03.02;19:00:00	2015.03.03;06:59:00
6	2015.03.15;19:00:00	2015.03.16;06:59:00
7	2015.03.20;19:00:00	2015.03.21;06:59:00
8	2015.04.07;19:00:00	2015.04.08;06:59:00

7.3.2 Minimal duration of the step

The important systematic error could arise if the experimental step is stopped too early, i.e. before reaching the steady state. The estimation of time needed to approach steady state can be based on the balance equation:

$$C\frac{\mathrm{d}T_i}{\mathrm{d}t} = \Phi_p - HLC(T_i - T_e)$$

(10)

where C (J/K) is thermal capacity of the box, HLC (W/K) is heat loss coefficient of the box, Φ_p(W) is heat flow from internal heat source, T_i is internal temperature and T_e is external temperature. The solution for step change in internal heat gain ($\Phi_p(t>0)= \Phi_p$) and external temperature ($T_e(t>0)= T_e$) is:

$$T_i(t) = T_e + \frac{\Phi_p}{HLC} + (T_{i0} - T_e - \frac{\Phi_p}{HLC})e^{-\frac{1}{\tau_c}t}$$

(11)

where τ_c (s) is time constant of RRTB (ratio C/HLC) and T_{i0} is initial internal temperature. Temperature $T_e + \Phi_p/HLC$ is the value of the internal temperature in steady state (see Figure 74). So, we can rewrite the equation to:

$$\Delta(t) = T_i(t) - \overline{T_i} = (T_{i0} - \overline{T_i})e^{-\frac{1}{\tau_c}t}$$

(12)

Difference between actual internal temperature and steady state temperature is minimized either when exponential term diminished, or initial internal temperature is close to the steady state temperature.
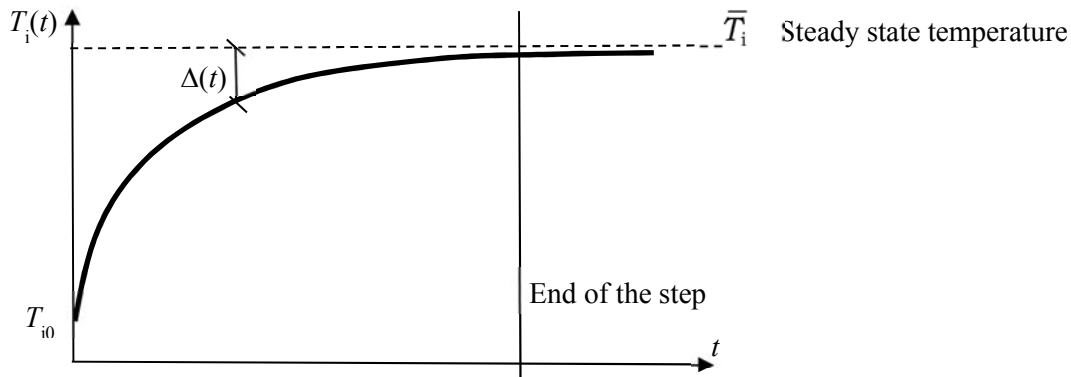
Figure 74: Temperature buildup compared with steady state limit

Some values of e^{-x} are: $e^{-3} \approx 0.05$; $e^{-4} \approx 0.02$. Time constant of the box is approximately one day (based on the previous data analysis performed with state space models in other common exercises). It means the internal temperature will exhibit more than 95 % of its move to steady state value after more than 3×24 h = 3 days. Therefore, data recorded after start of the experimental step should cover at least four days.

Example: HLC = 4 W/K, T_{i0} = 15 °C, T_e = 0 °C

1) Φ_g = 120 W

$\overline{T_i}$ = 0 +120 /4 = 30 °C

$\Delta(3\ d) = (15 - 30)e^{-3} = -15 \cdot 0.05 = -0.75$ °C

$\Delta(4\ d) = (15 - 30)e^{-4} = -15 \cdot 0.018 = -0.27$ °C

2) Φ_g = 200 W

$\overline{T_i}$ = 0 +200 /4 = 50 °C

$\Delta(3\ d) = (15 - 50)e^{-3} = -35 \cdot 0.05 = -1.75$ °C

$\Delta(4\ d) = (15 - 50)e^{-4} = -35 \cdot 0.018 = -0.63$ °C

7.3.3 Calculation model for estimation of HLC

The value of heat loss coefficient for RRTB is not measured directly. HLC is calculated assuming that the thermal balance of RRTB in steady state is:

$$\Phi_p - HLC(T_i - T_e) = 0 \tag{13}$$

The heat loss coefficient is thus power released from internal heat source related to temperature difference between internal and external environment:

$$HLC = \frac{\Phi_p}{T_i - T_e} \tag{14}$$

Since in reality the measured temperatures in the internal environment of the box are spatially different, the term internal temperature should represent the equivalent internal temperature somehow composed from distinct measured values. Similarly, the external temperature should represent the equivalent external temperature. Since the surfaces in climatic chamber had very similar temperature with air temperature in climatic chamber the external equivalent temperature around RRTB was represented by mean air temperature. The definition of internal temperature is of high importance since it influences the value of HLC.

The thermal network in Figure 75 depicts how the heat is released from the heat source towards surface 1. For simplicity the internal surface temperatures (surfaces 2 – 6) were already aggregated together into one value $T_{si,2\text{-}6}$ in the scheme. The surface temperature of the heat source T_s, the internal air temperature close to the surface 1 $T_{ai,1}$, and internal

surface temperatures T_{si} are known since they are measured during experiments. Of course, there is some uncertainty since the surface temperatures were measured only at the centre of the wall and the surface temperature of the heat source was measured only at two points.
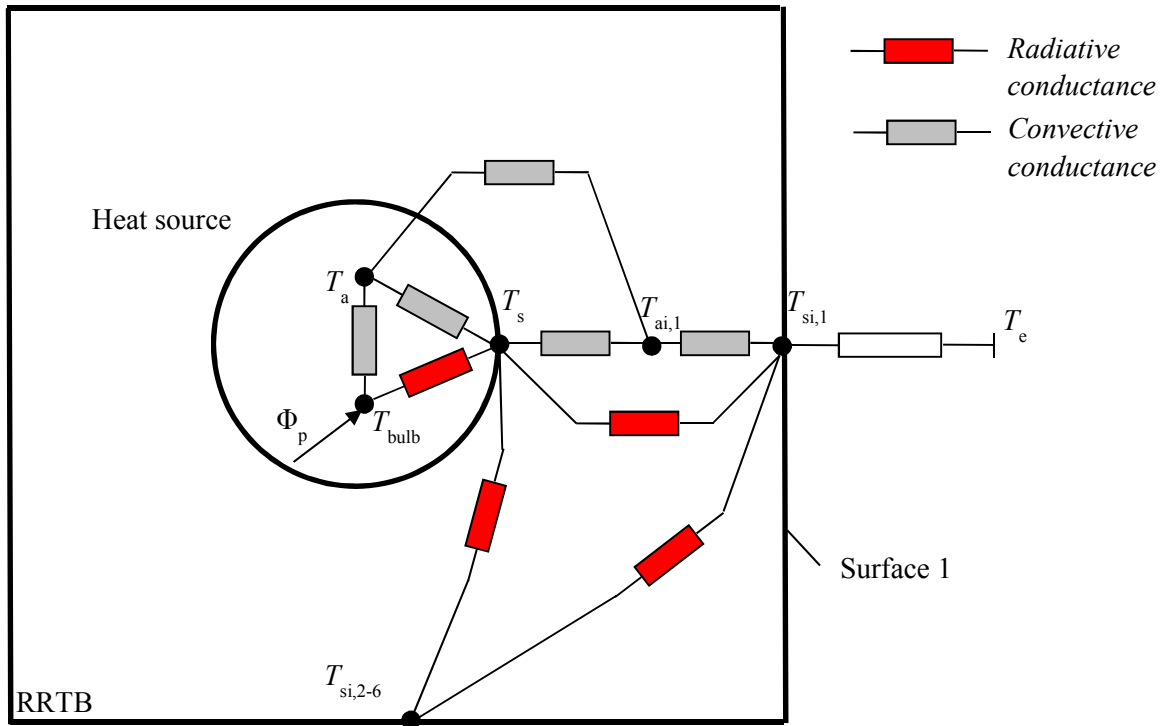
Figure 75: Thermal circuit of the problem

If one omits all the heat flow paths which do not directly influence the internal surface temperature $T_{si,1}$ the thermal circuit can be represented as depicted in Figure 76.
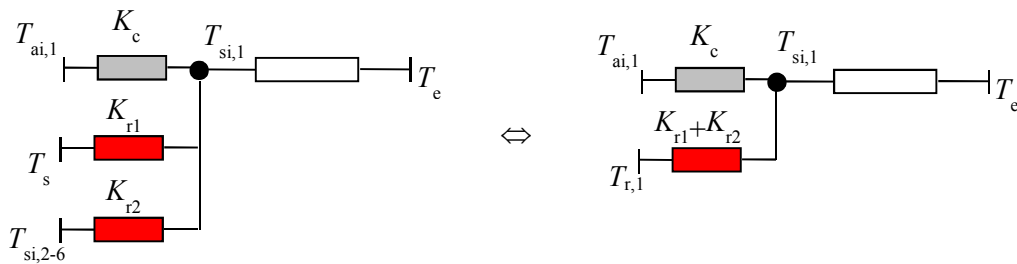
Figure 76: Equivalent thermal circuits

The surface temperatures T_s and $T_{si,2-6}$ can be replaced by equivalent temperature, often called mean radiant temperature for surface 1:

$$T_{r,1} = \frac{K_{r1}T_s + K_{r2}T_{si,2-6}}{K_{r1} + K_{r2}} \tag{15}$$

Example: Mean radiant temperature for the wall (surface 1). It is assumed that the heat source and surface 1 act like black bodies. Thermal conductance K_{r2} can be estimated as: $K_{r2} = A_1 4\sigma((T_{si,2-6}+T_{si,1})/2)^3 = (6 \div 7)A_1 = (6 \div 7)\times 0.92 = 5.5 \div 6.4$ W/K.

Thermal conductance K_{r1} can be estimated as: $K_{r1}=A_sF_{s\to s1}4\sigma((T_s+T_{si,1})/2)^3$ $=(6\div7)A_sF_{s\to s1}$. The value for view factor between heat source and surface 1 will be lower than 0.25, therefore $K_{r1}=(6\div7)\times0.42\times0.25 = 0.63 \div0.73$W/K. It is therefore estimated that mean radiant temperature is composed only by 10% from surface temperature of heat source. The following temperatures were typically observed in the RRTB: $T_s \approx 40$ °C, $T_{s,2-6} \approx 26$ °C, $T_{ai}\approx29$°C. It translates to mean radiant temperature $T_{r1} = 0.9\times26+0.1\times40 = 27.4$°C.

Mean radiant temperature and air temperature are now replaced by internal temperature for surface 1 (see Figure 77).
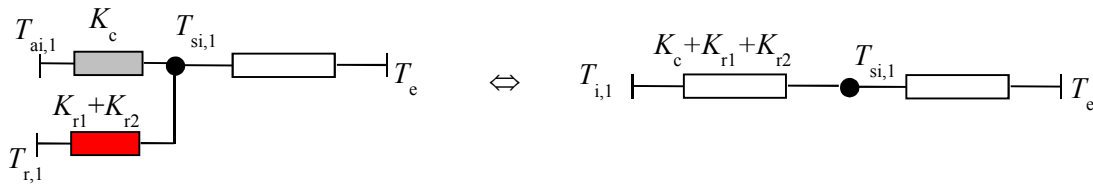
Figure 77: Equivalent thermal circuits

$$T_{i,1} = \frac{K_cT_{ai,1} + K_{r1}T_s + K_{r2}T_{s,2-6}}{K_c + K_{r1} + K_{r2}} \text{ or } T_{i,1} = w_1T_{ai,1} + w_2T_{s,2-6} + w_3T_s \qquad (16)$$

where w denotes weights.

Example: Internal temperature for the wall of RRTB. The convective conductance can be estimated as: $K_c = (2\div3)A_1= (2\div3)\times 0.92 = 1.8\div2.8$ W/K. The values of radiative conductances K_{r1} and K_{r2} were already estimated in the previous example. The estimated weights thus are:

Table 20: Estimated weights for calculation of $T_{i,1}$

w_1	w_2	w_3
0.23 ÷ 0.28	0.64 ÷ 0.69	1- w_1 - w_2

The internal temperature for wall is: $T_{i,1} = 0.25\times29 + 0.66\times26 + 0.09\times40 = 28$ °C. It seems that for the configuration of heat source in the RRTB the internal temperature for wall is probably rather close to the internal air temperature. However, it may not be true for co-heating test performed in real houses. Depending on the insulation thickness of the fabric, the internal temperature will be lower than the internal air temperature, especially in poorly insulated houses.

Now, it remains to derive how the total internal temperature of RRTB should be calculated from local values of the internal temperature for building component. Several heat transfer paths act in parallel, see Figure 78.
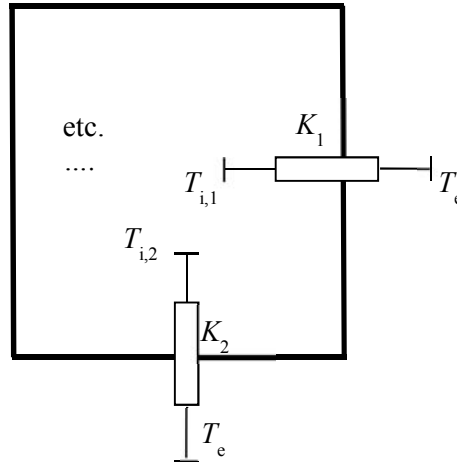
Figure 78: Parallel heat transfer paths through RRTB fabric

$$K_1(T_{i,1} - T_e) + K_2(T_{i,2} - T_e) + \dots = \left(K_1 + K_2 + \dots \right)(T_i - T_e) \qquad (17)$$

$$\frac{K_1 T_{i,1e} + K_2 T_{i,2} + \dots}{K_1 + K_2 + \dots} - T_e + \dots = T_i - T_e \qquad (18)$$

The total internal temperature of RRTB is weighted mean of individual internal temperatures for given surface according to local total heat loss coefficients of each external building component. However, the composition of RRTB was not known to participants of Annex 58. The box is nonetheless a perfect cube and five walls are assumed to have identical composition. Therefore, the total internal temperature of the RRTB can be roughly estimated as arithmetic mean from internal temperatures for each component:

$$T_i \approx \frac{T_{i,1} + T_{i,2} + \dots + T_{i,6}}{6} \qquad (19)$$

7.3.4 Uncertainties

The following uncertainties can be distinguished:

- uncertainty due do inaccuracy of sensors (accuracy stated by manufacturer),
- uncertainty due to the improper installation of sensors,
- uncertainty due to the fuzzy definition of internal temperature and external temperature,
- and uncertainty associated with the assumption of steady state.

The uncertainty that the experiment was not in steady state was not taken into account in the calculated values of *HLC* since the experiments were long enough to expect this error should be reasonably low.

The external temperature (equivalent temperature of the environment surrounding the RRTB) was calculated as mean value from all air temperature sensors placed in the climatic chamber. According to manufacturers, the used sensors have accuracy: ± 0.15 °C + 0.002|T|, *T* in degrees of Celsius. In calculation of HLC the temperature dependency was neglected. Instead, it was conservatively assumed the accuracy ±0.20 °C. The uniform probability was assumed between limit values. Standard deviation for uniform distribution is ±0.20/√3 = ±0.12 °C. This uncertainty should propagate through calculation of mean value from distinct air temperature sensors. The result would be lower value than 0.12 °C as

uncertainties likely compensate each other. Instead it was assumed the maximal value ±0.12 °C as uncertainty in the mean value of external air temperature.

The heat flow was measured by wattmeter HAMEG HM 8115. According to manufacturer the accuracy is: ±0.5% from measured value + 10×precision. Precision at used measuring range was 100mW. For example: (0.5/100)×200 W +10×(100/1000) = 1 + 1 = 2 W.

The uncertainty in the definition of the internal temperature is expected to be rather important. The exact values of weights w_1, w_2 are uncertain (see Table 20) and the measured values of temperatures are the subject of uncertainty as well. For uncertainty in internal air temperatures the uniform probability between -0.20°C and +0.20°C was assumed. For the surface temperature of the external building components somewhat higher uncertainty can be expected since the measured values were recorded only at one central point of building component. The uniform probability between -1°C and +0.3°C was assumed since it is more likely that the measured value of the internal surface temperature overestimates the real mean internal surface temperature due to the colder places near junctions between building components. For surface temperature of heat source even larger uncertainty could be expected since only two temperature sensors were used for measurement. Moreover, the temperature of the cylinder was not very uniform due to the local heat sources inside (three electric bulbs) and due to the low thickness of the metal. And finally, during some of the experiments with higher internal temperature, the tape attaching the sensor with heat source surface did not sustain hot environment and the sensor fell down. For uncertainty in surface temperature of heat source the uniform probability between -2°C and 2°C was assumed.

To evaluate how the input uncertainties propagate in the internal temperature the samples were randomly generated (by latin hypercube sampling) from the estimated weights in and from expected uncertainty of temperature measurements as specified above. Then, the internal temperature for each surface and finally total internal temperature in RRTB were calculated for each sample - see the example for step 3 and step 6 in Figure 79.
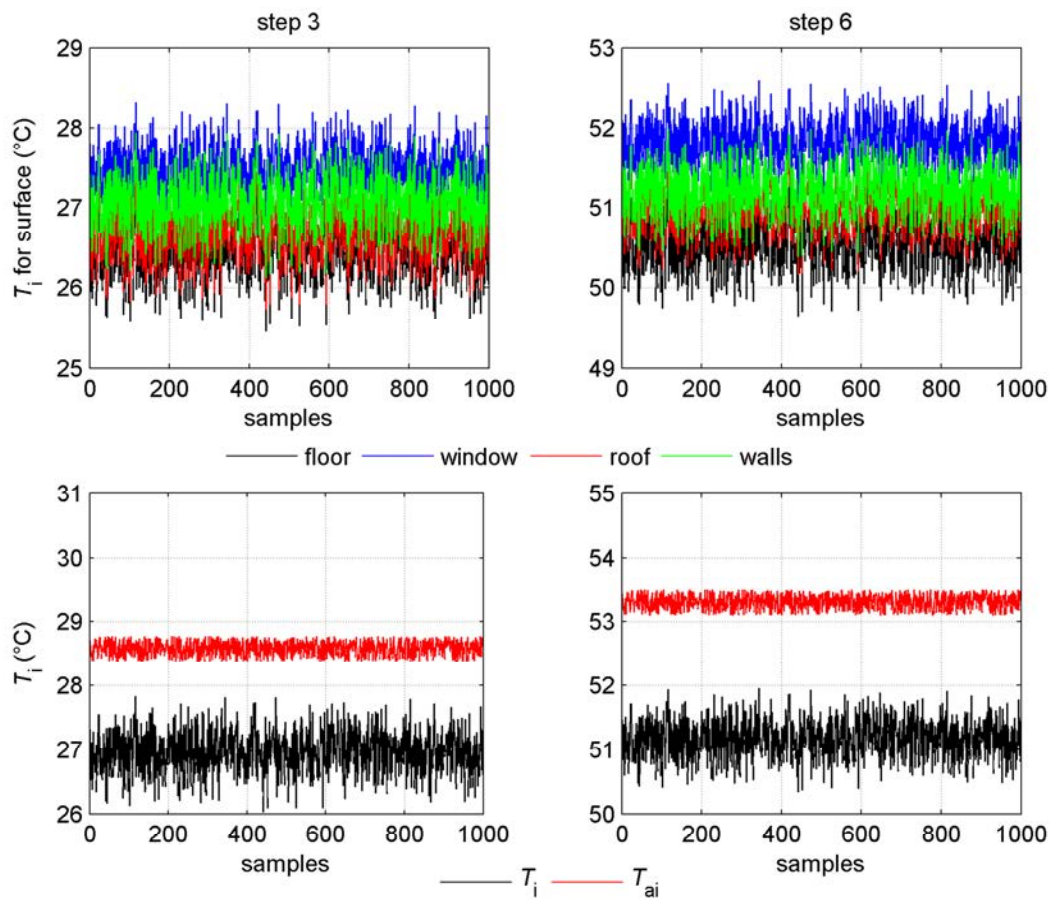
Figure 79: Internal temperature for given surface and total internal temperature compared with internal air temperature

The uncertainty in the internal temperature was estimated as one standard deviation from the values of T_i (see Figure 80).
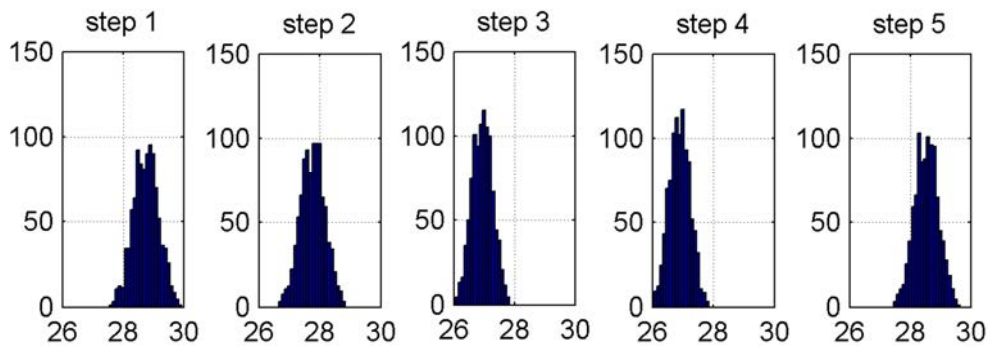
Figure 80: Distribution of the internal temperature for step 1 to step 5 (based on 1000 samples)

7.3.5 Measured values of HLC

The mean value of HLC was calculated according to equation (13). The total uncertainty of HLC was calculated as:

$$u_c = \sqrt{\left(c_1 \delta \Phi_p\right)^2 + \left(c_2 \delta T_i\right)^2 + \left(c_3 \delta T_e\right)^2} \tag{20}$$

where sensitivity coefficients are partial derivatives with respect to each variable in equation (13):

$$c_1 = \frac{1}{T_i - T_e} \tag{21}$$

$$c_2 = -\frac{\Phi_p}{\left(T_i - T_e\right)^2} \tag{22}$$

$$c_3 = \frac{\Phi_p}{\left(T_i - T_e\right)^2} \tag{23}$$

The expanded uncertainty is calculated as:

$$U = k_p u_c \tag{24}$$

where coverage factor k_p was assumed to be $k_p = 2$ (95 % measurements will fall into interval specified by the expanded uncertainty).

The results are specified in Table 21 and Table 22. Moreover, the results are depicted in Figure 81. The red points in Figure 81 are the values of HLC when the mean surface temperature was assumed to be the internal temperature. The blue points in Figure 81 are the values of HLC when the mean internal air temperature was assumed to be equal to the internal temperature.

Table 21: Heat loss coefficient of RRTB

step	Φ_p	T_i	T_e	HLC
nr	(W)	(°C)	(°C)	(W/K)
1	172.2	28.8	-17.1	3.75
2	147.6	27.8	-11.5	3.75
3	104.0	26.9	-0.5	3.78
4	89.1	26.9	3.3	3.78
5	129.9	28.5	-6.1	3.75
6	167.6	51.2	11.0	4.18
7	149.7	49.7	14.0	4.20
8	206.7	50.2	0.3	4.14

Table 22: Expanded uncertainty U

step	$\delta\Phi_p$	δT_i	δT_e	c_1	c_2	c_3	u_c	U
nr	(W)	(°C)	(°C)	(1/K)	(W/K^2)	(W/K^2)	(W/K)	(W/K)
1	1.1	0.41	0.12	0.022	-0.082	0.082	0.042	0.08
2	1.0	0.39	0.12	0.025	-0.096	0.096	0.047	0.09
3	0.9	0.34	0.12	0.036	-0.138	0.138	0.058	0.12
4	0.8	0.34	0.12	0.042	-0.161	0.161	0.067	0.13
5	1.0	0.38	0.12	0.029	-0.108	0.108	0.051	0.10
6	1.1	0.31	0.12	0.025	-0.104	0.104	0.044	0.09
7	1.0	0.29	0.12	0.028	-0.118	0.118	0.047	0.09
8	1.2	0.28	0.12	0.020	-0.083	0.083	0.035	0.07
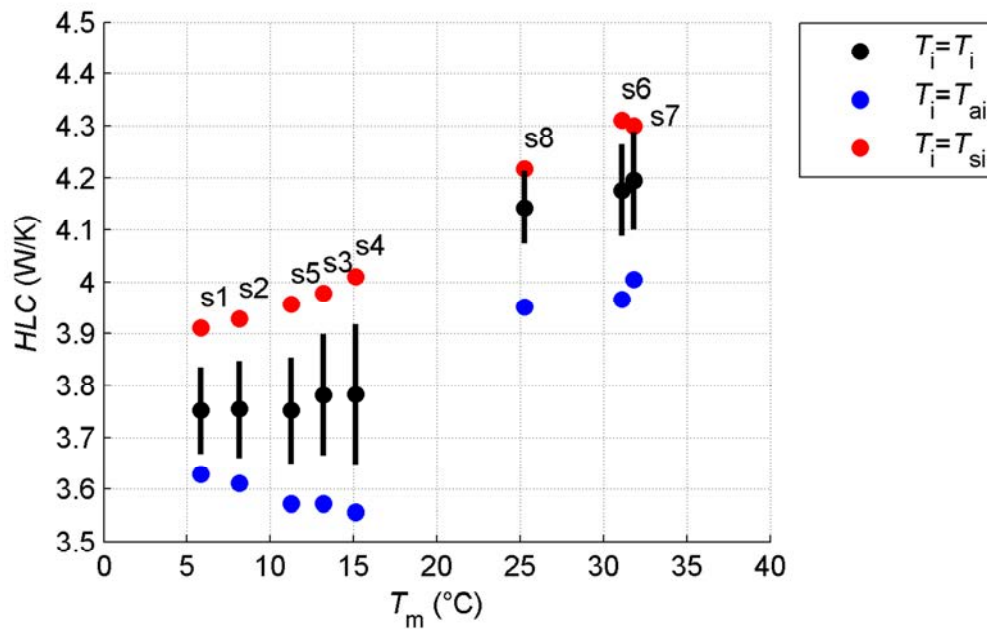
Figure 81: Measured values of HLC with expanded uncertainty ($k_p = 2$)

8. Twin house at Fraunhofer IBP experimental facility

8.1 Introduction

This chapter deals with the experiment used to support common exercise 5 in Subtask 3, which is based on one of the experiments carried out in one of the Twin Houses at IBP Fraunhofer in Germany, also considered for validation exercises in Subtask 4.1 described in (Ref. 23). The building and its heating and ventilation systems, experiment design, measurement devices, test sequences, and data are not described here in detail to avoid repetitions, because all this information is already included in (Ref. 23). But it must be taken into account that detailed description of these aspects is relevant to this case study. So reading (Ref. 23) complementarily to this chapter, is recommended to understand this case study. Then this chapter exclusively discusses those aspects which are considered relevant regarding the identification exercise, and not considered in the mentioned document. Data overview is included in this chapter to qualitatively analyse the degree of achievement of the considered optimisation objectives described in section 8.2.

Two experiments were conducted in the twin houses for the simulation exercise in Subtask 4.1. Experiment 2 is primarily considered here for the identification exercise in Subtask 3. Some features have been explicitly designed and implemented in this experiment set up, aiming to optimise it regarding data analysis for the given climatic conditions as discussed in section 8.2. Data corresponding to experiment 1, also available, can be used for additional validation, etc. Comparison of main variables in experiments 1 and 2 permits visualising the differences between experiments designed and not designed for identification (see section 8.3).

Analogous objectives to previous exercises have been set. However new challenges are incorporated when a full size building is considered. It represents an important step forward in the road from round robin box to real life conditions, in the sense that it consists in a full size test building which adds a relevant degree of complexity regarding the previous considered case studies. However other characteristics are still far from reality, which on the other hand simplifies somehow the analysis. This is the case of as the following: the building is non-occupied, it has a high degree of sensors and measurement points. Test sequences have been designed and controlled aiming to improve accuracy of parameter estimates.

8.2 Experimental aspects related to identification

This section discusses the aspects taken into account and the features implemented to optimise the test regarding data analysis for identification.

Analysis objectives

First, experiment design must take into account the final objectives of the identification analysis. In this case these objectives are the following:

- Characterize the heat losses of the main zone through 1. the heat loss coefficient to the outdoor ambient and 2. the heat loss coefficient to the other boundary zones.
- Characterize the solar gains of the main zone through its overall gA-value.

- Characterise the dynamic performance of the main zone through an effective heat capacity.

Main zone and boundaries

Main zone and boundaries must be well defined and clear for analysis and consequently they must be taken into account for experimental design. The same zone configuration used for the validation exercise in ST4.1. is considered for the common exercise 5 in ST3. This allows data from experiment 1, in principle not designed for identification, to be available for further validation and other identification studies.

In this configuration the three rooms on the north side of the house were sealed off from the 4 rooms on the south side which were linked by large door openings. There were no doors to the cellar from the ground floor, and only a small opening to the attic, which was sealed.
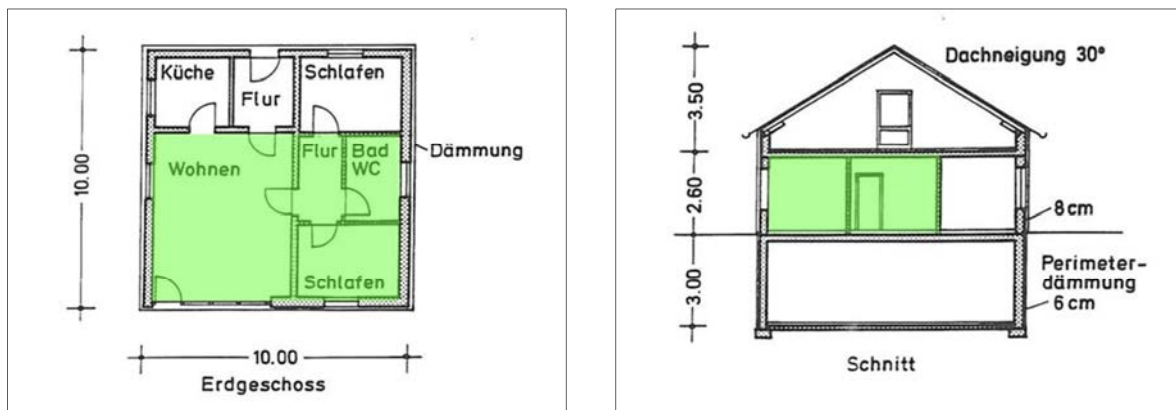
| (a) Cross section | (b) Vertical section |

Figure 82: Main zone (marked in green) and boundaries considered for the experiment set up.

According to this set up we define the following spaces as indicated in Figure 82:

- Main zone consisting in: living room, south bedroom, bathroom and corridor (Marked in green in Figure 82).
- Boundaries consisting in: cellar, attic, kitchen, north bedroom, hall and outdoor ambient.

Requisites related to the main inputs and driving variables

The experiment design must guarantee that the phenomena that must be characterised are strong enough. Phenomena are considered strong enough in this context, when the amplitude of the corresponding driving variable is significantly higher than the uncertainty in its measurement. Otherwise signal to noise is poor.

The same criteria must be applied to the amplitude of any other variable required to complete the energy balance equation used in the analysis.

Applying these conditions to this case study the following conditions are necessary:

- To identify **heat loss coefficient to the outdoors**, the experiment set up must ensure strong enough heat loss through the corresponding components. This is achieved maximising the temperature difference between the air in the main zone and the outdoor air, which is the driving variable in this case.

- Analogously to identify **heat loss coefficents to the boundaries**, the experiment set up must ensure strong enough heat loss through the corresponding components. This is achieved maximising the temperature difference between the air in the main zone and the air in the adjacent zones, which is the driving variable in this case.
- To identify the **overall gA-value**, solar gains must be strong enough along the experiment. This is achieved when the experiment contains sunny days, when solar radiation is high, which is the driving variable in this case.
- To identify the **effective heat capacity** the system must be excited by dynamic input signals in a wide range of frequencies covering the characteristic time constants of the system. This is achieved by ROLBS test sequence applied.
- Notice that **heating in the main zone** during the experiment is necessary to maximise temperature differences between indoor air and ambient and adjacent zones. Free running tests may lead to poor signal to noise ratios in the temperature difference measurements and problems with identifiability. Additionally, the heating power is an important variable to complete the energy balance equation used in the analysis, so it must be strong enough along the experiment.
- Correlation between the he internal boundary conditions and the external boundary conditions has been avoided, aiming to facilitate identification.

Experiment 2 has been designed aiming to maximise the degree of accomplishment of all these conditions, for the given weather in the test site and the constraints that are brought by the heating systems installed in the building (Cooling is not available, ROLBS in some boundary spaces is not possible).

To simplify set up all the spaces in the adjacent zones have been set to the same constant temperature. Set point in these boundary zones have been set to constant 22°C. Lower constant temperatures are not feasible due to the given weather conditions and because cooling is not available.

Blinds were down in the boundary rooms to facilitate temperature control in the adjacent zones avoiding solar gains. Blinds were up in the south rooms to allow solar gains in this zone and permit identification of gA-value.

Homogeneity of the indoor air temperature

The different sources of heat such as heating devices and solar radiation can lead to some degree of inhomogeneity contributing to the uncertainty budget of the parameter estimates.

A fan could help to achieve better homogeneity. However this strategy has been disregarded because it could introduce significant perturbations in the interior convection coefficients.

Assuming that air stratification will be present in realistic experimental campaigns, measurements giving information on air stratification have been included.

Vertical distributions of air temperature sensors have been included in the rooms in the south zone to have more information on the air stratification in the zones where heaters that were switched on could increase stratification. Vertical distribution of air temperature sensors was already included in the living room in Experiment 1. Additional vertical distributions of sensors were installed in the bathroom and south bedroom in Experiment 2.

This information on air temperature distribution is useful to investigate the following issues:

- Uncertainty in parameter estimates due to temperature stratification in indoor air.
- Different options to achieve an optimum representation of indoor air temperature, for example: considering spatial averages, weighted averages, a reduced selection of measurement points, or any other.

-

Measurements of heat flux density and internal surface temperature

Heat flux density and internal surface temperature were measured in the living room and south bedroom.

These measurements are useful to investigate if dependence of U-value of the opaque walls with surface temperatures and wind speed and direction, are relevant or negligible.

Measurements of heat flux density are very useful to analyse if the g-value of opaque walls and the contribution of solar radiation to the net heat flux through opaque walls, are relevant or negligible.

See section 11.6.2 in chapter 11 for further information.

8.3 Data overview

Data overview is used here to qualitatively analyse the degree of achievement of the optimisation objectives considered in section 8.2. Comparison of main variables in experiments 1 and 2 is used in this section to highlight the differences between experiments designed and not designed to optimise these criteria.

Figure 83 present the main variables considered in section 8.2 for Experiment 1 (left) and Experiment 2 (right). This figure evidences the differences implemented in Experiment 2 aiming to improve it regarding identification.

Particularly the following aspects show a better signal to noise ratio in the corresponding variables in Experiment 2 regarding Experiment 1.

- Higher differences between air temperature in the main zone and outdoors, and between boundary spaces and outdoors. (See Figure 83c and Figure 83d).
- Higher heating power supplied to the main zone (See Figure 83e and Figure 83f).

No significant difference is observed regarding solar radiation (See Figure 83a and Figure 83b). However both experiments Include cloudy and sunny days when it is strong enough.

Air temperature is not perfectly homogeneous in both experiments as expected. Temperatures in the boundary spaces in Experiment 2 are a bit different which is a bit deviated from specifications (22°C set point in all the boundary spaces). Air temperatures in cellar and attic are very similar. However the rooms in the north zone show some differences in some time intervals, as can be seen in Figure 83d. Figure 84 and Figure 85 show the temperatures measured in the different rooms in the south zone at different heights. These figures also evidence some degree of inhomogeneity. This issue should be taken into account and discussed in the analysis.

8.4 Common exercise 5

The requested outputs proposed for this exercise are presented in the following sections **¡Error! No se encuentra el origen de la referencia.** and 8.5.1.

8.4.1 Modelling Report – Common exercise for identification

Considering the south zone of the ground floor which consists of living room, bathroom, south bedroom and corridor, participants are requested:

- To estimate the heat loss coefficients to the outside, to the adjacent spaces (north room, attic and basement), the effective heat capacity and the solar aperture.
- Using models identified on the basis of measurement campaigns performed in this second experiment, predict the output on the basis of input data recorded in the free float period.

The submitted reports need to comprise a detailed description of the applied analysis and validation carried out. The level of detail in the report is intended to allow anyone, using the same approach, to repeat the analysis described in the report and achieve the same results. This report should contain at least the following items:

1. Name of the organisation.

2. Name of the modeller.

3. <u>Pre-processing</u>: Any pre☐processing carried out must be reported. Participants are encouraged to report data overview based on plots, discussion about quality of data and their suitability to fit objectives, etc.

4. <u>Modelling approach:</u> The methods and models used must be described. The hypotheses and approximation about the physics behind the model used must be justified. Schematic representations of heat flows in the building are recommended to support explanations. The process of model selection and the decisions made in this process must be explained. The software tools used to identify the parameters must be mentioned.

5. <u>Validation:</u> The validity of the results must be demonstrated. The process followed to demonstrate the validity of the results must be explained. Discussion on the consistency of the results based on physical criteria must be included.

6. <u>Results:</u> A value estimated for each parameter and its corresponding uncertainty must be clearly marked as the final result.

7. <u>Conclusions:</u> Any relevant finding resulting from the analysis, about results themselves, about the experiment set up and measurement campaign, etc., must be summarised.

8.5 Results of common exercises 5 – discussion of the results

Very few contributions have been submitted to this exercise. Although very few written paper are available, some participants have worked on it and presented their analysis and results in annex 58 expert meetings. Discussions related to experiment set up, and data analysis, were held on these meetings.

Some participants reported difficulties in identifying the requested parameters, which is somehow considered normal taking into account on the one hand the increase of difficulty regarding previous case studies, and on the other hand that we are working in a research context where finding problems that need solutions is part of normality.

Reference 24 reports a comprehensive and advanced analysis of this case study by one of the participants. This paper illustrates the application of grey-box models for the identification of the heat loss coefficient of the house based on the short term provided data. It concludes that while the estimate of the heat loss coefficient to the exterior H_e is within the range of expectations, the grey-box models fail to estimate the heat loss coefficient to the boundary zone H_b and the effective thermal capacities. On the other hand, both H_e and H_b were estimated roughly by use of ARX-models on 5 days data while both zones kept at a constant, but different, indoor temperature.

Other participants that didn't submitted written paper also reported problems in identifying the boundary zone H_b and the effective thermal capacities. Discussions trying to explain and solve these problems were held on the expert meetings. Some opinions pointed to correlations among input variables. Experiment set up was also mentioned as a possible source of difficulties. However experiment set up was already optimised as far as possible as explained in section 8.2. Additionally it must be taken into account the increase of the presence of correlation between input variables, is linked to the process of approaching to reality in many applications. Consequently being able to deal with correlation is relevant issue regarding future research.

Some techniques to deal with correlation problems such as multi-output models (Ref. 25), or reducing the search intervals of unknown parameters taking into account physical constraints, or applying regularization techniques such as Tikhonov (Ref. 26), have been already applied to different published case studies. The application of these techniques has a relevant potential regarding future research. However no one of them has been explored to solve the problems arisen in this common exercise.

A comprehensive dataset is available for those wishing to test identification techniques on a slightly more complicated experimental facility than a wall or test box.

8.5.1 Results – Common exercise for identification

Participants are requested to:

- Provide a full analysis report in a .doc-file or .pdf-file: ST3_CE5_country_institute.doc/pdf.
- Complete the provided .xls-file (either the 10 minutely or the hourly version) for the free float period with the predicted output based on models fitted to this second experiment. Rename the .xls-file to: ST3_CE5_ Free Float _country_institute.xls.

Please note that ST3_CE5_ Free Float _country_institute.xls and ST3_CE5_country_institute.doc/pdf need to be renamed to the participant's actual country and institute name, as e.g. ST3_CE5_Spain_CIEMAT.xls.

Data of the measured temperatures in the south rooms in the free float period are not included in the provided datasets – participants are expected to predict temperatures in this period. There was a period of missing house data from 23rd May 17:29 to 26th May 10:24 in this free-float period. However, weather data is available and it can be assumed that temperature control of the adjacent spaces was maintained in this period.
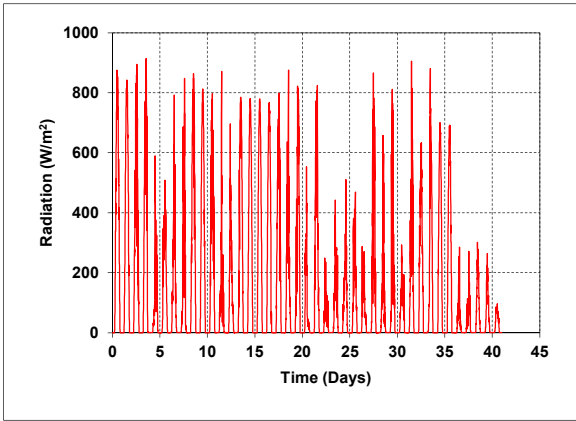
(a) Horizontal global solar radiation.
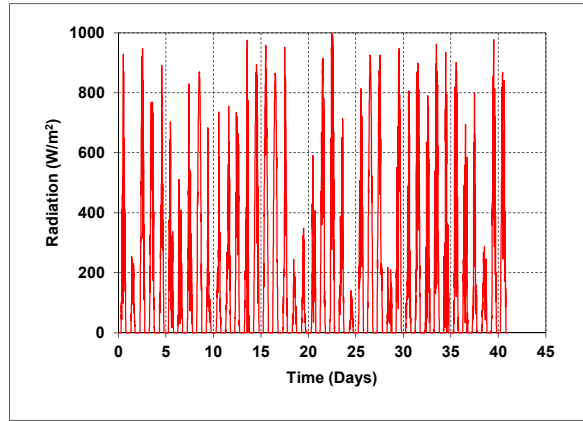
(b) Horizontal global solar radiation.
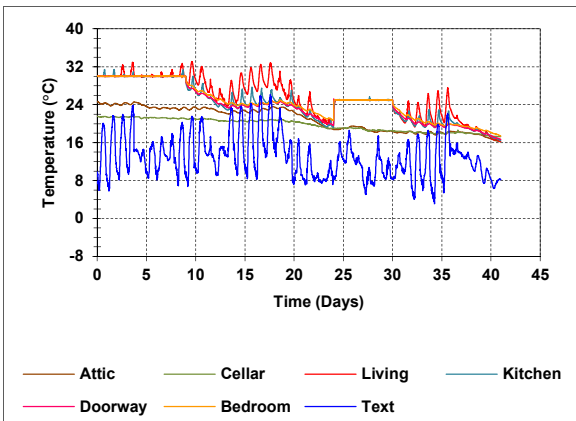
(c) Indoor and outdoor air temperatures.
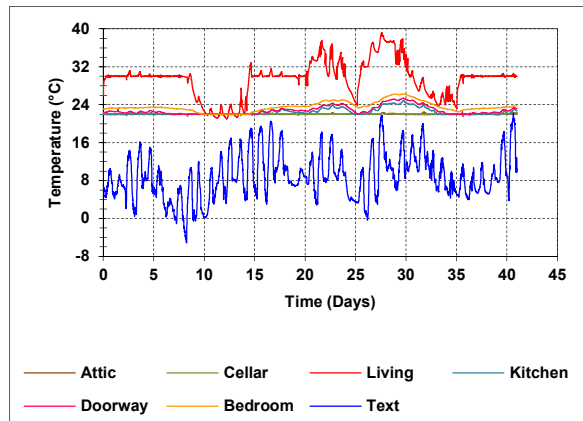
(d) Indoor and outdoor air temperatures.
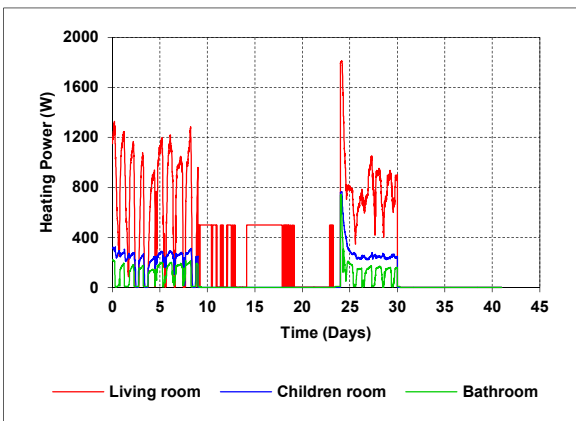
(e) Heating power.
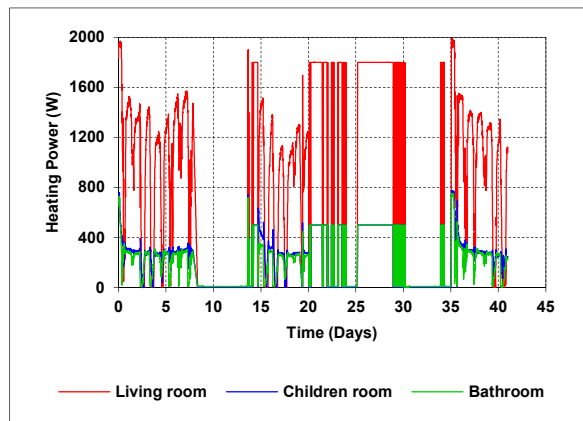
(f) Heating power.

Figure 83: Data overview. Left: 1ˢᵗ Experiment (23ʳᵈ August to 29ᵗʰ September 2013). Right: 2ⁿᵈ Experiment (14ᵗʰ April to 2ⁿᵈ June 2014)

108
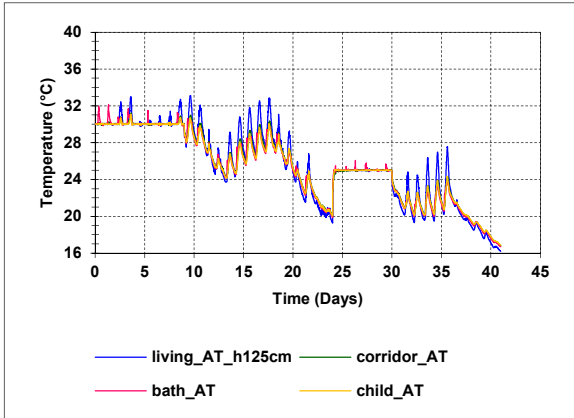
(a) Rooms in the south zone.
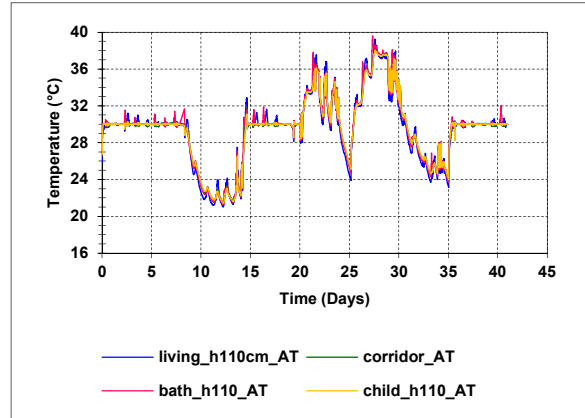
(b) Rooms in the south zone.
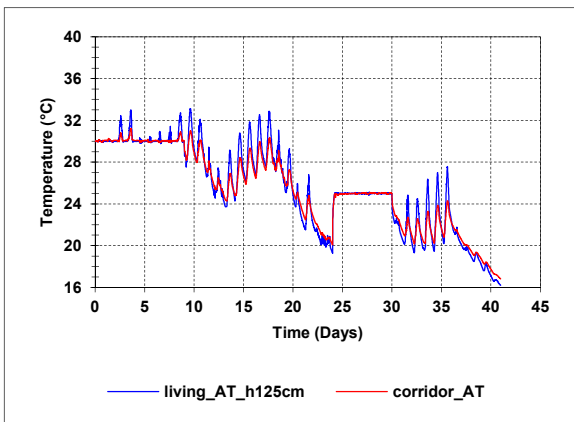
(c) Living room and corridor.
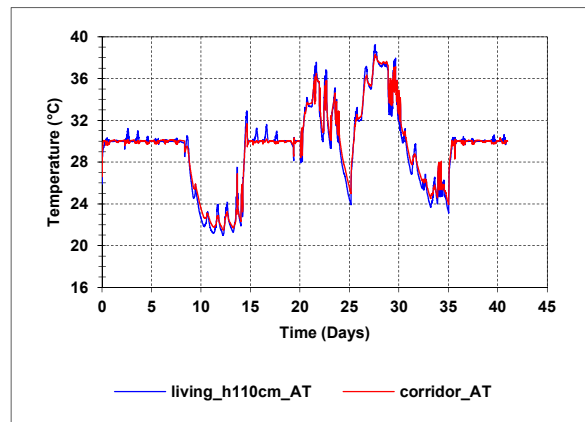
(d) Living room and corridor.
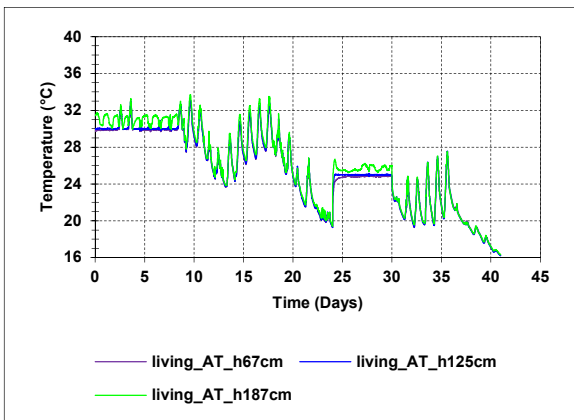
(e) Stratification in the living room.
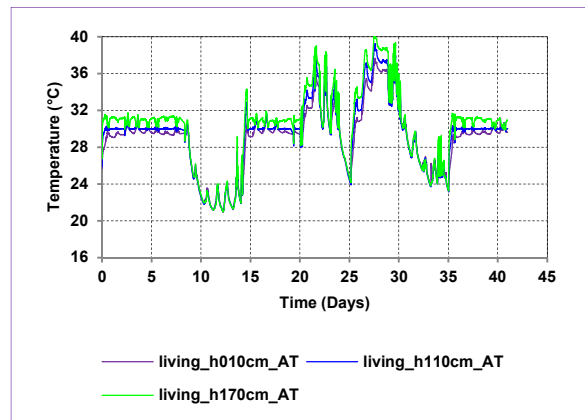
(f) Stratification in the living room.

Figure 84: Distribution of air temperature in the south zone for Experiment 1 (left) and Experiment 2 (right).

109
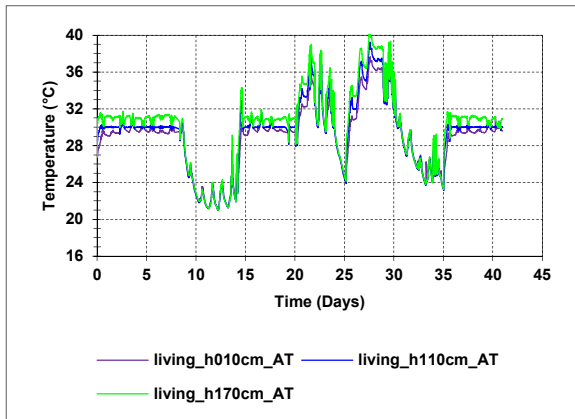
(a) Stratification in the living room.
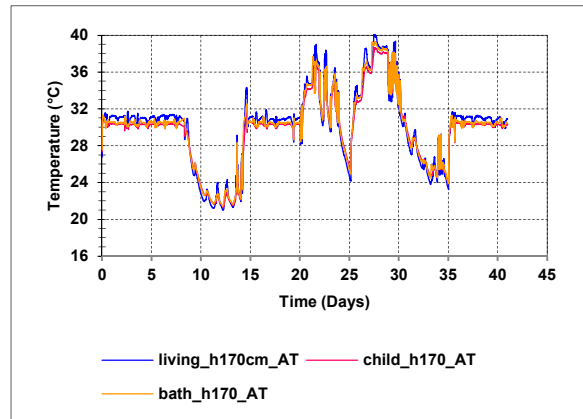
(b) Temperatures in the rooms of main south zone. 170cm high.
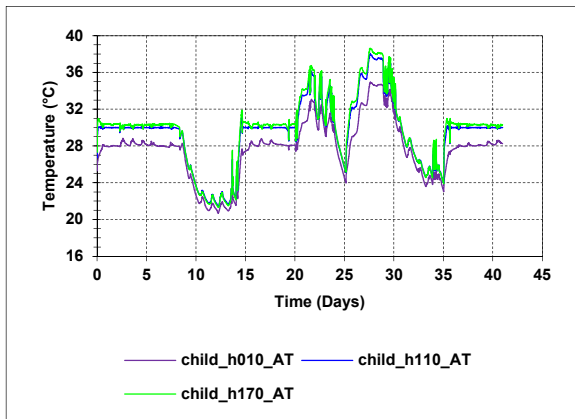
(c) Stratification in the south bathroom.
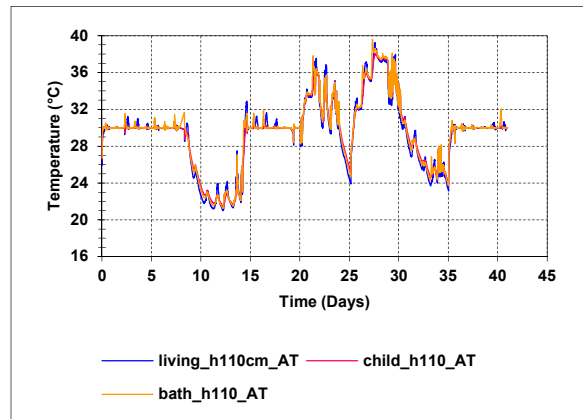
(d) Temperatures in the rooms of main south zone. 110cm high.
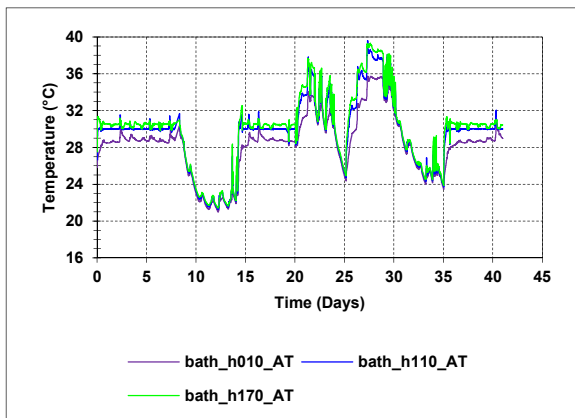
(e) Stratification in the bathroom.
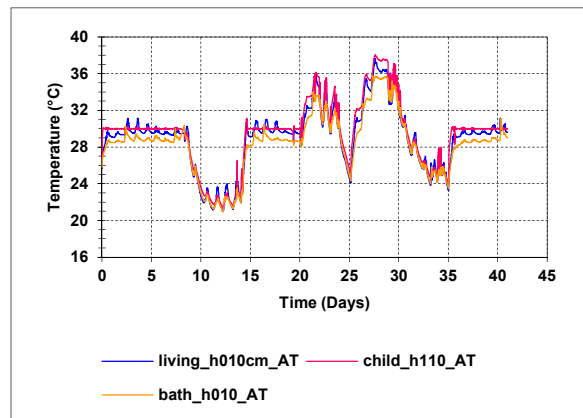
(f) Temperatures in the rooms of main south zone. 10cm high.

Figure 85: Stratification in the different rooms of the south zone (left). Comparison of measurement in the same level for all the rooms in the south zone (right).

9.   IDEE. BBRI

9.1 Introduction

The IDEE house, a full-scale experimental building located at the BBRI facilities in Limelette (Belgium), has been used for the last common exercise CE6. Aim was to characterize the heat loss coefficient of this test house based on different data sets generated by several measurement campaigns. The proposed requested output was the same proposed for common exercise 5 (see section 8.4).

9.2 Description of the IDEE house

The building comprises a ground floor, basement and attic and is situated on a small hill, in a wide open place. The main façade is oriented southwards, between S and S-SW. The heated surface area is about 86 m², with a ceiling height of 2.55 m. Hence, heated building volume is 220 m³. The outdoor dimensions are 8.2 m by 13.2 m. Hence, total envelope surface is 325.6 m². The outside walls are cavity walls filled with 10 cm of mineral wool. The ceiling (between the ground floor and attic) is a light construction, consisting of wooden floor and insulated with mineral wool. The floor between the ground floor and the basement is heavy and insulated only to a limited extent. The windows are composed of double glazing and wooden frames.

Figure 86 shows an picture of the IDEE building. As illustrated, the building is detached and exposed to winds. The main "living" room is facing south and is highly glazed.

Figure 86 : the IDEE experimental house, Limelette (Belgium)

Figure 87 depicts a ground floor plan and numbers the various rooms and collects associated dimensional characteristics.
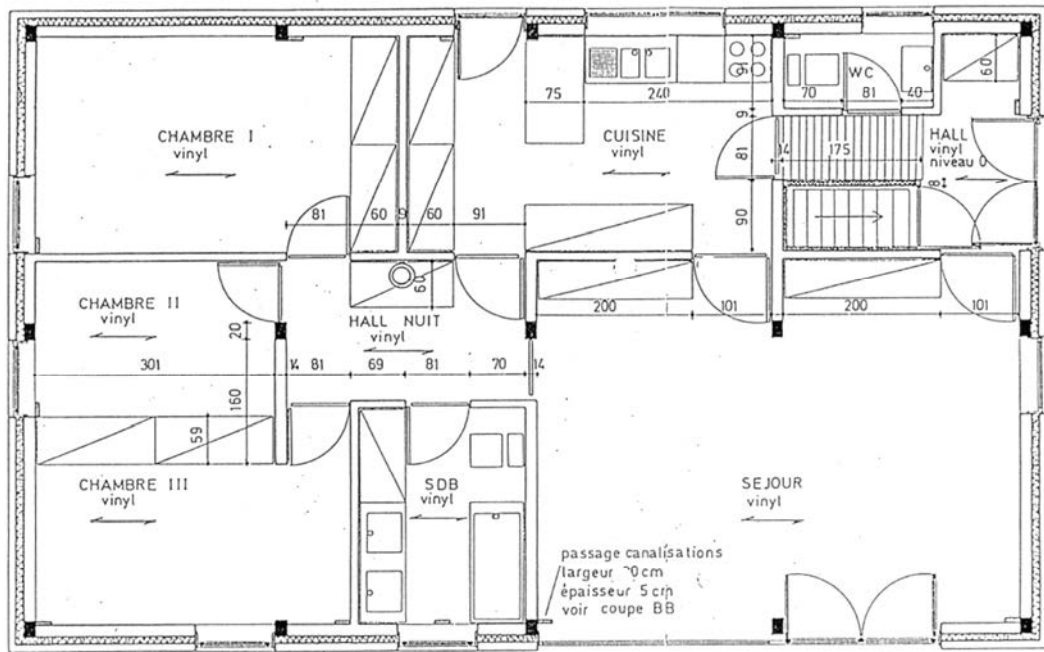
Figure 87 : plan of the IDEE experimental house, Limelette (Belgium)

Table 23 : numbering, naming and dimensions of the rooms

Room #	Room name	l (m)	w (m)	S (m²)	h (m)	Vol (m³)
0	entrance hall	3.01	1.71	5.15	2.55	13.1
-	WC	1.91	0.91	1.74	2.55	4.4
1	Living	6.16	4.71	29.01	2.55	74
3	'bathroom'	2.11	2.6	5.49	2.55	14
4	sleeping room 3	3.96	2.3	9.11	2.55	23.2
-	night hall	3.01	2.11	6.35	2.55	16.2
5	sleeping room 2	2.41	3.01	7.25	2.55	18.5
6	sleeping room 1	4.56	2.71	12.36	2.55	31.5
7	'kitchen'	3.66	2.71	9.92	2.55	25.3
	TOTAL					220.3

An elaborate set of plans is included in Appendix 9.2.

9.3 Boundary conditions

The IDEE house is located at the BBRI facilities (Belgian Building Research Institute) in Limelette, Belgium (lat. 50°41' N, long. 4°31' E), at 30 km from Brussels.

In general, the weather climate at this test site is maritime temperate, consisting of mild winters and rather cool summers. It is usually rainy, humid and cloudy.

The experiments have been made during spring 2014.

Data collected from the weather station located near the building includes outdoor air temperature (shielded from solar radiation and ventilated) and relative humidity, vertical

global solar radiation on the East, South and West façades and finally, wind speed and direction (north = 0°, east = 90°). An additional weather station is located somewhat further, i.e. 200 m, from the IDEE house. Here, horizontal global solar radiation, horizontal diffuse solar radiation, long wave radiation on the vertical south and horizontal planes, among others, are measured. See Table 25.

The dataset used for the CE6 only makes available a relevant subset of these data and leaves out redundant measurements (see 9.7).

9.4 Performed experiments

A large number of measurement campaigns were performed. For the purpose of the CE6, we've selected both a stationary and dynamic heating experiment. Both are performed using the exact same experimental setup, explained in the following section. Moreover, a limited 10 days period is offered for both of them. The first is a co-heating test, from 3 to and including 12 April 2014. The latter is an experiment with a dynamic heating power dictated by a PRBS (pseudo random binary sequence), from 1 to and including 10 February 2014. Table 24 lists the details:

Table 24 : list of considered datasets for CE6

Data set name	Start	Finish
Coheating	03/04/14	12/04/14
PRBS	01/02/14	10/02/14

The ventilation system was shut down and sealed during the measurements.

The actual air change rates (air infiltration) have been measured during the experiments, using the constant concentration tracer gas technique with SF6 gas and a Bruël&Kjaer apparatus (see Appendix 9.1).

9.5 Testing infrastructure

The testing infrastructure consists of "kits" installed in each zone and connected to the central control & acquisition unit. The communication between the central main unit and the local kits happens via a serial port and an Advantech/ADAM 4011 multifunctional module (Figure 88).

Figure 88: Advantech ADAM4011 module with electric fan and heater

This module takes care of actuator control and measures indoor air temperature and energy consumed by actuators. The communication happens continuously with instructions updated every 100 seconds. For instance, if the required power in a zone is 500W and we have a

controlled heater with nominal power of 1000W and a fan with nominal power of 50W, then we need 450W from the heater. Hence, it will be made active during 45 (out of 100) seconds. Note that the energy meter gives 1 pulse per Wh, which allows to monitor heating power in discrete steps of 36W per cycle of 100 seconds, or 6W per 10 minutes time steps. Evidently, these meters are not reset at the end of each cycle, such that the associated measurement accuracy remains very good at a larger time scale.
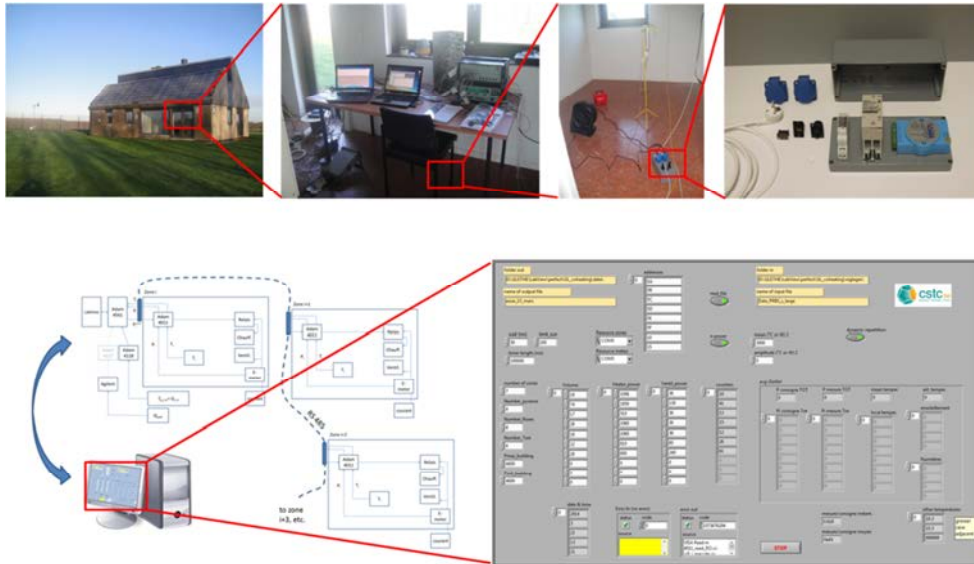
Figure 89 : Overview of the experimental setup infrastructure

A software user interface (Figure 89) is also developed such that the type of experiment can be selected and adjusted, and current variables can be monitored. It is possible to activate a functionality that will be in charge of adaptively spreading the total power in the various zones of the building with the objective to achieve as homogeneous temperatures as possible inside the building, when performing a PRBS or other complex measurement.

The infrastructure is further illustrated in Figure 90.
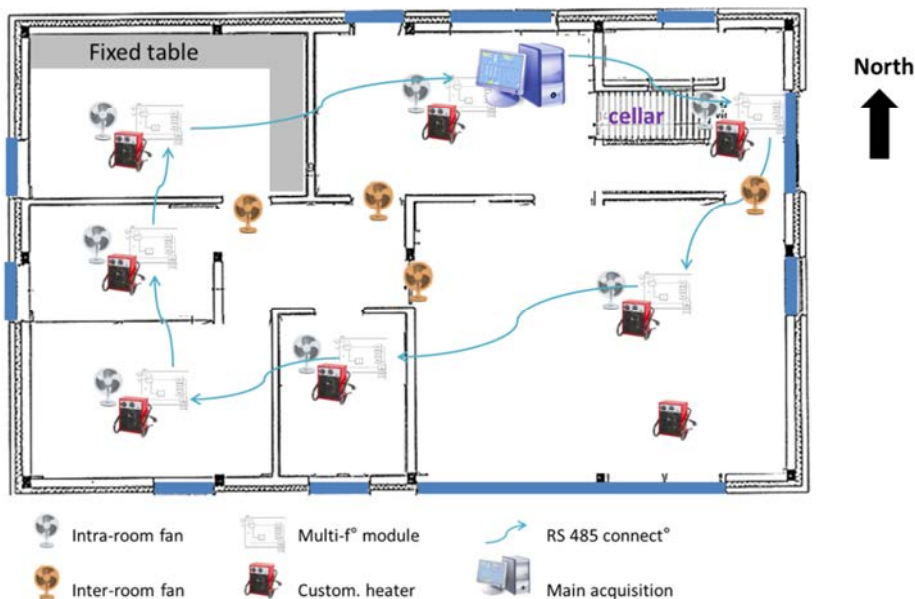
Figure 90 : Experimental setup components and positioning in the house

Inside the building, multi-zone data are available. Data include heating power, temperature, air change rate and local heat fluxes. More details are given in the next section.

9.6 Measurement devices

Table 25 shows all sensors which have been installed.

More detailed information on the transducers and sensors used during the experiments is given below :

- Surface temperature : type T thermocouple (copper-constantan), temperature at the cold junction measured by a Pt100 sensor.
- Air temperature : type T thermocouple (copper-constantan), temperature at the cold junction measured by a Pt100 sensor. Shielded and naturally ventilated.
- Horizontal and vertical solar irradiance : pyranometer, model CM11 manufactured by Kipp and Zonen. The diffuse horizontal solar irradiance is measured by means of a shadow ring.
- Heat flux density : sensor (thermopile), model HFP01 manufactured by Hukseflux, thickness 5mm, total size diameter 80mm, calibration constant supplied with each individual sensor, accuracy +- 5%.
- Heating power : measured via an energy meter (Finder module (7E.13)) and then with a DAS composed by an ADAM module (model 4011, pulses). Concerning the accuracy of the energy measurement, the documentation of the Single-phase meter EcoCount® WSD32 modules that has been use (www.nzr.de) mentions a class-B level. Using the norm NBN EN 50470-3, 2007 on "Electricity metering equipment (a.c.), Part 3 : Particular requirements - Static meters for active energy (class indexes A, B and C)", the accuracy should be about 1 to 1.5%.

Table 25 : measured data

Name	Measurement	Unit	sensor type	Acquisition System
Time	Time	DD/MM/AAAA hh:mm		
P_heat	Heating delivered power (Wh/h)	W	Finder Type 7E.13	LabView + ADAM 4011
Ti	Inside air temperature (volume weighted)	°C	thermocouple type T	LabView + ADAM 4118
Te	Outside air temperature (shielded and ventilated)	°C	thermocouple type T	LabView + ADAM 4118
T_attic	air temperature in the attic	°C	thermocouple type T	LabView + ADAM 4118
T_cellar	air temperature in the cellar	°C	thermocouple type T	LabView + ADAM 4118
sol_dir_East	Vertical 'East' façade global solar radiation	W/m²	Kipp & Zonen CM11	LabView + ADAM 4118
sol_dir_West	Vertical 'West' façade global solar radiation	W/m²	Kipp & Zonen CM11	LabView + ADAM 4118
ACH_measured	bounded building air change (SF6) volume weighted	1/h	B&Kjaer 1302/1303	Lumasense 7620
ACH_predicted	predicted airchange	1/h	B&Kjaer 1302/1303	Lumasense 7620
WS	Wind velocity	m/s	Thies Clima 4.3519	portable : Onset (Hobo) H21-001
GS	Wind gust velocity	m/s	Thies Clima 4.3519	portable : Onset (Hobo) H21-001
WD	Wind direction (East = 90°)	°	Thies Clima 4.3129	portable : Onset (Hobo) H21-001
0GHE01	Horizontal global solar radiation	W/m²	Kipp & Zonen CM11	HP3852A
0DHE01	Horizontal diffuse solar radiation	W/m²	Kipp & Zonen CM11	HP3852A
0GVE01	Vertical South global solar radiation	W/m²	Kipp & Zonen CM11	HP3852A
tsi_sol	Internal surface temperature	°C	thermocouple type T	HP Agilent 34970A
tse_sol	External surface temperature	°C	thermocouple type T	HP Agilent 34970A
tsi_mur	Internal surface temperature	°C	thermocouple type T	HP Agilent 34970A
tse_mur	External surface temperature	°C	thermocouple type T	HP Agilent 34970A
tsi_plaf	Internal surface temperature	°C	thermocouple type T	HP Agilent 34970A
tse_plaf	External surface temperature	°C	thermocouple type T	HP Agilent 34970A
Q_sol	Heat flux density at the internal face	W/m²	Huksflux HFP01	HP Agilent 34970A
Q_mur	Heat flux density at the internal face	W/m131	Huksflux HFP01	HP Agilent 34970A
Q_plaf	Heat flux density at the internal face	W/m132	Huksflux HFP01	HP Agilent 34970A

Note that only a part of this information has been used for CE6 (see section 9.7).

As can be seen, 5 different acquisition systems are used, and data are manually synchronized back into the GMT timeframe.

9.7 Data

Two data files are supplied, one for each test:

- Test 1 : co-heating test
- Test 2 : PRBS test

The data files are text files organized in rows and columns. Each column corresponds to a variable. The first row represents the headers of the respective columns and refers to the recorded variables as indicated in Table 26 below. Data are read and recorded in each row every 5 minutes (GMT timeframe).

For the air change measurements, maximum 4 dosing/sampling channels were available. Therefore some rooms were joined together in order to create a smaller number of zones. Here, we only provide the building average air change, not the individual zone air change.

The data are made available on the DYNASTEE website.

Table 26 : data available for CE6

Name	Measurement	Unit	Sensor type	Acquisition system
Time	Time	DD/MM/AAAA hh:mm		
Ti	Indoor air temperature (volume weigthed)	°C	thermocouple type T	Labview+ADAM4118
Ta	Outdoor air temperature (shielded and ventilated)	°C	thermocouple type T	Labview+ADAM4118
Qh	Heating deliver power	W	Finder Type 7E.13	Labview+ADAM4011
Tattic	air temperature in the attic	°C	thermocouple type T	Labview+ADAM4118
Tcellar	air temperature in the cellar	°C	thermocouple type T	Labview+ADAM4118
qsw.h	Horinzontal global solar radiation	W/m²	Kipp & Zonen CM11	HP3852A
Ws	Wind velocity	m/s	Thies Clima 4.3519	Onset (HOBO) H21-001
Wd	Wind direction (East = 90°)	°	Thies Clima 4.3519	Onset (HOBO) H21-001
ach	measured/predicted air change rate	1/h	B&Kjaer 1302/1303	Lumasense 7620

Appendix 9.1: Tracer gas measurements

Introduction

The constant concentration tracer gas method has been chosen because it allows measuring continuously and hence obtain dynamic data. The tracer gas that is used is SF6 (Sulfur Hexafluoride). The acquisition instruments is composed of two Bruel&Kjaer units: one monitor (B&K 1302) and one multiplexer (B&K 1303) illustrated in Figure 91. Both the monitor/analyzer and multiplexer have been calibrated prior to the measurements.

Figure 91: Tracer gas test equipment (here mounted in another investigated building)

The relatively uniform repartition of tracer gas is ensured because each zone is controlled independently of each other and the air is mixed using fans and heaters inside each of them.

Constant concentration method

The monitoring system is composed of several elements, as illustrated in Figure 92. Software that controls the central unit is connected to the multiplexer of 6 channels (with all the valves dozers and analyzers or samplers). The central unit manages the opening of the valves to allow appropriate dosage and sampling of each of the channels via a connecting pipe. The dozers are located inside the multiplexer and are calibrated at the beginning of the measurement. The sampler is located in the monitor and is calibrated by a specific laboratory externally. The tracer gas concentration in each zone is analyzed at recurrent intervals and tracer gas is re-injected zone per zone according to a predefined algorithm. The objective is to obtain a constant concentration (stabilization) of tracer gas in each zone. The sampling and dosing data are post-processed to compute the air change rate in each zone.
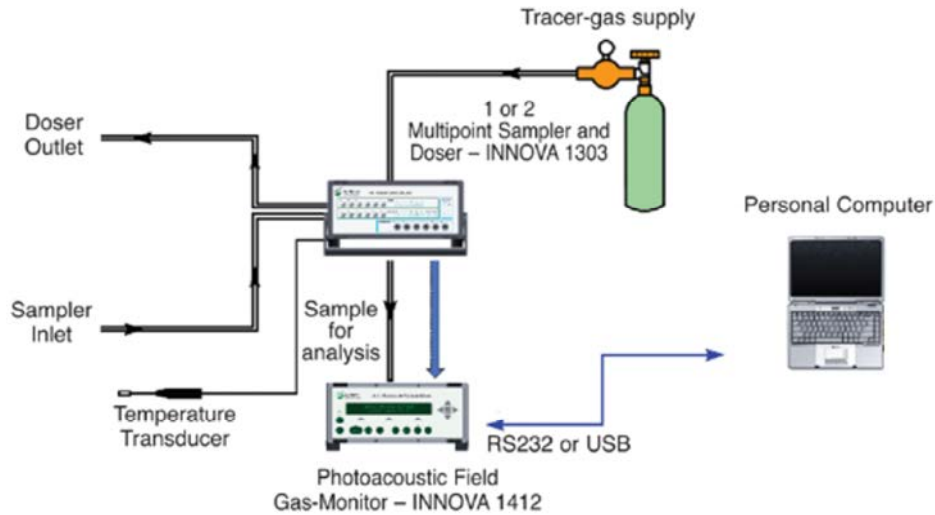
Figure 92 : Acquisition system architecture

The equation used to compute the airchange rate is :

$$N_k = \frac{\frac{V_t}{R} + (C_{k-1} - C_k)}{T_a(C_{avg} - C_b)} \qquad [h^{-1}] \qquad (1)$$

Where

N_k is the air change a time step k [h-1]

V_t is the total dosage of tracer gas in the building during the previous time interval Ta [mg]

R is the total volume of the building [m³]

C_{k-1} is the average concentration at the beginning of the time interval [mg/m³]

C_k is the average concentration at the end of the time interval [mg/m³]

T_a is the averaging time interval used for the calculation of the airchange [h]

C_{avg} is the average concentration during the time interval [mg/m³]

C_b is the background concentration during the measurement [mg/m³]

If the concentration is perfectly constant from one time step to the other and the tracer gas used is not naturally present in the atmosphere, equation (1) becomes:

$$N_k = \frac{V_t}{RT_aC_{avg}} \qquad [h^{-1}] \qquad (2)$$

hence air change is directly proportional to the dosage of tracer gas per time unit, for a defined concentration and building volume.

Equation (2) defines the air change inside a unique and homogeneous zone. Since the building is composed of several zones, the air change in each zone must be computed separately and then weighted depending on their relative volume:

$$N_{tot} = \frac{\sum_i N_i R_i}{R_{tot}} \quad [h^{-1}] \quad (3)$$

where the « i » indices represent the various zones of the building and Rtot indicates the global volume of the zones.

Figure 93 depicts a schematic of the installed equipment.
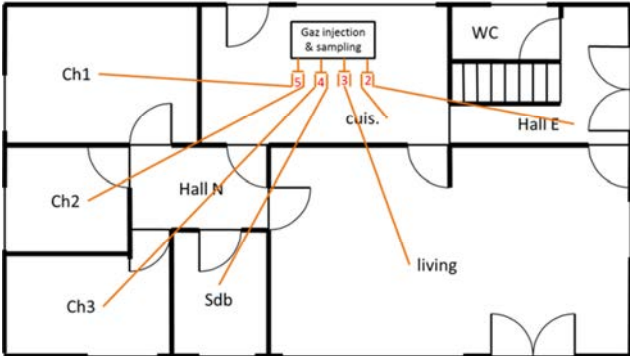
Figure 93 : airchange measurement setup inside the experimental X2 building

Appendix 9.2: Plans of the IDEE test house

The following table gives an overview of the characteristics of the IDEE dwelling.

Room	Floor dimensions (m²)		Glas areas (m²)			Glas area (m²)
	L x B	A	Door	W 1	W 2	
Living	6.16 x 4.68	28.8	2x(.77 x 1.8) 2.78	.84 x 1.04 0.87	2.84 x 1.84 5.23	8.88
Bathroom	2.78 x 2.13	5.9		0.76 x 0.93 0.71		0.71
Bedroom 1	4.55 x 2.76	12.6		0.76 x 0.93 0.71		0.71
Bedroom 2	L-shape	16.4		0.76 x 0.93 0.71	0.76 x 0.93 0.71	1.42
Kitchen	4.72 x 2.76	13.0	0.59 x 1.65 0.97	2(.71x0.93) 1.32		2.29
WC	1.86 x 0.97	1.8		0.65 x 0.93 0.60		0.60
Entry hall			0.59 x 1.65 0.97			0.97

B2

201

B 2

B A

119

10 2

40

20

171

390

40

280

710

B2

122

Bż

38
201
91
182
118
21
21
91x118

REZ - DE - CHAUSSEE

SEJOUR vinyl

CUISINE vinyl

WC

HALL vinyl niveau 0

HALL NUIT vinyl

SDB vinyl

CHAMBRE I vinyl

CHAMBRE II vinyl

CHAMBRE III vinyl

passage canalisations largeur 10 cm, épaisseur 5 cm voir coupe BB

A

B

COUPE BB

COUPE AA

125

SOUS - SOL

B2

COUPE BB

B 2

COUPE A A

128

contreventement

ferme

ferme

21x31

129

CHAMBRE I
vinyl
31,9 M³

CHAMBRE II
vinyl
41,5 M³

CUISINE
vinyl
32,9 M³

11,4 M

SEJOUR
vinyl
72,9 M³

S.D.B
vinyl
14,9 M³

H. DE NUIT
vinyl

hauteur 2,53m

ALL
nyl
eau D

passage canalisations
largeur 20cm
épaisseur 5 cm
voir coupe BB

10. Free papers and papers in Scientific Journals

10.1 Introduction

Calls for free papers focussing on topics which are relevant regarding the overall objective of this subtask have been made for each expert meeting. Contributions were discusses in these meetings. Most presented papers were related to thermal performance analysis of building "fabric". Many of these contributions report the study of different issues of modelling considering simplified situations either by simple cases studies, or by carrying out analysis based on simulated data. Relevant findings have been reported even from these simplified approaches.

Requisites on measurements and experimental set up, derived from requisites of data analysis was also considered in several contributions. In general it was concluded that the developed methodologies for dynamical analysis provide much more information about the characteristics of the building or the component than steady state methods, and moreover the results are provided using much shorter periods of experiments.

Some participants have already proven rather promising results regarding the analysis of full size buildings with a number of sensors and a number of rooms, even in the case of occupied buildings.

All the free papers presented along the Annex 58 expert meetings in Subtask 3, are listed in the following section 10.2. Some of these works were further elaborated and published in scientific journals. A list of all these published papers is also included in section 10.3. Relevant results have been presented in different events organised by DYNASTEE network and their corresponding proceedings and other dissemination documents can be downloaded from its webpage (www.dynastee.info).

10.2 List of free papers presented in Annex 58 expert meetings

All the free papers presented along each expert meeting of Annex 58 as contribution for discussion in Subtask 3, are listed in the following:

3rd Expert meeting: Leeds. United Kingdom. 24-26 September 2012.

- Determination of hygrothermal properties for building materials using inverse modeling. Jos Van Schijndel – Eindhoven University of Technology.
- CSTM-R. P. Bacher – DTU.

4th Expert meeting: Holzkirchen. Germany. 8-10 April 2013

- Regression method based in averages, applied to estimate the thermal parameters of a room in an occupied office building in Madrid . L. Castillo, R. Enríquez, M.J. Jiménez – CIEMAT.

- Feasibility of grey-box models for thermal characterisation of an opaque single and double masonry wall by means of system identification. A.H. Deconinck, S. Roels. – KU Leuven.
- Why performance indicators are not always reliable. D. Saelens – KU Leuven.
- Grey box building models for model order reduction and building control. R. De Coninck – KU Leuven.
- Characterisation of heat dynamics of arctic low-energy house with floor heating. P. Delff, M.J. Jimenez, H. Madsen, C. Rode – DTU, CIEMAT.
- QUB: Validation of a Rapid Energy Diagnosis Method for Buildings. G. Pandraud, R. Fitton. Saint-Gobain Isover, University of Salford.

5th Expert meeting: Hong Kong. China. 14-16 October 2013

- Using subspace identification methods to characterise the thermal performance of buildings. G. Bauwens, S. Roels, E. Reynders, T. Quirijnen, M. Wassink – KU Leuven.
- Quality of grey-box models and identified parameters as function of the accuracy of input and observation signals. G. Reynders, D. Saelens – KU Leuven.
- Parameter Identifiability in Graybox Models of Heat Dynamics of Buildings. P. Delff, R. Juhl, U. Høgsbro Thygesen, H. Madsen. – DTU.
- Dynamic parameter estimation of different wall types' thermal characteristics – Influence of indoor dynamics and comparison with linear regression methods. A.H. Deconinck, S. Roels – KU Leuven.

6th Expert meeting: Ghent. Belgium. 14-16 April 2014

- Estimation of the Round Robin Test Box's thermal resistance by semi-stationary and dynamic characterisation methods – An-Heleen Deconinck, Staf Roels – KU Leuven
- Inverse modelling of a conditioned climate chamber. Rick Kramer, Jos Van Schijndel – Eindhoven University of Technology
- Dynamic analysis of flux and co-heating test measurements in a low-energy house for characterisation of the energy performance. Julio Efrain Vaillant Rebollar, Arnold Janssens, Eline Himpe - Ghent University.
- An adapted co-heating test and grey-box modelling for thermal dynamic response of a building. Paul Steskens, Guillaume Lethé, Gilles Flamant – BBRI
- Calibration using stochastic methods with detailed simulation programs. - Filippo Monari - Strathclyde University

7th Expert meeting: Berkeley. EEUU. 17-19 September 2014

- Identification of the hygrothermal properties of a building component by CMA Evolution Strategy. S.Rouchier, M. Woloszyn - LOCIE
- Identifying the temperature dependent thermal resistance of building components. – An-Heleen Deconinck, Staf Roels – KU Leuven.
- Modelling the infiltration airflow in a building based on measured weather conditions. P. Steskens, G.Lethé, G. Flamant – BBRI.
- Building Envelope Real Energy performance in situ characterisation. – G. Lethé - BBRI.

8th Expert meeting: Prague. 13-15 April 2014

- Reducing time duration of full-scale thermal transmission coefficient measurements (Htr) on constructed building envelopes: first analytical criteria to define physical limitations due to thermal storage. R. Bouchie, S. Thébault S. – CSTB.
- A physically interpretable solar aperture identification method based on a nearly-white-box modelling and a hybrid experimental protocol – G. Lethé.
- Grey-Box modelling of a tertiary building for heating system optimisation. F. Moretty, P. Bacher, G. Comodi, S. Pizzuti, H. Madsen – DTU.
- Parameter Identification of Building Material Properties using Inverse Modeling Techniques. – W. Vink - Eindhoven University of Technology.
- Identifiability analysis of grey-box models by evaluating the profile likelihood. – An-Heleen Deconinck, Staf Roels – KU Leuven.
- Hidden Markov Models for indirect classification of occupancy behaviour. – J. Liisberg, J.K. Møller, H. Madsen, J. Cipriano, H. Bloem. DTU, CIMNE-UPC, JRC.
- Mechanical ventilation rate estimation in buildings during occupancy: the role of metabolic CO_2. – R. Enríquez, D. Bravo, M.J. Jiménez. – CIEMAT
- Measurements and characterization of the RR-box. – I. Ruiz de Vergara, A. Erkoreka, C. Escudero, C. García – LCCE, UPV/EHU
- Characterisation of the Thermal Performance of a Test House based on Dynamic Measurements – E. Himpe, A. Janssens – Ghent University.
- Characterising the thermal performance of the twin test houses: improved solar radiation modelling and application of ARX-models. – G. Bauwens, S. Roels – KU Leuven

10.3 Papers published in scientific journals

Papers derived from different contributions to subtask 3 and published in Scientific Journals are listed in the following:

M.J. Jiménez, J.J. Bloem. 2015. "Energy performance assessment of buildings and building components. Guidelines for data analysis from dynamic experimental campaigns part 1: physical aspects". *Energy Procedia*. 78, pp. 3306-3311. "6th International Building Physics Conference, IBPC 2015".

S. Roels, P. Bacher, G. Bauwens, H. Madsen, M.J. Jiménez. 2015. "Characterising the actual thermal performance of buildings: current results of common exercises performed in the framework of the IEA EBC Annex 58-project". 78, pp. 3282-3287. "6th International Building Physics Conference, IBPC 2015".

K. Chávez, R. Enríquez, M.J. Jiménez. 2015. "Experimental energy performance assessment of a simplified building: study of robustness of different analysis approaches under different test conditions". *Energy Procedia*. 78, pp. 2328-2333. "6th International Building Physics Conference, IBPC 2015".

Eline Himpe, Arnold Janssens. 2015. "Characterisation of the Thermal Performance of a Test House based on Dynamic Measurements". *Energy Procedia*. 78, pp. 3294-3299. "6th International Building Physics Conference, IBPC 2015".

Glenn Reynders, Jan Diriken, Dirk Saelens. 2015. Impact of the heat emission system on the identification of grey-box models for residential buildings. *Energy Procedia*. 78, pp. 3300-3305. "6th International Building Physics Conference, IBPC 2015".

An-Heleen Deconinck, Staf Roels. 2015. "A maximum likelihood estimation of the thermal resistance of a cavity wall from on-site measurements". *Energy Procedia*. 78, pp. 3276-3281. "6th International Building Physics Conference, IBPC 2015".

G. Reynders, J. Diriken, D. Saelens. 2014. "Quality of grey-box models and identified parameters as function of the accuracy of input and observation signals". *Energy and Buildings*. 82, pp. 263–274.

L. Castillo, R. Enríquez, M.J. Jiménez, M.R. Heras. 2014. "Dynamic integrated method based on regression and averages, applied to estimate the thermal parameters of a room in an occupied office building in Madrid". *Energy and Buildings*. 81, pp. 337-362.

P. Delff Andersen, M.J. Jiménez, H. Madsen, C. Rode. 2014. "Characterization of heat dynamics of an arctic low-energy house with floor heating". *Building Simulation*. 7, pp. 595–614.

I. Naveros, P. Bacher, D.P. Ruiz, M.J. Jiménez, H. Madsen 2014. "Setting up and validating a complex model for a simple homogeneous wall". *Energy and buildings*. 70, pp. 303-317.

Rick Kramer, Jos van Schijndel , Henk Schellen. "Inverse modeling of simplified hygrothermal building models to predict and characterize indoor climates". *Energy and buildings*. 68, pp. 87–99

I. Naveros, M.J. Jiménez, M.R. Heras. 2012. "Analysis of capabilities and limitations of the regression method based in averages, applied to the estimation of the U value of building component tested in Mediterranean weather". *Energy and Buildings*. 55, pp. 854-872.

11. Guidelines for data analysis from dynamic experimental campaigns. Physical aspects

11.1 Summary

This chapter presents guidelines for using time series analysis methods and tools for estimating the thermal performance of buildings and building components. The specific target is to obtain key performance metrics such as heat loss coefficients, time constants, solar aperture, effective thermal capacity etc.

The document is integrated in a more comprehensive work. This chapter is the first part is mainly dealing with physical aspects and specific complexity and problems that may occur due to the experimental conditions. It may be considered as a question: what quality and what information does the data contain for analysis? Minimum steps to carry out data analysis are reported and different alternative analysis approaches are outlined.

The focus is mainly on the most critical aspects particularly regarding energy performance assessment of buildings and building components. More general techniques also required to carry out data analysis are briefly presented in this document including references for more comprehensive information.

Common exercises described in previous chapters facilitated to identify frequent mistakes leading to unjustified high spread in the results and inaccurate parameter estimates. This chapter focuses on criteria that must be considered to avoid these mistakes. Graphs are used to illustrate the considered aspects.

It is assumed that the reader is familiar with basic principles of heat transfer. There are many text books dealing with this topic such as Refs. 17, 27, etc. It is also assumed that the reader has some background on measurement techniques that are well described in the literature and standards (Refs. 28 to 31, etc.).

A case study is considered to facilitate the understanding of some of the recommendations given in this report. The presented case study consists of a round robin test box built in the framework of IEA EBC Annex 58. References are given for additional case studies that help to understand the different aspects discussed and are included within this document.

A second part (Report of Subtask 3 – Part 2, Ref. 19) focuses on statistical aspects and may help to make decisions in choosing a correct model and analysis of residuals. Both documents must be considered as complementary and on some occasion they may overlap, in particular for processing data for input to the modelling work.

11.2 Introduction

Analysis and modelling of data obtained from experiments under real climate conditions require special attention to the treatment of the data during all steps of the elaboration process. The interest for these techniques and their application has grown in recent years by industry. This interest has pushed standardisation activities such as CEN/TC 89/WG13 and research initiatives such as IEA EBC Annex 58. In general it concerns numerous observations by measurements at regular interval of physical processes. For the case of

experimental work and analysis for the energy performance assessment of buildings the physical processes are importantly thermal transfer between a controlled indoor environment and a variable outdoor environment. In principle all these thermal transfer processes are well known physical ones, e.g. conduction, convection and radiation. On many occasions data is produced by people carrying out the technical work of setting up an experiment and controlling the process of data acquisition. Raw data is made available for analysis with the purpose of producing one or a few output results (see Table 2 for clarification).

Often mathematicians do not have the profound knowledge about the experiment and receive the data with limited information. The guidelines will address therefore also a brief introduction on the most common issues and will address several issues that deal with examining the data before any data treatment takes place.

As an introduction some basic information on temperature measurements is given as it is considered as important for a proper analysis of the measured data. The measurement of temperatures and thermal flows is performed by sensors based on the applied physical properties of the sensitive part of it: resistances (PT100), thermo-couples (like Cu-Co) and electronic devices. A correct measurement of the target temperature is required and a closer look will be given within the context of thermal performance of a building corresponding to the transfer of heat through the building envelope.

In

Figure *94* a schematic view is given of a building for which it is important to recognise that an indoor- and outdoor environment exists, separated by the building envelope. The heat transfer is importantly defined by the air temperatures.
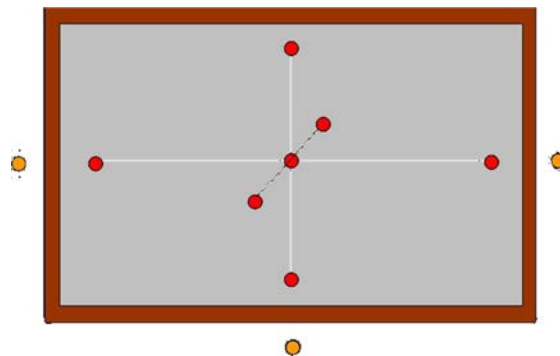
Figure 94: Schematic view of a building.

To guarantee an accurate temperature measurement, the temperature of the sensing element must be identical to the temperature of the measurand. Different strategies can be followed to fit this objective, depending on the kind of temperature that is measured. For example:

- Air temperature measurement: Convection is the main mechanism helping to equalise air and sensor temperatures so it must be enhanced, and the conductive and radiative heat transfer should be avoided. This can be achieved by using a fan and shielding of the sensor.
- Surface temperature measurement: a surface is the separation between two distinctive entities, usually air or water and solid. Installation of the sensor must guarantee, that its response to the different heat transfer phenomena (conduction, convection, and radiation), must be as similar as possible to the response of the measured surface. This is achieved using small sensing elements and integrating them as much as possible with the corresponding surface. This may be done by different techniques depending on the surface, for example: painting the sensors in the same paint as the surface, or covering them with tapes having similar properties

as the surfaces, etc. If sensor integration is not good enough high uncertainties can be found mainly associated to the different response of sensor and measured surface to the radiative component.

- Comfort temperature measurement: the perceived temperature from radiation and convection is usually measured with a black bulb. The conductive thermal component is avoided.

Radiation is the main source of wrong temperature measurements that give false signals from the sensor and hence false information to the mathematical models about the physical processes. The disturbing radiation may arrive from solar radiation, heat sources such as badly shielded electric heaters and incandescent light bulbs. Shielding of air temperature sensors is therefore necessary in particular for those that could be hit by solar radiation near to window openings and those sensors that are placed in a space where electric heaters or light bulbs are used. Ambient air temperature is usually measured with a special device that is double shielded and ventilated by natural or forced ventilation (with a small fan that draws air past the sensor). See Figure 96.
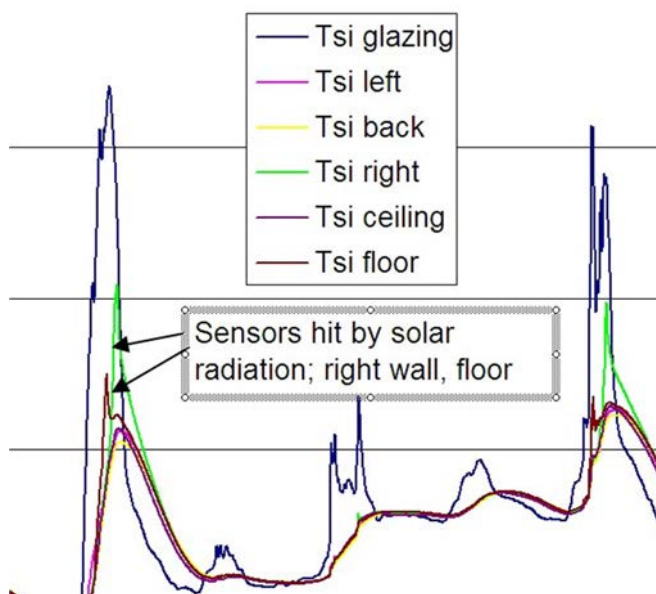
Figure 95: Surface temperature sensors hit by solar radiation as function of time.

Figure 96: Air temperature measurement.

In Figure 95 an example is given of the effect of solar radiation on the sensor. The temperature given by the sensors not hit by solar radiation is lower than the temperature given by sensors hit by solar radiation. Compare the surface temperature of the ceiling with that of the floor or right wall. One important question here is: does this sensor installation guarantee that the temperatures of the sensing elements are the same as the measured surfaces? Good documentation of experiment set up including detailed description of sensor installation is an indispensable complement for high quality data sets, and would be very helpful to answer this kind of questions.

As schematically illustrated in Figure 94, air temperatures are measured at different places. The reason is that for indoor environments without forced ventilation and sometimes where there is mechanical ventilation (for example with displacement ventilation systems), stratification occurs that can result in temperature difference in the order of several degrees. When the model is working with one signal representing the indoor temperature one has to know the uncertainty of that signal. The experiment can reduce that uncertainty by using a

ventilator guaranteeing a certain limit on the stratification which provides a better quality input signal for the mathematical model. In Figure 97, the differences to average and extremes (minimum and maximum of 7 sensors as positioned in Figure 94) are given for a space of $37m^3$ that can serve as input for analysis work. Note that the increase is during a 24 hour heating period.
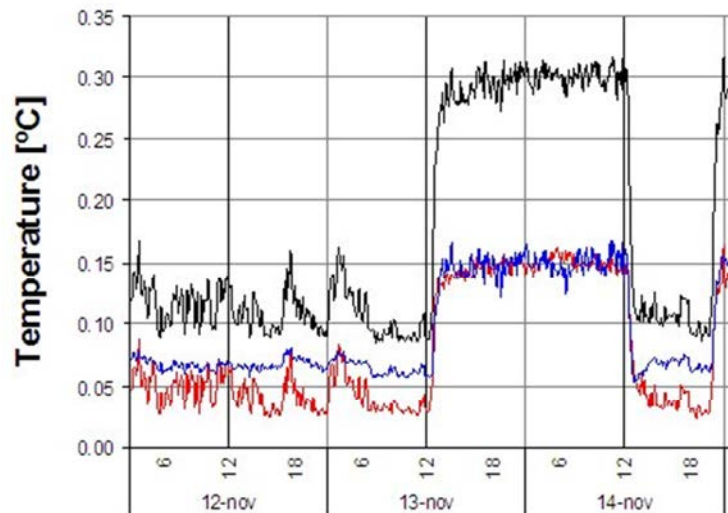
Figure 97: Indoor air temperatures; difference to average

The main conclusion from this introductory section is that in general one has to understand what a measured signal represents. What information is available from the single sensor signal or from a group of signals (such as the average from 7 indoor air temperatures that are supposed to represent one indoor air temperature)?

To get more knowledge about measurements and what information is contained in the observations a pragmatic approach for checking is proposed:

- Graphical plot of signals; it may indicate outliers, sudden changes as function of expected time constants.
- Statistical methods; average and variance of group of sensors; check of expected limits.

The measured data leads to 'raw data' with a certain accuracy. It should be stored and documented for later analysis or modelling work.

It leads to the following overview of the interaction between experimental work and analysis of the obtained measured data. It can be applied to heat transfer through the building envelope, either a wall or the whole building.

Table 1: Summary of interaction between experimental work and data analysis

Physical processes and Experiments	Mathematics and Statistics
Physical Object, Processes, Parameters	
Feedback	General mathematical description of methodology for object, processes, etc.
Experimental set-up Data information required Data collection	
Data pre-processing	Mathematical method, model and parameters Analysis techniques
Parameter conversion	Parameter identification and Mathematical assessment
Physical parameters and performance expression	
	Reporting of performance value and estimated uncertainty

One may recognise 8 steps:

1. the measurement of several phenomena of the physical process under investigation
2. the production and storage of raw data including quality aspects
3. pre-processing of data at measurement level (controlled by the acquisition system)
4. processing of data for model input (depends on analysis method)
5. representation of the physical system by a mathematical model
6. model identification from measured data
7. post-processing of the results and applied model
8. conversion and reporting of the final result, including uncertainty

Part 1 of the guidelines is mainly concerned with items 4, 5 and 7. Some overlap may occur where items 5 and 7 are concerned. Part 2 of the guidelines are dealing mainly with items 6 and 7.

As may be clear from the statements above, the measurements and the analysis of the observed data are dealing with variable conditions, sometimes induced, sometimes unexpected. The way to deal with it is the use of appropriate dynamic mathematical and statistical techniques complemented with general knowledge of the physical processes.

The next paragraph introduces the application of dynamic methods for the assessment of limited number of physical parameters to be identified from a huge amount of available data.

Dynamic tests allow modelling buildings and building components from experimental test campaigns carried out under dynamic test conditions. One of the main strength of these methods is that they permit the extraction of intrinsic characteristic parameters from time varying measurements. These features are very useful to carry out energy performance assessment of "as built" buildings, under outdoors weather and in occupied conditions where these conditions are dynamic.
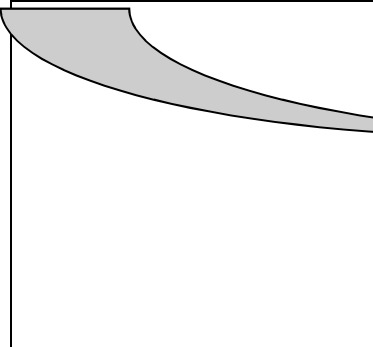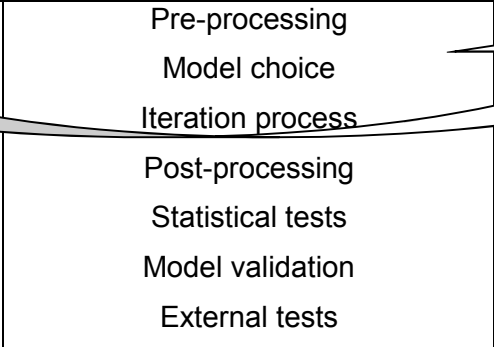
These analysis approaches must be able to deal with features of the particular experimental conditions of these test campaigns. Although some characteristic parameters can be obtained from dynamic tests applying steady state approaches under certain test conditions (section 11.6.3), it is evident that, in general, time varying measurements call for the application of system identification techniques and time series analysis tools. However as built, in outdoors weather and in occupancy conditions requires the capability to take into account any other phenomena brought by these test conditions. In practice, this means that these test conditions require modelling additional terms to complete energy balance equations that may be not necessary in other different test conditions (such as well controlled tests in laboratories and steady state).

These real test conditions are usually linked to many complex physical phenomena, which case modelling may become very difficult. In this case simplifications criteria discussed in section 11.6.2 play an important role to obtain accurate results.

GENERAL CONCEPT

The objective is the identification of a mathematical modelling with application to energy performance assessment in the built environment. The problem is stated as: from many measured data to a few estimated values.

Table 2: Process to obtain a few estimated values (characteristic parameters) from many measured data. Main elements of the methodology.

INPUT	METHODOLOGY	OUTPUT
Many observations from time and space Physical processes Literature General knowledge	Description of physical processes into mathematical equations. Method should fulfil the aim taking into account the searched output	Limited value(s) Period Performance Efficiency Data
	Pre-processing Model choice Iteration process Post-processing Statistical tests Model validation External tests	

How to get from many observations as input for the calculation process to one or a few limited output values for reporting? In that process the accuracy of input data, the propagation of the errors in the calculation process and the required accuracy of the reported value are of high importance.

Once data has been produced (raw data), from a dedicated experiment, it is assumed that these data contain all information describing the physical processes that a mathematical model is supposed to analyse. Treatment of the raw data is therefore crucial and should be performed by someone who has knowledge about the physical processes as well as the experimental set-up. Pre-processing of data for the purpose of mathematical modeling is therefore important and should be carried out with caution.

Reduction of observations and signals on the input side implies the examination of the uncertainty of the input data to the calculation model. More about this aspect can be found below and illustrated in the figures.

It is very frequent confusing and misinterpreting dynamic test conditions with time dependent parameters. Test conditions can be steady state or dynamic. Parameters can be constant (intrinsic) or time varying. Dynamic analysis must be robust giving stable estimates for constant parameters and allowing the identification of clear dependencies for non-constant indicators. Dynamic conditions don't change classical definitions of physical parameters. Equations used to extract these parameters from experimental data must take into account all the relevant effects which are present in given test conditions. Consequently dynamic conditions should not change parameters but call for equations adapted to the test conditions.

It must be taken into account that some performance characteristics, which are not constant by definition, can be can be handled as constant in practice provided that their variation is under the range of uncertainty of the parameter estimates. Discerning when these

approximations are valid requires some knowledge of building physics. For example U-value is not a constant parameter. However it is used as constant in many practical applications. This is a reasonable assumption under some conditions, but could it be incorrect in some cases such as poorly insulated walls and windows.

This document describes guidelines for dynamic analysis for estimating the thermal performance of buildings and building components focusing on physical aspects. Minimum steps to carry out data analysis are reported and different alternative analysis approaches are outlined. This document is mainly focused on the most critical aspects particularly related energy performance assessment of buildings and building components. More general techniques which are also required to carry out data analysis are briefly presented in this document including references to more comprehensive information. Case study considered in chapters 3, 4, 5, 6 and 7, is used to facilitate the understanding of some of the recommendations given in this chapter. References for additional case studies that help to understand the different aspects discussed are included in the document.

This is considered as a multidisciplinary problem that requires application of knowledge in different areas such as physics and statistics. This first part is mainly dealing with physical aspects. A second part focused in statistical aspects has been also elaborated. Both documents must be considered as complementary.

11.3 Physical parameters

Definition given by International standards are used in this document - particularly the following included in ISO 7345:1987 (Thermal Insulation – Physical Quantities and Definitions):

- **Thermal resistance, R:** Temperature difference divided by the density of heat flow rate in the steady state condition. Units: m^2K/W.
- **Thermal conductance, Λ:** Reciprocal of thermal resistance from surface to surface under conditions of uniform density of heat flow rate. Units: $W/(m^2K)$.
- **Thermal transmittance, U:** Heat flow rate in the steady state divided by area and by the temperature difference between the surroundings on each side of a system. Units: $W/(m^2K)$.

The following are defined by the ISO 13790:2008(E) (Energy performance of buildings - Calculation of energy use for space heating and cooling).

- **Heat transfer coefficient:** Heat flow rate divided by the temperature difference between two environments; specifically used for heat transfer coefficient by transmission or ventilation. Units: W/K.
- **Transmission heat transfer coefficient:** Heat flow rate due to thermal transmission through the fabric of a building, divided by the difference between the environment temperatures on either side of the construction. Units: W/K.
- **Ventilation heat transfer coefficient:** Heat flow rate due to air entering an enclosed space, either by infiltration or ventilation, divided by the difference between the internal air temperature and the supply air temperature. Units: W/K.

Characterization by system identification techniques requires a lumped representation of building fabric. The following parameters are usually considered in such lumped representation of a given building envelope:

If you want to list something, proceed as follows:

- UA: Overall thermal transmittance coefficient: the heat flow rate in the steady state divided by the temperature difference between the surroundings on each side of the system or component, in W/K. For the 1-D case the U-value, in W/m^{2}K.
- gA: Total solar energy transmittance or solar aperture: the heat flow rate leaving the component at the inside surface, under steady state conditions, caused by solar radiation incident at the outside surface, divided by the intensity of incident solar radiation on the component, in m^2. For the 1-D case the g-value [-].

gA and g can show some variability, taking into account the theoretical expressions to calculate the g value of opaque components (equation (6) in chapter **¡Error! No se encuentra el origen de la referencia.**) and glassing (equation (9) in chapter 5). This variability can be assumed negligible for opaque components, in most practical applications. Considering glassing, these parameters depend also on the transmittance of the glassing that depends on the incidence angle, and consequently on the time of the year. Smaller variability than the uncertainty on the parameter estimates is expected, but it should be analysed and discussed in each particular case study. The variability of these parameters for the opaque wall and round robin box is discussed in sections 2.2.1 and 0 respectively.

Interpretation of effective heat capacities in lumped representations: As mentioned in the introduction, dynamic tests allow modelling buildings and building components from experimental test campaigns carried out under dynamic test conditions. The starting point of this analysis is considering energy balance equations that include the measured variables and characteristic parameters that must be identified. Dynamic energy balance equations of any given system must include terms representing energy accumulated in the system. This accumulation is governed by effective heat capacities that can be estimated as the other defined parameters. However these heat capacities can be considered as auxiliary parameters that regulate the energy that is accumulated in the system and depend on the characteristics of the system and its boundaries. Then these parameters are considered effective heat capacities and must not be compared to the theoretical heat capacities obtained from the characteristics of the construction materials of the building envelope.

11.4 Experimental aspects related to identification

This section discusses the aspects that must be taken into account and the features that must be implemented to optimise the test regarding data analysis for identification.

<u>Analysis objectives</u>

First, experiment design must take into account the final objectives of the identification analysis. The generic objectives listed below will be considered for the following discussion:

- Characterize the heat losses of the envelope of one given zone through the heat transfer coefficient to its boundary zone. The boundary could be the outdoor or any other zone.

- Characterize the solar gains of the main zone through its overall gA-value.

- Characterise the dynamic performance of the main zone through an effective heat capacity.

<u>Main zone and boundaries</u>

The main zone and boundaries must be well defined and clear for analysis and consequently they must be taken into account for experimental design.

Requisites related to the main inputs and driving variables

The experiment design must guarantee that the phenomena that must be characterised are happening and strong enough for their analysis. Phenomena are considered strong enough in this context, when the amplitude of the corresponding driving variable is significantly higher than the uncertainty in its measurement. Otherwise signal to noise is poor.

The same criteria must be applied to the amplitude of any other variable required to complete the energy balance equation used in the analysis.

Applying these conditions to the considered generic objectives, the following conditions are necessary:

- To identify **heat transfer coefficient to the outdoors**, the experiment set up must ensure strong enough heat loss through the corresponding components. This is achieved maximising the temperature difference between the air in the main zone and the outdoor air, which is the driving variable in this case.

  This maximisation must be implemented taking into account the limitations due to the safety recommendations of the construction materials. Limitations due to the variability of characteristic parameters with temperature must be also considered. Too high indoor temperature that could lead to damage construction materials as well as variations of parameters that are not seen in actual operational conditions, must be avoided.

- Analogous considerations must be done to identify **heat transfer coefficients to the boundaries**. In this case the main driving variable, is the temperature difference between the air in the main zone and the air in the adjacent zones. This difference must be maximised taking into account the limitations mentioned in the previous paragraph.

- To identify the **overall gA-value**, solar gains must be strong enough during the experiment. This is achieved when the experiment contains sunny days, when solar radiation is high, which is the driving variable in this case.

- To identify the **effective heat capacity** the system must be excited by dynamic input signals in a wide range of frequencies covering the characteristic time constants of the system. This is achieved e.g. by applying a ROLBS power sequence. See statistical guidelines for further information of the ROLBS sequence (ref. 19). Some examples can be seen in section 4.2.5 chapter 4, section Figure 98 in this chapter, and ref. 23

- Notice that **heating in the main zone** during the experiment is necessary to maximise temperature differences between indoor air and ambient and adjacent zones. Free running tests may lead to poor signal to noise ratios in the temperature difference measurements and problems with identifiability. Additionally, the heating power is an important variable to complete the energy balance equation used in the analysis, so it must be strong enough in the experiment.

The experiment should be designed aiming to maximise the degree of accomplishment of all these conditions, for the given weather in the test site and the constraints resulting from the heating systems available in each case.

Homogeneity of the indoor air temperature

The different sources of heat such as heating devices and solar radiation can lead to some degree of inhomogeneity of the indoor air temperature contributing to the uncertainty budget of the parameter estimates.

A fan could help to achieve better homogeneity. However it must be taken into account that this strategy could introduce perturbations in the interior convection coefficients, so its usefulness is limited to cases when these perturbations could be considered as negligible.

When unavoidable air stratification is present in realistic experimental campaigns, the uncertainty in parameter estimates due to temperature stratification in indoor air must be taken into account and evaluated. Measurements giving information on air stratification are very useful. This information on air temperature distribution is useful to investigate the following issues:

- Uncertainty in parameter estimates due to temperature stratification in indoor air.

- Different options to achieve an optimum representation of indoor air temperature, for example: considering spatial averages, weighted averages, a reduced selection of measurement points, or any other.

11.5 Minimum steps for data analysis

Data analysis must consider at least the following steps:

1 Pre−processing: Any pre-processing carried out must be reported. Participants in the analysis exercises were encouraged to report data overview based on plots, discussion about quality of data and their suitability to fit objectives, etc.

2 Modelling approach: The methods and models used must be described. The hypotheses and approximation about the physics behind the considered candidate models must be justified. Schematic representations of heat flows in the building are recommended to support explanations. The process of model selection and the decisions made in this process must be explained. The software tools used to identify the parameters must be mentioned.

3 Validation: The validity of the results must be demonstrated. Statistical criteria are very useful in this process. Results must not contradict physical consistency. The process followed to demonstrate the validity of the results must be explained.

4 Results using different data must be compared. Since the data comes from the same physical system the best model should give similar results for two (or more) data series.

5 Results: A value estimated for each parameter and its corresponding uncertainty must be clearly marked as the final result.

6 A list of the hypotheses and approximation of the physics behind the model finally selected to give the final results, must be given together with the final result.

7 Conclusions: Any relevant finding resulting from the analysis, about the results, about the experiment set up and measurement campaign, etc., must be summarised.

8 Reporting: Reports must include at least a section devoted to each of points 1 to 5.

Feedback among the different points should be made in every phase of the process. Is the model accepted? It is advisable to apply more than one method to get a better understanding of the whole problem. Common sense should always be used and all the available physical and statistical knowledge should be used whenever possible.

11.6 Data analysis

This section summarises the aspects that must be considered. Sub-sections 11.6.1, 11.6.2 and 11.6.4 are common to all the analysis approaches considered in this document. Section 11.6.3 focuses on specific aspects of some different approaches that can be chosen.

11.6.1 Preprocessing

Data analysis starts with a qualitative analysis of the quality of the data based on data overview. The objective of this data overview is to detect any abnormal behaviour in the tendencies of the measured variables, sensor failures, etc.

This qualitative analysis is based on the prior physical knowledge of the thermal system under study. Knowledge of the measurement principles of the sensors, transducers and data acquisition systems, can help to interpret unexpected behaviour of the recorded data.

The result of this analysis can be the rejection of some measurements, the decision of correcting some problem on the experiment set up and repetition of the experiment, or the acceptance of the data for the analysis.

Averaging and filtering

Averaging is frequently used as filtering and also as resampling technique. Other filtering and resampling techniques can be applied. Discussing filtering and resampling techniques is out of the scope of this document. However some relevant issues regarding their application are discussed in the following.

In general any averaging and filtering carried out must be justified, explaining its interpretation, which are the beneficial performances that are expected applying it, why improvements are expected, etc.

The application of filtering techniques is useful when there is certainty that their effect is removing information in the data that doesn't correspond to the phenomena that we are studying in the building or building component. However filtering and averaging could have harmful effects if it removes relevant information to the process under study.

As an example the tests of the round robin box in Almería is considered, where tests have been optimised regarding analysis. Particular focus was put in these tests in optimising the accuracy of the measurement of heating power, and regarding amplitude and time resolution (see section 5.5.1 of this document). Amplitude of the heating power, set point of indoors air temperature and dead band have been set such that switching frequencies in the heating power are lower enough than the sampling frequency to guarantee good time resolution. Wrong resampling can make ineffective this experimental set up optimization, and lead to conclude erroneously that signal to noise ratio is poor. See Figure 98 and Figure 99.

In addition it is known that the amplitude of the heating power in these tests only can have two values depending on the status of the switch (on/off), with very small fluctuations around the "on value" (due to the stability of the power source). However averaging can bring some values very far from the actual values of the heating power, and consequently introduces an unnecessary source of uncertainty. See Figure 100.

Consequently in this case this resampling gives poorer signals than the originals so it makes no sense.

The effects of different averaging and resampling periods in other measured variables which are relevant in this case study are shown in Figure 101 (indoor air temperature), Figure 102 (vertical south global solar radiation in clear sky days), Figure 103 (vertical south global solar radiation in cloudy and clear sky days) and Figure 104 (outdoor air temperature).

Averages are suitable in steady state methods which are integral approaches where averages are used to represent integrals. The situation is radically different in differential approaches where the interpretation of time averaging as integration makes no sense.

11.6.2 Construction of candidate models based on hypotheses derived from prior physical knowledge

The starting point of the analysis is considering energy balance equations that include the measured variables and characteristic parameters that must be identified. The characteristics of the studied component and given test conditions are taken into account to build all the candidate models. This step is common to all the analysis approaches.

Then candidate models must be written trying to answer the following questions:

- What is the system to which the energy balance equation will be referred to?. Is it a volume?, is it a flat surface? What is the considered system and their boundaries?

  Some case studies where the energy balance considered for modelling is referred to a surface are reported in Refs. 34 and 35. A case study where the energy balance considered for modelling is referred to a volume is reported in Ref. 36.

- What are the phenomena that theoretically participate in the considered energy balance equation?
- Which of these phenomena are relevant in practice to the considered case study under the given test conditions?
- What is the most efficient way of modelling each phenomena considered as relevant in each case study?. Notice that here efficiency is referred to model accuracy, cost of used measurement devices, and model simplicity. Modelling should include in its objectives the maximisation of accuracy and the minimisation of costs of measurement devices as well as minimising model complexity.

  It must be taken into account that sometimes expressions that could be considered more accurate in principle, could in practice give bad performance. This behaviour could be explained since these expressions bring to the models information and also uncertainty, and in some cases the weight of the introduced uncertainty could be higher that the weight of the introduced information. Any of the following issues could explain this behaviour:

  ➤ Sometimes these expressions are approximation themselves. In this case including effects that have low influence on the global energy balance could bring more uncertainty than information.

  ➤ The contributions associated to each of the variables incorporated in such expressions (the more variables the more uncertainty). As a consequence, including effects that have low influence and are depending on many measured variables could lead to models with bad performance.

    Statistical tests can give very useful support to study this issue.

  ➤ Being far from the scope of applicability of these expressions.

    Consequently it is possible that using more sophisticated expressions could lead to more inaccurate models at the end. Conversely we can find very simple expressions that however capture the main essences of the studied process leading to accurate models.

- Which are the main driving variables of each of the phenomena recognised as relevant for the considered case study?
- Which variables must be considered inputs and outputs according to causality?

If it is not possible to answer some of these questions a priori, several candidate models according to the different possibilities can be considered and evaluated.

If too many options are identified constructing candidate models in this way, it is useful to stablish some prioritised order first studying independently each of the relevant effects identified and then combining those that evidence improvement regarding models not including them. This strategy to construct candidate models was followed in the work reported in ref. 48.

Specific recommendations to construct candidate models for a case study: round robin text box.

This section further discusses criteria to construct candidate models focusing on the round robin test box considered in chapters 3, 4, 5, 6 and 7.

The first step to construct candidate models to fit this objective is to identify the system to which the energy balance equation will be referred to. In this case this energy balance will be referred to the volume of air confined by the building envelope.

To propose candidate models we need to formulate hypotheses according to the following questions 1 to 3. Candidate models must be based on approximations derived from these hypotheses.

1   Are the solar gains through the opaque walls (outside to inside) relevant regarding the other terms in the energy balance equations?.

-   Candidate models considering only solar gains through the window make sense for this case study for data recorded in Belgium during winter (chapter 4), taking into account: 1. The low levels of solar radiation (mainly diffuse), 2. Due to the sun position in winter, the strongest global solar radiation is on the south vertical external surface, 3. Probably high insulation materials in the opaque walls, 4. White external surface that contribute to reduce solar gains.

-   This issue can be investigated considering mono-dimensional analysis, based on energy balances of energy flows through the internal surfaces of the opaque walls. Heat flux measurement devices, on the internal face of each wall, measure the net heat flux density through the internal surface of each wall. These devices are used to carry out this analysis:

  ➢   Studying if solar radiation influences this net heat flux through these surfaces, is useful to discern if solar radiation through the opaque walls is relevant or negligible.

  ➢   The identification of U and g values of the walls using this measurement and the energy balance through the corresponding surface is useful to discern if g-value of the opaque walls is relevant or negligible.

  The mono-dimensional analysis of the roof in Spain (chapter 5) in summer can be studied as an unfavourable case with high levels of incident solar radiation, to evaluate if the g value is or isn't negligible on the opaque walls. In this surface the global solar radiation is high compared to other orientations and also compared to tests in Belgium. If it is concluded that solar radiation is not relevant in this roof we could extrapolate that it is not relevant in any other opaque wall of the round robin box.

  Carrying out analogous mono-dimensional analysis to study floor, and all the others opaque walls is strongly recommended because it would be very useful to confirm and validate the results and conclusions obtained from the analysis of the roof.

- Would it be sufficient to compare plots of the heat flux measurements through the different walls, to conclude that solar gains are relevant when we observe differences in the heat fluxes and these differences are correlated to solar radiation?.

No, this is not enough to do this affirmation. If we see that heat flux through the roof is lower than heat flux through the floor it may be: either because we have solar gains that reduce the net heat losses through the roof, or because the solar radiation that enters through the south window reaches the internal surface of the floor and increases the net heat flux through the floor. Similar considerations can be done for east and west walls. See Figure 105.

It must be taken into account that differences smaller than the uncertainty in the measurement of the heat flux sensor cannot be interpreted as actual differences. It must be remembered that the minimum uncertainty in this measurement is 5% (Uncertainty of the heat flux sensor).

2   Is it possible to assume a constant UA value?, Has the external surface heat transfer coefficient a relevant dependence on the wind speed?, Have the surface coefficients a relevant dependence on the temperature of the corresponding surfaces?, Have the thermophysical properties materials a relevant dependence on temperatures?.

Mono-dimensional analyses are useful and recommended also to study these issues.

3   Is air leakage relevant to the energy balance equation when the whole volume is considered to calculate the UA value?. If it is relevant we need to model this term. It makes sense to consider this contribution negligible in this case study, but there are alternatives that can be considered in case of being not negligible as justified below.

- Preliminary tests for air-leakage were done and reported by BBRI (see Chapter 4 in this document). These tests demonstrated that air-leakage is negligible.

- Even if air leakage is not negligible, the corresponding contribution to the energy balance equation could be considered negligible if the outdoor air flow is already heated up to the indoor air temperature level before being delivered to the room, then there is no heat loss involved. (Ref. 38, page 45).

- If the air enters the test room via a shortcut, then a 100% correction for the effect of air flow on heat balance is required. In practice this phenomena can have an effect on the HLC between zero (fully pre-heated) and maximum (no preheating at all). (Ref. 38, page 45).

- When air leakage between indoors and outdoors is not negligible, a coefficient depending on the pressure difference between both environments could be included. In practice pressure difference is dependent on temperature difference and also on wind speed and direction. Several options for this effect considering first order approximations of these two variables are suggested by Ref. 38 (section 5.1.).

- Improvements could be investigated considering other alternatives reported for this effect in the literature (ref. 40).

11.6.3 Modelling

This section briefly introduce some of the most usual modelling approaches and make emphasis on the physical aspects in each particular case. The main focus on these sections is on the key steps that require application of physical criteria, which are highlighted here. These aspects are crucial to obtain accurate results.

Relevant statistical aspects of these modelling approaches are described in detail in the statistical guidelines (Ref. 19).

Steady state approaches

In steady state all the physical quantities are time independent, according to the definition of steady state given by ISO 9251: 1987. Consequently steady state equations applied to raw data are not valid in dynamic test campaigns.

However integrated dynamic equations become analogous to steady state equations, using time averaging to represent integrals when the integration period is long enough for the accumulation terms to become negligible compared to the other energy flows in the equation. In this case steady state equations can be applied to dynamic test campaigns.

The applicability of these methods to dynamic data has significant constraints as discussed by Ref. 42. This reference reports on the study of the errors in the U-value estimates for different walls, using the steady-state equation. This study is done for instantaneous measurements as well as considering averages representing integrals. It concludes that instantaneous measurements can't provide accurate estimates of the U-values but its accuracy is significantly improved if time integrated variables are used. It is also shown that the error in the U-value estimation is minimised by using a multiple of 24 hours as the integration period. It affirms that the minimum valid integration period depends on the characteristics of the wall and weather conditions. It also demonstrates that longer integration periods are required when temperature fluctuations are higher, temperature difference between indoors and outdoors are lower and walls are heavier.

Average method and (multi-) linear regression methods based on averages belong to this family of models, which base their validity in using averages having their origin as integrals of dynamic formulations.

These models give very bad results when:

- Premises for applicability are not met. More details about these requisites for applicability for average methods are reported in ISO 9869 (Ref. 43).
- Inappropriate energy balance equations are applied in (multi-) linear regression methods. It must be remembered that criteria given in section 3.2 are valid also in this approach to construct candidate models.

It must be remarked that when a product or other operation with different variables is considered in a model, all the products and other operations must be done before the average. This is easily understood keeping in mind that time integral of dynamic energy balance equations are behind time averaging in the origin of these approaches.

These approaches applied to dynamic test campaigns are not efficient, but they can be useful in certain applications. Their main drawback is that sometimes extremely long test periods are required.

These methods were considered at the beginning of the PASSYS project (ref. 44), but were superseded by dynamic approaches that are more accurate, efficient and suitable for dynamic experimental conditions (Refs. 45 to 47).

This analysis is recommended as a first exploratory approach to each new problem. Such preliminary analysis is useful for indicating the order of magnitude of thermal parameters, to investigate which are the most relevant effects in the energy balance equations, what approximations are more suitable for each relevant effect, etc. (Refs. 7 and 48).

Linear models in transfer function form

These models are described in Refs. 49 and 50. Ref. 47 presents the application of this type of models to estimate the thermal properties of building components from outdoor dynamic testing, imposing appropriate physical constraints.

The following is focused on ARX models as an example without losing generality. In these models the output, y(t), is expressed as linear function, using constant coefficients, a_i and b_i, of a number, s, of past readings from the inputs, u(t), and also from a number, r, of past readings of output itself as follows:

$$y(t)+a_1 y(t-\Delta t)+...+a_r y(t-r\Delta t)=b_0 u(t-b\Delta t)+...+b_s u(t-(b+s)\Delta t)+e(t) \tag{25}$$

Where Δt is the sampling interval, e(t) represents the model error.

Considering a dynamic ARX model including the same variables as the steady state energy balance equation of the given system, the required physical parameters are found from the coefficients of the dynamic ARX model, by imposing as physical constraint that the following equations must be coincident:

1. The steady-state energy balance equation of the considered system.
2. The ARX model, when all its inputs and outputs are constant.

This implies that the coefficient of each variable must be the same in both equations. In the case of steady steady-state energy balance equation these coefficients are the target physical parameters. In the case of the ARX model, with constant inputs and outputs, the coefficients become algebraic combination of the a_i and b_i, parameters obtained for the dynamic ARX model.

Then the steady-state physical parameters can be found by comparing these two equations (ref. 47). This comparison is possible provided that the ARX model contains the same variables as the steady state energy balance equation of the considered system. Consequently the first step in this analysis approach is to deduce and write the appropriate steady state energy balance equation that must be based on previous physical knowledge.

For example, if the steady-state energy balance equation for a given system is $\Phi = U(T_i-T_e)-gG_v$, then the dynamic ARX model used to obtain the U and g values must contain the following variables: Φ, T_i, T_e and G_v.

Different candidate models can be taken into account as discussed in section 11.6.2, taking into account different approximations to write the steady-state energy balance equation.

Once the variables that must be included in the model have been identified, it is necessary to decide which of them are considered inputs and which of them are considered as outputs. This assignment must be based on causality of these variables. Usually, either indoor temperature or heat flux is selected as the model output. Multi-output models can be also considered and have shown very good performance in some case studies where test were carried out under unfavourable test conditions (Ref. 51).

Notice that although this is a linear approach, some non-linear effects can be considered by a change of variable. An example is reported in ref. 58. In that work, long wave effects depending on surface temperature raised to the fourth power T^4, were included in the models through a new variable $y=T^4$.

Models in continuous time state space form based on SDE

The continuous–discrete stochastic state space model is a model that consists of a set of nonlinear discrete, partially observed stochastic differential equations (SDEs) with measurement noise, i.e.

$$dx_t = f(x_t, u_t, t, \theta)dt + \sigma(u_t, t, \theta)d\omega_t \tag{26}$$

$$y_k = h(x_k, u_k, t_k, \theta) + e_k \tag{27}$$

where $\theta \in \Theta \ R^p$ is parameter vector; $f(\cdot) \in R^n$, $\sigma \in \Theta \ R^{nxn}$ and $h(\cdot) \in R^l$ are nonlinear functions; $\{\omega_t\}$ is an n-dimensional standard Wiener process and $\{e_k\}$ is an l-dimensional white noise process with $e_k \in N(0, S(u_k, t_k, \theta))$.

This class of models is further described in Ref. 52 and treated by the tool called Continuous Time Stochastic Modelling (CTSM), Ref. 53.

The state space representation is very useful and flexible to represent physical systems governed by differential equations, which offers a very high potential to model a wide variety of physical systems.

Diffusion terms and modelling errors ($\sigma(u_t, t, \theta)d\omega_t$ and e_k in the previous equations) allow achieving very accurate parameter estimates.

It must be highlighted that the system equations can include measured as well as non measured states which is a very useful feature in modelling physical systems.

RC models can be considered here. However these family of models are a reduced subset of the state space models that can be used and don't make use of these capabilities to their full extent.

Case studies applying this approach are reported in Refs. 35, 54 and 55. Ref. 54 reports the application of RC models to a full size building. Ref. 35 reports the modeling of a building integrated and ventilated photovoltaic system. It demonstrated that a description of the nonlinear heat transfer is essential for modelling of surface effects due to long wave radiation and convection in this particular system. It showed also the usefulness of certain approximations to take into account unmeasured effects. Ref. 55 reports the application of the same model to evaluate the effect of different set ups in the heat transfer coefficient for the same PV integrated modules.

11.6.4 Model validation

Validation is a key issue of the problem. Statistical criteria are very useful guiding and optimising the process of model selection. Results must not contradict physical consistency.

The following criteria for model selection and validation suggested by Norlén (ref. 56) are recommended:

1. Fit to the data. The model residuals should be 'small' and 'white noise'. A necessary condition for 'white noise' is that there should be neither autocorrelation in the residuals nor correlation between the residuals and the input variables.
2. Internal validity. The model should agree with data other than that used for parameter estimation (cross validation).
3. External validity. The model results should not (without strong reason) conflict with previous experience or other known conditions.
4. Dynamic stability. In steady state, the model should provide an output after a temporary change in an input variable that gradually fades out (if the model is intended to describe dynamic characteristics).
5. Identifiability. It should be possible to determine the parameters of the model uniquely from the data.
6. Simplicity. The model should be as small as possible.

If the residuals contain periodicities, a study of the correlation in the frequency domain can be more useful to reveal such periodicities than the autocorrelation function. The periodogram shows how the variation of the residuals is distributed on frequencies. For white noise this variation is equally distributed, i.e. the cumulative periodogram is a straight line from (0,0) to (0.5,1). See Ref. 57 for further details.

Particular care must be taken in the interpretation of residuals with a frequency of 24 hours. In a first approach a non-negligible correlation between the model residuals and solar radiation could lead to the suggestion for a more detailed description of the solar radiation in the model for further improvements. However it must not be forgotten that, many variables can show a relevant correlation with solar radiation, so any other effect not properly modelled can show problems in the residuals in the same frequency as the solar radiation. This behaviour is highlighted in sunny locations where levels of solar radiation are high. The effects in the following list can be mentioned as examples of phenomena that could produce this behaviour.

If you want to list something, proceed as follows:

- Air leakage that can depend on wind speed and/or outdoor air temperature, both depending on solar radiation.
- Long wave effects resulting from high surface temperatures due to solar radiation. One example of this issue is reported in 58.
- U depending on thermal conductivities which depend themselves on the temperature of the materials that finally depend on solar radiation.
- Wrong resampling disregarding the sampling theorem (See section 0 and Figure 99).
- Etc.

If validation criteria don't fit, models must be rejected and new models must be reformulated. Conclusions from the previous analysis and validation process are very useful to construct new models, reconsidering hypothesis and rewriting candidate models according reviewed hypothesis. Redesigning experiment set up and carrying out new experiments might be necessary.

Practical recommendations

This section reports some practical recommendations reported in 38. These recommendations are based on experience from different European projects related to energy assessment of building components, such as IQ-TEST, etc. (ref. 39).

A.   Preliminary check on residuals:

Plot of average and root mean square of the residuals are very useful in a preliminary analysis to detect problems related to data and modelling. In particular the following checks are recommended:

- If the root mean square (RMS) value of residuals is 'unexpectedly' large: check data file or model for errors.
- The mean value of residuals should be significantly smaller than the RMS value; if not: systematically biased output and check data file or model for errors.
- If at certain point the residual is (or starts to be) higher than roughly three times the RMS value: check for erroneous input or output data at that point.

B.   Evaluation on the basis of confidence intervals:

If a parameter has a very high large confidence interval: Look at parameter significance and correlation between parameters then adapt the model to remove insignificant and highly correlated parameters:

- If not highly correlated with one or more other parameters, freeze the parameter at some value indicated by the identification result or at a value which is physically meaningful.

- If highly correlated with one or more other parameters, then freeze one of this group of parameters: choose the one with the highest deviation from what seems physically feasible.

Freezing parameters and establishing constraints among for different parameters in the model according to physical knowledge is usually helpful to solve these problems.

C.   Evaluation of the characteristic parameters and individual parameters with physical meaning:

It must be taken into account that some individual parameters have only mathematical and no physical meaning; these cannot be checked for their physical meaning; for instance individual conductances and capacitances inside a construction without internal measurements.

The following checks are useful regarding parameters with physical meaning:

- Check if values deviate from values expected based on prior knowledge......
- Check if the confidence interval of a function of parameters is unexpectedly high; if so the test sequence is not appropriate for this function or the model is not appropriate (non-linearities?,...etc.).

D.   Residual statistical analysis:

Autocorrelated residuals indicate that the model is not capable of following the dynamics of the system. This may be due to any of the following issues:

If you want to list something, proceed as follows:

- A missing input or error in the input data. This can be solved trying to find the missing input variable
- A higher order influence of one or more already known input variables. In this case a higher order model may lead to improved results.

Combining parameter values such as string of identical resistances and capacitances can be an useful strategy to avoid that the model becomes overparametrised.

A statistical post processing program may help to detect which information is still contained in the residuals.

E.   Cross-validation:

Compare results with results on different data set. A convenient way is to repeat the identification on the data set with twice the original length and check for consistency. Since the data comes from the same physical system the best model should give similar results for both (or more) data series.
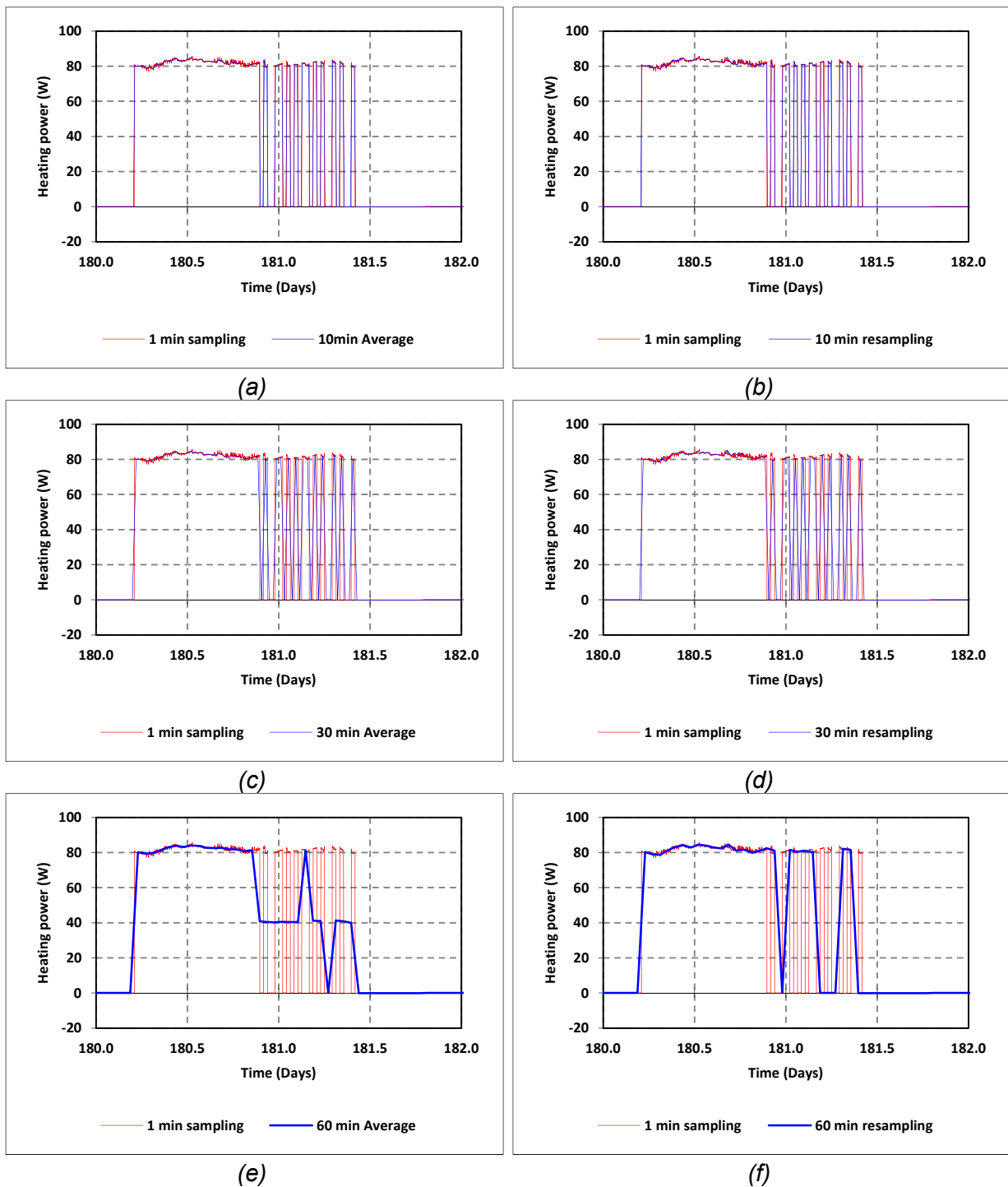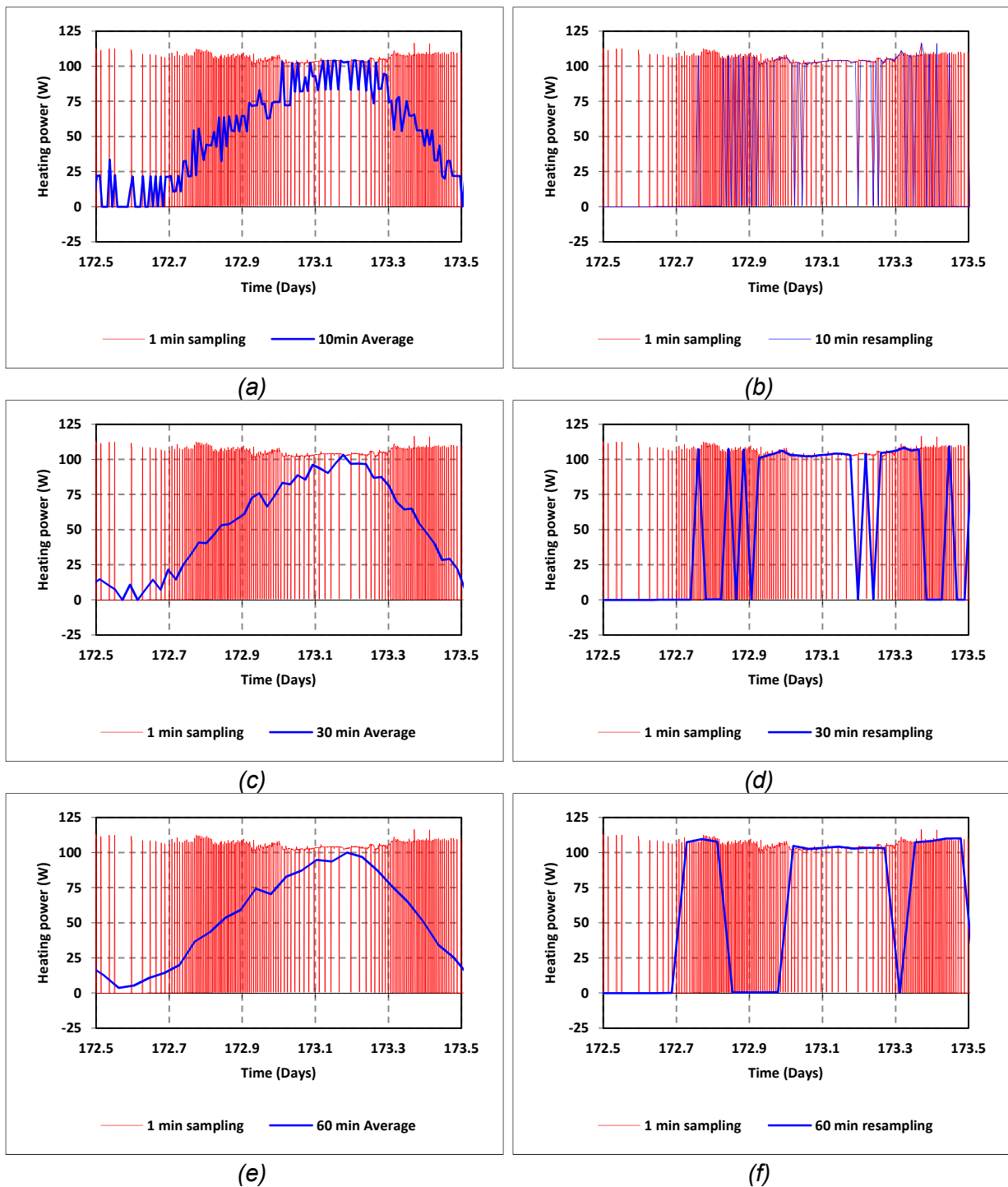
Figure 98: Effects of different resampling periods and techniques on power measurement in a ROLBS sequence. (Series 5 CE4. Test in Almería). Different behaviour is observed for the different averaging and resampling intervals. Faithful representation of the actual variable for 10 minutes resampling and averaging is seen in graphs (a) and (b). However relevant information on the measured variable is lost in some periods when longer intervals are considered for resampling and averaging. This is particularly evident in graphs (e) and (f), with 60 minutes averaging and resampling, around the time interval 181.0 to 181.5.

Figure 99: Effects of different resampling periods and techniques on measurement of heating power. (Series 4 CE4. Test in Almería). Relevant information on the measured variable is lost when resampling and averaging are applied in all cases.
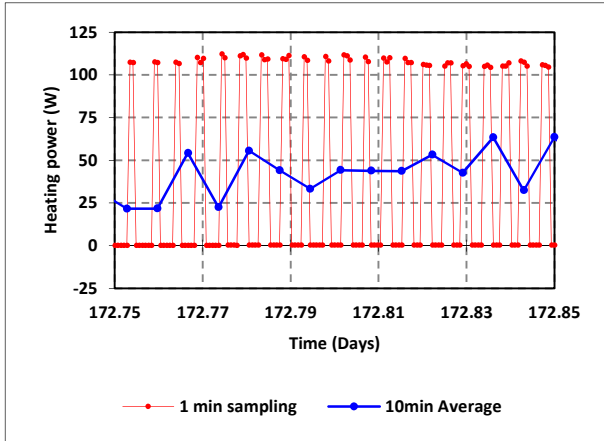
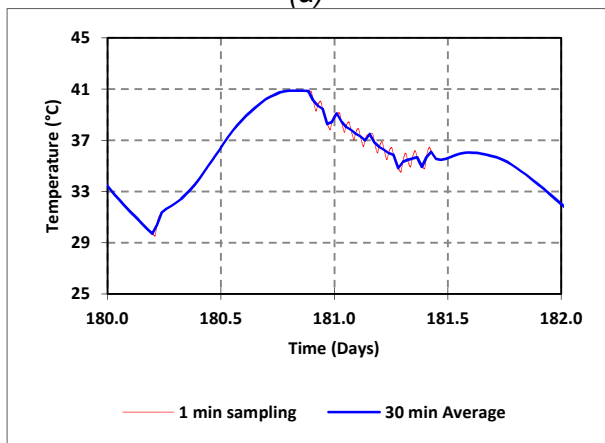*(a). Power measurement in a Co-heating test. (Series 4 CE4. Test in Almería).*

(b) Power measurement in a ROLBS sequence. (Series 5 CE4. Test in Almería).

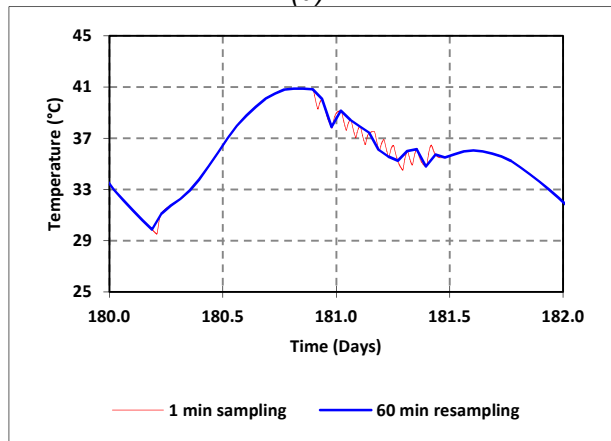*Figure 100: Some examples of resampling eliminating relevant information.*
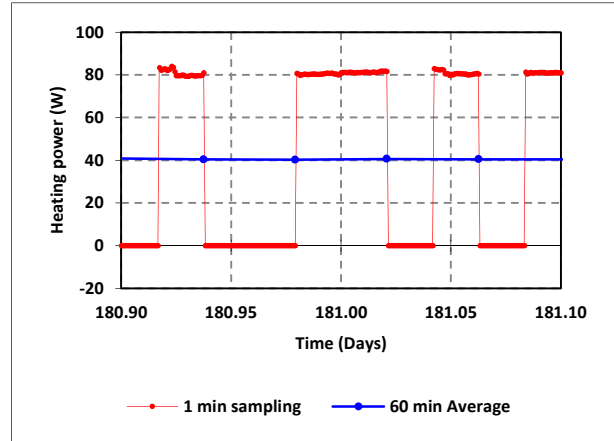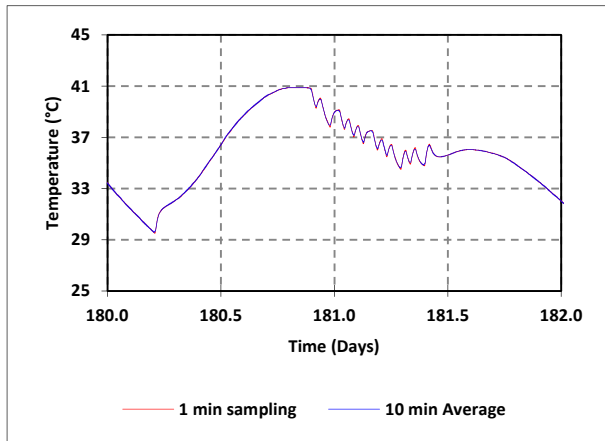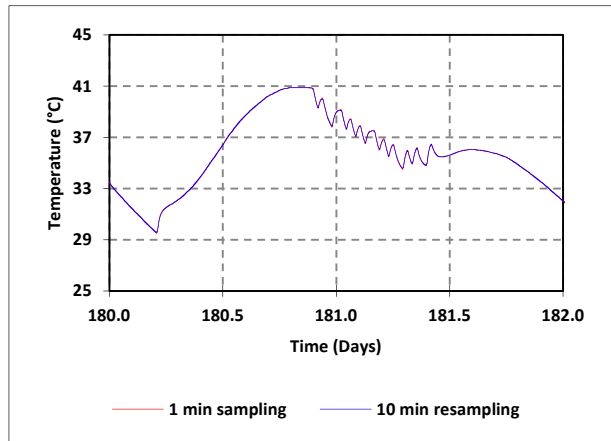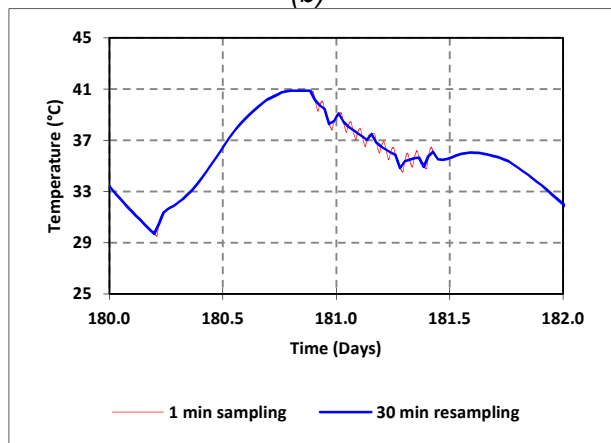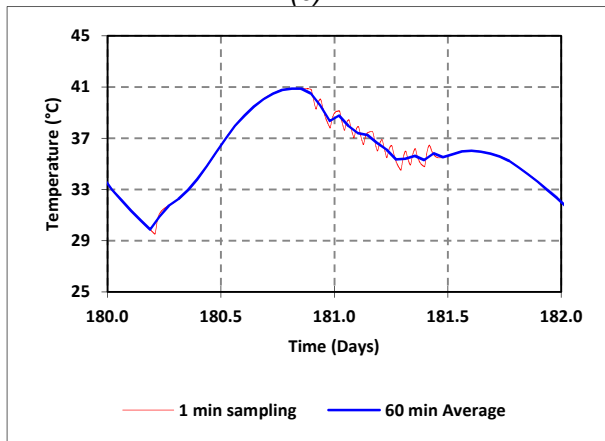
Figure 101: Effects of different resampling periods and techniques on measurement of indoor air temperature. (Series 5 CE4. Test in Almería). Faithful representation of the actual variable for 10 minutes resampling and averaging is seen in graphs (a) and (b). However relevant information on the measured variable is lost in some periods when longer intervals are considered for resampling and averaging. This is particularly evident in graphs (e) and (f), with 60 minutes averaging and resampling, for the time interval 181.0 to 181.5.
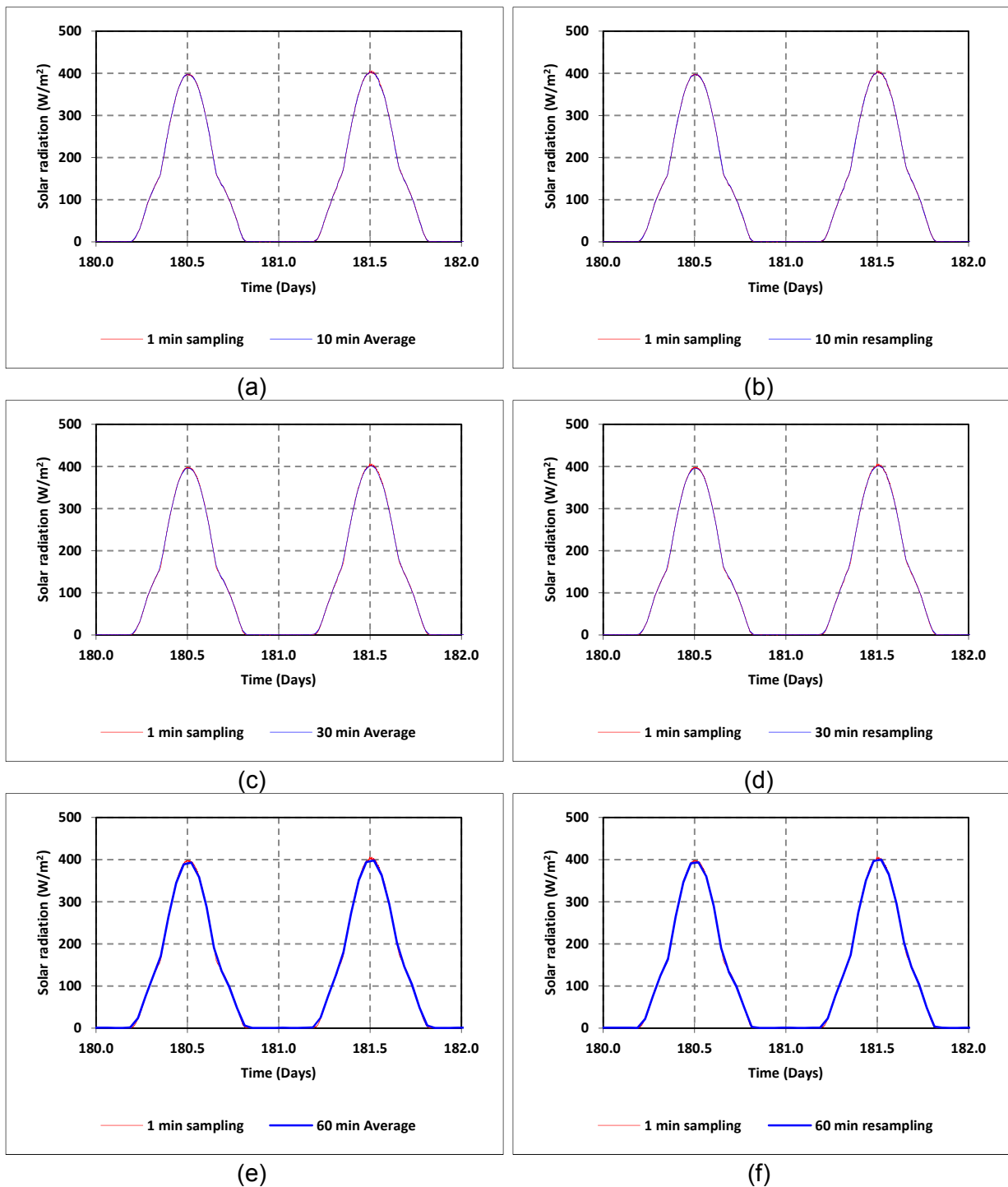
Figure 102: Effects of different resampling periods and techniques on measurement of vertical south global solar radiation. (Series 5 CE4. Test in Almería). The different averaging and resampling frequencies give faithful representation of the actual variable on sunny days. Different performance is observed for cloudy days (see Figure 103).
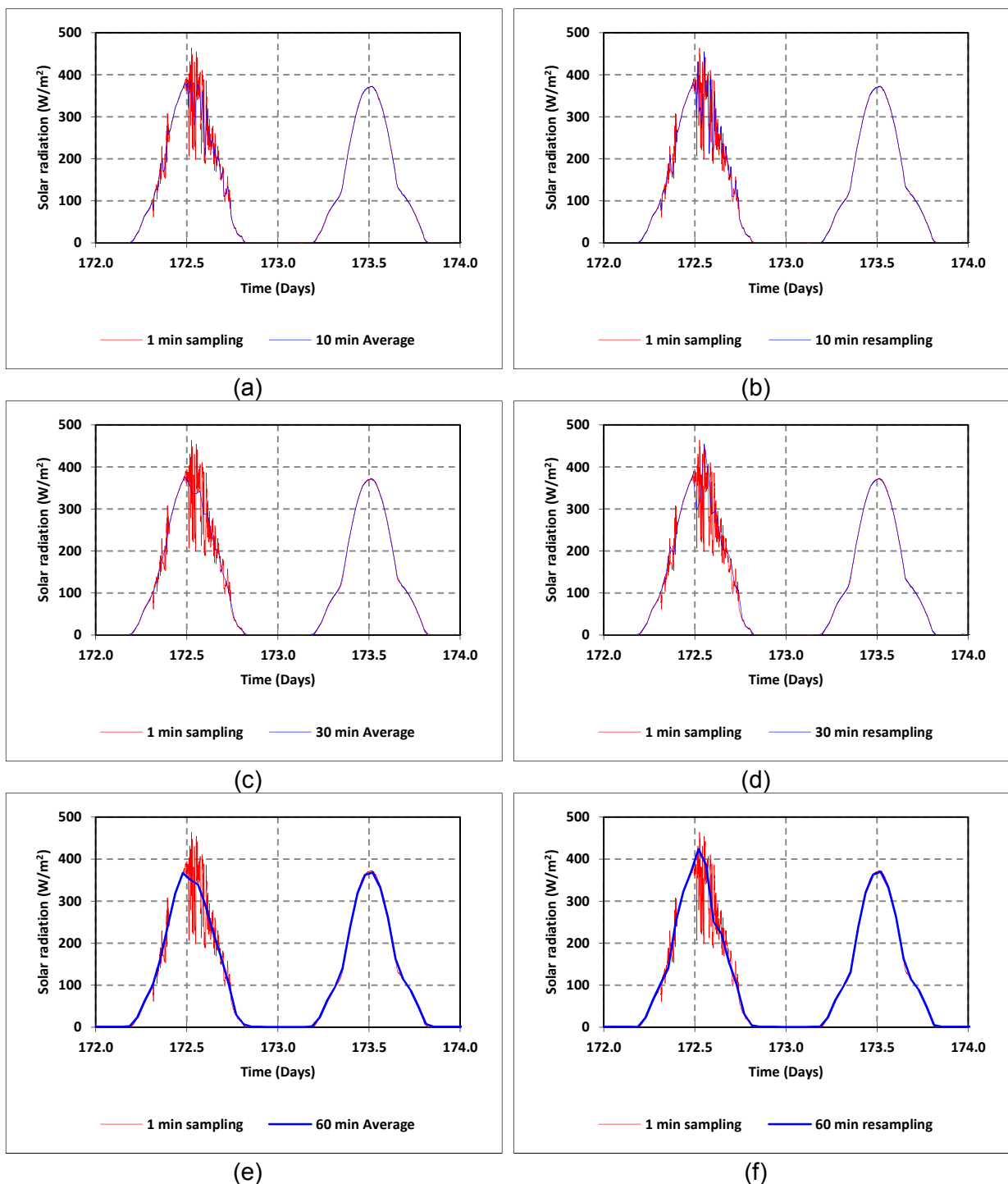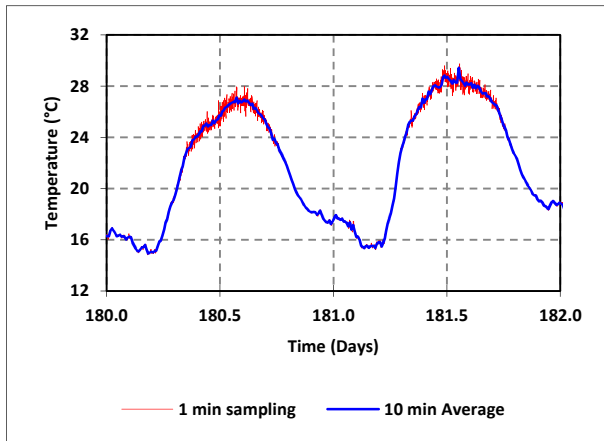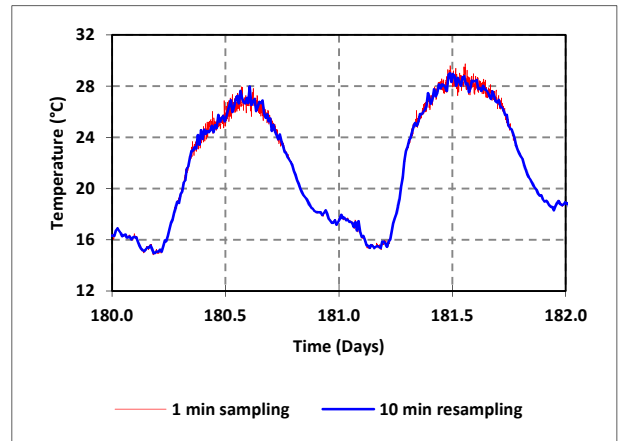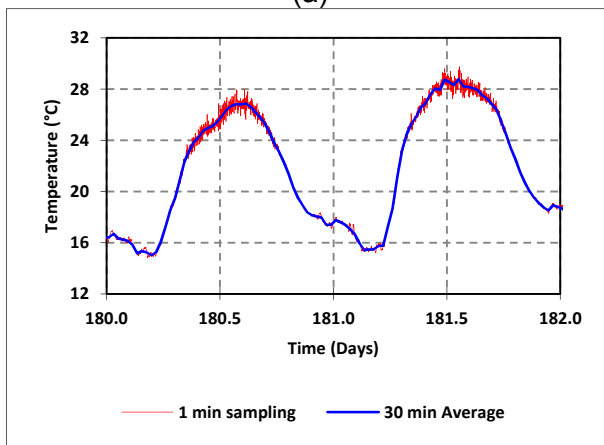
Figure 103: Effects of different resampling periods and techniques on measurement of vertical south global solar radiation for sunny and partly cloudy days. (Series 5 CE4. Test in Almería). Different behaviour is observed for clear sky and partly cloudy days. In the case of clear sky, the different averaging and resampling frequencies give faithful representation of the actual variable. However when days are partly cloudy the original measurement present relevant variations that are lost when resampling and averaging are applied.
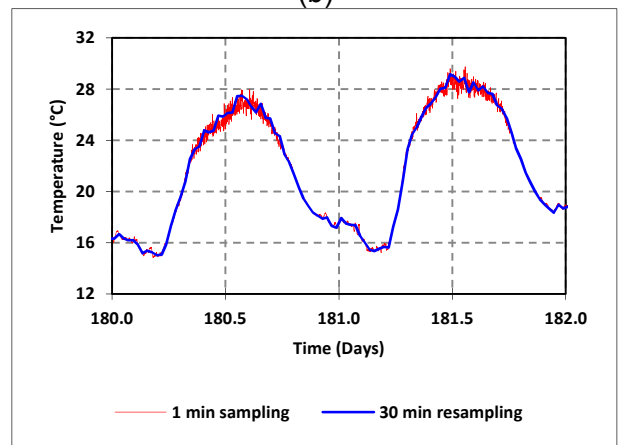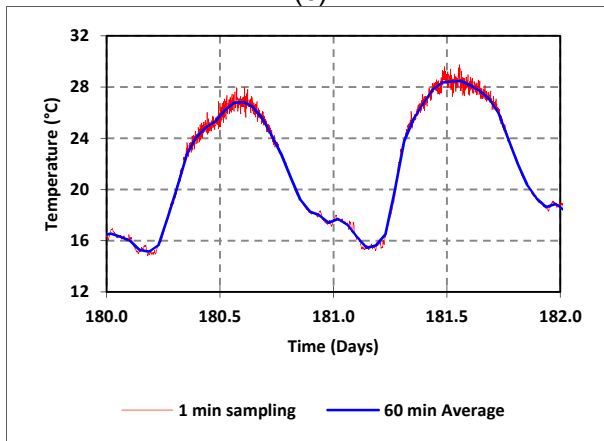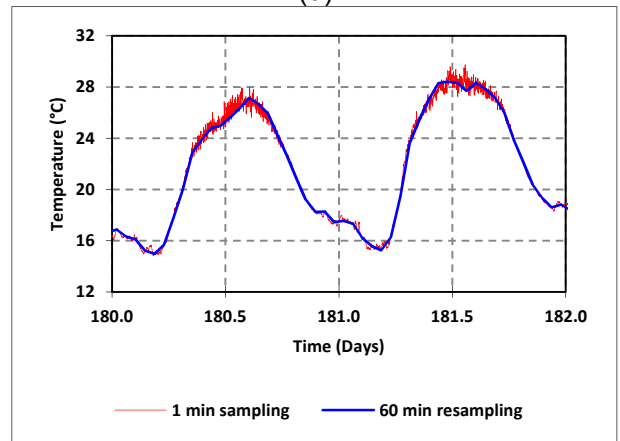
Figure 104: Effects of different resampling periods and techniques on measurement of outdoor air temperature. (Series 5 CE4. Test in Almería). Some information is lost for the different frequencies of averaging and resampling applied. Equivalent behaviour is observed for the different averaging frequencies, which eliminate small oscillations in high frequencies mainly around midday. In principle this filtering is not considered harmful because these oscillations seem to follow a white noise pattern in the range of the uncertainty in the measurement of this variable.
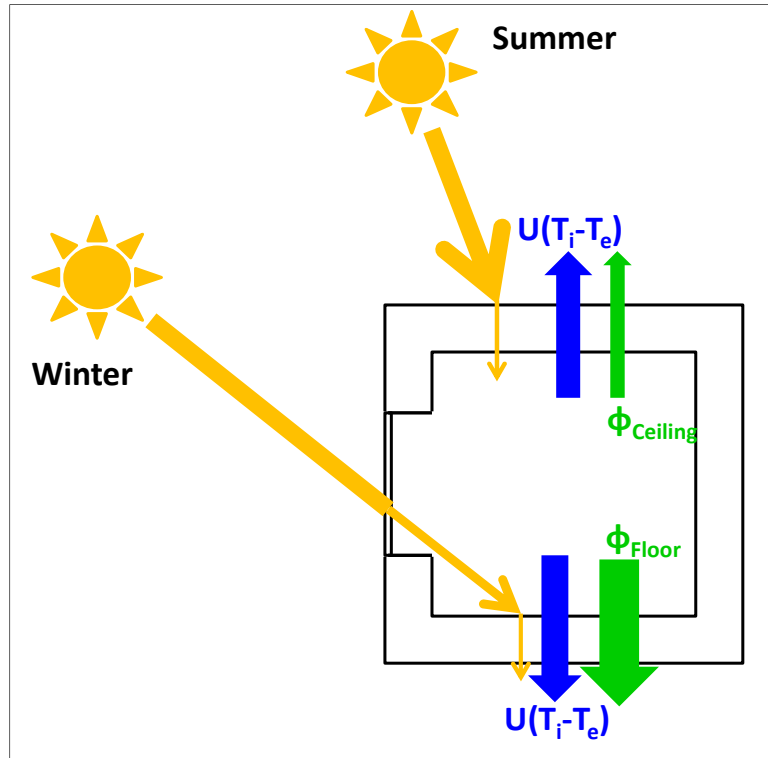
Figure 105: Different possibilities of heat flows due to solar radiation: 1.- Negligible. Then the net heat flow (green) is due to heat lost (blue). 2.- Non negligible from outdoor to indoor. Then the corresponding contribution is subtracted from the heat lost to give the net heat flow (as shown in this example through ceiling). 3.- Non negligible from indoor to outdoor. Then the corresponding contribution is added to the heat lost to give the net heat flow (as shown in this example through the floor).

Acknowledgements

References

1. CTE. 2006. Código técnico de la Edificación. R. D. 314/2006, B.O.E. 28th March 2006. (Spanish regulation for thermal conditions in buildings).
2. ISO 6946:2007. Building components and building elements -- Thermal resistance and thermal transmittance -- Calculation method.
3. W. H. McAdams. 1954. "Heat Transmission". 3rd ed., McGraw-Hill, New York.
4. J. H. Watmuff, W. W. S. Charters, D. Proctor. 1977. "Solar and Wind Induced External Coefficients for Solar Collectors". COMPLES Nº2, 56.
5. J. A. Duffie, W. A. Beckman. 1991. "Solar Engineering of thermal processes". Ed. J. Wiley & Sons. Inc. ISBN 0-471-51056-4
6. ASHRAE Handbook Applications. 1999.
7. I. Naveros, M.J. Jiménez, M.R. Heras. 2012. Analysis of capabilities and limitations of the regression method based in averages, applied to the estimation of the U value of building component tested in Mediterranean weather. Energy and buildings. 55. pp. 854–872.
8. I. Naveros, P. Bacher, D.P. Ruiz, M. J. Jimenez, H. Madsen. 2014. Setting up and validating a complex model for a simple homogeneous wall. Energy and buildings. 70. pp. 303–317.
9. EN 673:2011. Glass in building. Determination of thermal transmittance (U value). Calculation method.
10. ISO 6946:2007. Building components and building elements -- Thermal resistance and thermal transmittance -- Calculation method.
11. A.H. Deconinck, S. Roels. Estimation of the Round Robin Test Box's thermal resistance by semi-stationary and dynamic characterisation. 6th Expert meeting Annex 58 ECBCS IEA. Ghent (Belgium), 14-16 April 2014.
12. ISO 9869:1994. Thermal insulation -- Building elements -- In-situ measurement of thermal resistance and thermal transmittance.
13. H. Hens. 2012. Applied Building Physics - Boundary Conditions, Building Performance and Material Properties. Ernst & Sohn. ISBN: 978-3-433-60127-3.
14. ISO 6946:2007. Building components and building elements -- Thermal resistance and thermal transmittance -- Calculation method.
15. W. H. McAdams. 1954. "Heat Transmission". 3rd ed., McGraw-Hill, New York.
16. J. H. Watmuff, W. W. S. Charters, D. Proctor. 1977. "Solar and Wind Induced External Coefficients for Solar Collectors". COMPLES Nº2, 56.
17. J. A. Duffie, W. A. Beckman. 1991. "Solar Engineering of thermal processes". Ed. J. Wiley & Sons. Inc. ISBN 0-471-51056-4
18. ASHRAE Handbook Applications. 1999.
19. H. Madsen, P. Bacher, G. Bauwens, A-H. Deconinck, G. Reynders, S. Roels, E. Himpe, G. Lethé. Report of Subtask 3 – Part 2. Thermal performance characterization using time series data - statistical guidelines. IEA EBC Annex 58. Final Reports.
20. S. Roels, P. Bacher, G. Bauwens, H. Madsen, M.J. Jiménez. 2015. "Characterising the actual thermal performance of buildings: current results of common exercises performed in the framework of the IEA EBC Annex 58-project". "6th International Building Physics Conference, IBPC 2015". Energy Procedia. 78, pp. 3282-3287
21. K. Chávez, L. de la Torre, S. Castaño, R. Enríquez, M.J. Jiménez. 2015. "Experimental energy performance assessment of a simplified building: study of robustness of different analysis approaches under different test conditions". "6th International Building Physics Conference, IBPC 2015". Energy Procedia. 78, pp. 2328-2333.

22. P. Baker. 2008. Evaluation of round-robin testing using the PASLINK test facilities. Building and Environment. Special issue on Outdoor testing, analysis and modelling of building components. 43(2), pp. 181–188.

23. Strachan et al. 2015. Verification of common BES☐models based on in situ dynamic data. IEA EBC Annex 58. Final Report Subtask 4.1

24. Eline Himpe, Arnold Janssens. 2015. "Characterisation of the Thermal Performance of a Test House based on Dynamic Measurements". "6th International Building Physics Conference, IBPC 2015". Energy Procedia. 78, pp. 3294–3299.

25. Jiménez M.J.; Heras M.R. 2005. "Application of multi-output ARX models to estimate the U and g values of building components from outdoors testing". Solar Energy. 79(3), pp. 302-310.

26. R. Enríquez, L. Zarzalejo, M.J. Jiménez, M.R. Heras. 2012. "Ground reflectance estimation by means of horizontal and vertical radiation measurements". Solar Energy. 86(11), pp. 3216-3226.

27. F. P. Incropera, D. P. De Witt. 2002. "Fundamentals of Heat and Mass Transfer". 5th ed., John Wiley, New York.

28. World Meteorological Organization. 1996. "Guide to Meteorological Instruments and Methods of Observation.WMO-Nº8". ISBN: 92-63-16008-2

29. International Electrotechnical Commission. 1983. CEI IEC 751. Industrial platinum resistance thermometer sensors.

30. F. van der Graaf. 1990. Heat Flux Sensors. Chapter of book: Sensors a Comprehensive Survey. (W. Göpel, J. Hesse, J.N. Zemel, ed.). ISBN 3-527-26770-0 (VCH, Weinheim, Germany).

31. DIN EN 60688. 2002. Electrical measuring transducers for converting a.c. electrical quantities to analogue or digital signals (IEC 60688:1992 + A1:1997, modified + A2:2001)..

32. IEA ECBCS, Annex 58 Reliable Building Energy Performance Characterisation Based on Full Scale Dynamic Measurements. http://www.ecbcs.org/annexes/annex58.htm. Last viewed the 30th of November 2015.

33. M.J. Jiménez, S. Castaño, L. de la Torre, H. Madsen, G. Flamant, G. Lethé, G. Bauwens, S. Roels. Annex 58 ECBCS IEA. ST3. 4th Common Exercise on Data Analysis. Instruction Document. Annex 58 EBC IEA internal report. July 2013.

34. M.J. Jiménez, B. Porcar, M. R. Heras. 2009. Application of different dynamic analysis approaches to estimate the U value of building components. Building and Environment. 44(2), pp. 361-367.

35. M.J. Jiménez, H. Madsen, H. Bloem, B. Dammann. 2008. Estimation of Non-linear Continuous Time Models for the Heat Exchange Dynamics of Building Integrated Photovoltaic modules. Energy and Buildings. 40, pp. 157-167.

36. M.J. Jiménez, H. Madsen. 2008. Models for Describing the Thermal Characteristics of Building Components. Building and Environment. Special issue on Outdoor testing, analysis and modelling of building components. 43(2), pp. 152-162.

37. M.J. Jiménez, H. Madsen, G. Flamant, G. Lethé, G. Bauwens, S. Roels. Annex 58 ECBCS IEA. ST3. 3rd Common Exercise on Data Analysis. Instruction Document. Annex 58 EBC IEA internal report. March 2013.

38. PASLINK-EEIG. IQ-TEST FINAL TECHNICAL REPORT. PART 2. Training of test site managers and data analysis. (Dick van Dijk, Hans Bloem, Paul Baker. Eds). IQ-TEST project, CONTRACT N°: ERK6-CT1999-20003, PROJECT N°: NNE5-1999-0511. 1st August 2003.

39. Strachan P. A., Baker P. H. 2008. Special issue on Outdoor testing, analysis and modelling of building components. EDITORIAL. Building and Environment, 43, pp. 127-128.

40. Rabl A. 1988. Parameter estimation in buildings: methods for dynamic analysis of measured energy use. J. Solar Energy Eng, 110, pp. 52-66.

41. ISO 9251:1987. 1987. Thermal insulation. Heat transfer conditions and properties of materials. Vocabulary.

42. Modera M.P., Sherman M.H., Sounderegger R.C. Determining the U-Value of a Wall from Field Measurements of Heat Flux and Surface Temperatures. In Building Applications of Heat Flux Transducers, ASTM STP 885, Bales, E., Bomberg, M., Courville, G.E., (eds.); Philadelphia: American Society for Testing and Materials, 1985, pp. 203-219.

43. ISO 9869:1994. 1994. In-situ measurement of thermal resistance and thermal transmittance.

44. Van Dijk, H.A.L.;Van Der Linden, G.P. 1993. The PASSYS Method for Testing Passive Solar Components. Building and Environment. 28 (2), pp. 115-126.

45. O. Gutschker. 2004. LORD – Modelling and identification software for thermal systems, user manual, BTU Cottbus.

46. O. Gutschker. Parameter identification with the software package LORD. Special issue on Outdoor testing, analysis and modelling of building components. Building and Environment. 43(2), pp. 163-169.

47. M.J. Jiménez, H. Madsen, K.K. Andersen. Identification of the Main Thermal Characteristics of Building Components using MATLAB. Special issue on Outdoor testing, analysis and modelling of building components. Building and Environment. 43(2), pp. 170-180.

48. L. Castillo, R. Enríquez, M.J. Jiménez, M.R. Heras. 2014. Dynamic integrated method based on regression and averages, applied to estimate the thermal parameters of a room in an occupied office building in Madrid. Energy and Buildings. 81, pp 337-362.

49. Ljung, L. 1999. System Identification. Theory for the User. New Jersey: Prentice Hall.

50. Box, G.E.P., and G.M. Jenkins. 1976. Time Series Analysis, Forecasting and Control. Holden-Day.

51. M.J. Jiménez, M.R. Heras. 2005. Application of multi-output ARX models to estimate the U and g values of building components from outdoors testing. Solar Energy. 79(3), pp. 302-310.

52. N.R. Kristensen, H. Madsen, S.B. Jørgensen, 2004. Parameter estimation in stochastic grey-box models, Automatica 40 (2). 225–237.

53. Kristensen N.R., Madsen H. 2003. Continuous Time Stochastic Modelling - CTSM 2.3 User Guide. Technical University of Denmark, Lyngby, Denmark.

54. Madsen H., Holst J. (1995). Estimation of continuous-time models for the heat dynamics of buildings. Energy and Buildings, 22, pp. 67-79.

55. Friling N., Jiménez M.J., Bloem J.J., Madsen H., 2009. "Modelling the heat dynamics of building integrated and ventilated photovoltaic modules". Energy and Buildings. 41(10), pp. 1051-1057.

56. U. Norlén. Determining the Thermal Resistance from In-Situ Measurements. In: Workshop on Application of System Identification in Energy Savings in Buildings (Edited by Bloem, J.J.), 402-429. Published by the Commission of The European Communities DG XIII, Luxembourg.1994.

57. Madsen, H. 2008. Time Series Analysis, Chapman and Hall.

58. M.J. Jiménez, B. Porcar, M.R. Heras. 2008. Estimation of UA and gA values of building components from outdoor tests in warm and moderate weather conditions. Solar Energy. 82(7), pp. 573-587.